TEL-AVIV UNIVERSITY

Direct Moving Transmitter Geolocation Based on Delay and Doppler

by

Itamar Weiss

A thesis submitted in partial fulfillment for the
degree of Master of Science

in the
Faculty Name
Department or School Name

June 2011

"Write a funny quote here."

If the quote is taken from someone, their name goes here

TEL-AVIV UNIVERSITY

Abstract

Faculty Name
Department or School Name

Master of Science

by Itamar Weiss

We analyze the problem of geolocating a single moving transmitter using an array of stationary receivers, and propose a one-step algorithm. Although many common methods address this problem, they all consist of suboptimal two-step algorithms: at the first step, several signal parameters are extracted at each receiver such as Time Of Arrival (TOA) or Angle Of Arrival (AOA), while at the next step the extracted parameters are used to estimate the location of the transmitter. The proposed algorithm uses the same data used in common methods. However, it is performed in a single step by maximizing a cost function that depends on the unknown position and velocity only. This is a natural extension of the Direct Position Determination (DPD) algorithm for the scenario in which the transmitter is moving in an unknown velocity. In this work, we model the problem, present the Maximum-Likelihood (ML) cost function, explore the ML cost function for its characteristics, suggest algorithms relevant to different scenarios, present the Cramer-Rao lower Bound (CRB) of the problem and compare numerically the performance of the suggested algorithms to the CRLB and to the performance of the classical two-step methods. We show that the suggested algorithm achieves better performance than classical methods, especially in low Signal to Noise Ratio (SNR) scenarios.

Acknowledgements

The acknowledgements and the people to thank go here, don't forget to include your project advisor...

Contents

List of Figures

Abbreviations

AOA	**A**ngle **O**f **A**rrival
CRB	**C**ramer **R**ao lower **B**ound
DD	**D**ifferential **D**oppler
DPD	**D**irect **P**osition **D**etermination
FDOA	**F**requency **D**ifference **O**f **A**rrival
FIM	**F**ischer **I**nformation **M**atrix
ML	**M**aximum **L**ikelihood
SNR	**S**ignal to **N**oise **R**atio
TDOA	**T**ime **D**ifference **O**f **A**rrival
TOA	**T**ime **O**f **A**rrival

Symbols

L	the number of receivers
$\vec{p_\ell}$	the position of the ℓ-th receiver
$\vec{p}$	the position of the moving transmitter
$\vec{v}$	the velocity of the moving transmitter
$r_\ell(t)$	the complex signal received by the ℓ-th receiver at time t
b_ℓ	the complex attenuation of the signal at the ℓ-th receiver
T_ℓ	the time delay of the signal at the ℓ-th receiver
f_ℓ	the carrier frequency Doppler shift obseved by the ℓ-th receiver
$\tilde{f}_\ell$	the carrier frequency of the signal observed by the ℓ-th receiver
$w_\ell(t)$	the noise observed by the ℓ-th receiver at time t
f_c	the nominal carrier frequency of the transmitter
ν	the carrier frequency shift due to source instability of the transmitter
μ_ℓ	the ratio between the Doppler shifted frequency and the original transmitted frequency observed by the ℓ-th receiver
θ_ℓ	the angle between the line connecting the transmitter and the ℓ-th receiver and the x-axis
ϕ_ℓ	the angle between the velocity of the transmitter and the line connecting the transmitter and the ℓ-th receiver
B	the signal's bandwidth
c	the speed of light
$s(t)$	the envelope of the transmitted signal at time t
Ts	the time between samples
T	the observation time interval

For/Dedicated to/To my...

Chapter 1

Introduction and Literature Survey

In this work, we analyse the problem of passive geolocation of a moving transmitter, using a stationary array of receivers. We suggest a one-step algorithm for estimating the position and velocity of the transmitter based on one sampling interval. The performance of this algorithm is analyzed, tested using Monte-Carlo simulations and compared to the performance of conventional methods.

The signal processing problem of passive transmitter geolocation has been greatly discussed since World War I. It has both civil and military related applications. Among the military applications we can mention passive geolocation of communication systems, radars, GPS blockers and passive low-signature geolocation of air-planes. Among the civil applications we can mention navigation. The extensive use of cellular telephony these days has increased the popularity of this field, and geolocation of cellular phone users is one of the major civil application nowadays, for focused advertising, network load monitoring and enhanced emergency services. The wireless enhanced 911 (E911) review by Zagami et al.[1] is one example to the implementation of passive geolocation methods. The wide spread and high density of Wi-Fi networks in highly populated cities nowdays, can serve passive geolocation methods for nevigation inside buildings, or where

is no GPS reception. In [2] a method for geolocation inside buildings using the Wi-Fi signal strength is presented.

Unlike active localization systems such as radar or sonar, that transmit a known signal and process the signal after it was returned from the target, in passive gelocation systems the transmitted signal is usually unknown. Known signals scenarios include, for example, beacon tracking, where a system transmits a known signal in order to be tracked, and scenarios in which there is a communication system that has a known training sequence. In scenarios in which the transmitted signal is known, better performance and lower algorithm complexity can be achieved.

While exploring passive geolocation methods, two main approaches can be found: two-step methods and one-step methods. Many two-step methods for passive transmitter geolocation have been suggested in the past [3–10]. The two-step methods first estimate parameters characterizing the signal in each receiver, or in each pair of receivers, and then use these estimated parameters to estimate the location of the transmitter. One step methods were thoroughly discussed in literature and are considered, in general, the classical passive geolocation methods. Two step methods were very popular in the past, and also today, because the parameters characterizing the signals, such as time of arrival, frequency of arrival, signal strength etc., could have been extracted using simple analog components, and because sending the extracted parameters from all the receivers to a central processing station required low-bandwidth communication that was available in the past. Obviously, due the incomplete data used in each receiver or pair of receivers and over-parametrization, two-step methods are sub-optimal. Recently, one-step methods [11–14] have been suggested and shown to have greater results than the one-step methods. The one-step methods use the sampled signals collected at each of the receivers to simultaneously estimate the position of the transmitter. High frequency digital samplers and high-bandwidth communication systems that exist today, make it possible to employ the one-step methods.

Although geolocation of a stationary transmitter by moving receivers has been discussed thoroughly in the literature, the problem of geolocating a moving transmitter has been less discussed. The problem of geolocating a moving transmitter shows greater complexity than geolocating a stationary transmitter, because both the position and velocity of the transmitter are unknown and need to be estimated.

In this work, we employ the concepts of the one-step methods for passive geolocation of a moving transmitter.

Along this work, we present only the two-dimensional scenario, where the position and velocity of the transmitter lie on a two-dimensional plane. It is simpler to demonstrate the principles of geolocation using the two-dimensional scenarios, and the two-dimensional scenario can be easily expanded to the three-dimensional scenario. Although many applications, such as passive air-plane geolocation, are in-fact three-dimensional scenarios, in many other applications, such as mobile phone geolocation, the plane on which the transmitter could be found is usually known.

In the following chapter, we introduce several two-step and one-step methods suggested for passive geolocation of a stationary transmitter based on delay and doppler. The two-steps methods we introduce are TOA, TDOA, FOA and FDOA, while the one-step methods introduced are DPD and its derivatives.
At the last section of this chapter, we introduce the outline for our work.

1.1 Two-Step Localization Methods

1.1.1 Extracting TDOA and FDOA measurements

The first step in time and frequency shifts based two-step methods is estimating the time and frequency shifts between the received signal and another signal [15, 16]. Depending on the method, the estimation can be performed between each pair of receivers, between all the receivers and a reference receiver, or between each receiver and a known reference

signal, in the case where the transmitted signal is known.

The ML estimation of the delay and Doppler suggested by S. Stein [15] presents the following formulation. Two noisy signals $y_1(t)$ and $y_2(t)$, observed over the interval $(0, T)$, are assumed to contain a common signal $x(t)$, appearing in $y_2(t)$ with a relative complex gain factor α, at a differential delay τ and with a frequency offset ν, all unknown. In complex envelope notation:

$$\begin{aligned} y_1(t) &= x(t) + n_1(t) \\ y_2(t) &= \alpha x(t+\tau) e^{2\pi j \nu (t+\tau)} + n_2(t) \end{aligned} \tag{1.1}$$

For spectrally flat noise, the ML suggested estimator is shown to be the maximum of the complex cross-ambiguity function.

$$R(\tau, \nu) = \left| \frac{1}{T} \int e^{-2\pi j f \tau} Y_1^*(f-\nu) Y_2(f) df \right| \tag{1.2}$$

Or in the time domain:

$$R(\tau, \nu) = \left| \frac{1}{T} \int e^{-2\pi j \nu (t+\tau)} y_1^*(t+\tau) y_2(t) dt \right| \tag{1.3}$$

And in the discrete time domain:

$$R(\tau, \nu) = \left| \frac{1}{N} \sum_{n=0}^{N-1} e^{-2\pi j \nu t_{n+m}} y_1^*[n+m] y_2[n] \right| \tag{1.4}$$

Where $m = \lfloor \tau F_s \rfloor$ is the discrete time delay, N is the number of samples in the interval, $t_{n+m} = \frac{1}{F_s}(n+m)$ and F_s is the sampling frequency.

1.1.2 TOA and TDOA Based Passive Geolocation

In this subsection we discuss the methods to geolocate a transmitter using TOA and TDOA measurements.

Assuming that the TOA of the Signal-Of-Interest(SOI) to a receiver is known, the transmitter is known to be located on a circle around the receiver.
Adding another receiver will limit the location of the transmitter to two possible points of intersection, that using additional a-priori information about the location of the transmitter can reduce the estimation to a single position. An example for the TOA scenario can be seen in figure (1.1): Two stationary receivers are located in (-300,0) and (300,0). The estimated TOA for each receiver forms a circle of possible transmitter locations around each receiver. The two circles intersect at two points that are the two possible transmitter locations. Using a-priori information regarding the position of the transmitter, the two possible transmitter positions can be reduced to a single estimated position. In the case that additional receivers are added, the spheres will not intersect in one point because of noise and errors that cause estimation errors of the TOA, and the need to use estimation methods arises.

TOA methods for passive geolocation are seldom used, because in order to measure the TOA, each receiver needs to know the exact time when the signal was transmitted, which is usually unknown. Therefore, the more common methods use the TDOA measurements between pairs of receivers.

In TDOA based methods, each TDOA measurement locates the transmitter on a hyperbola of possible transmitter locations. At least another TDOA measurement is necessary in order to locate the transmitter at several points of intersection of the two hyperbolas. Using a-priori information about the transmitter location the several possible points can be reduced to a single solution. Again, as additional receivers are added, the hyperboloids will not intersect in one point because of noisy measurements and errors, and the need to use estimation methods arises. Chan and Ho [17] suggested a simple and efficient estimator for hyperbolic location systems, and Chestnut [18] suggested a method for estimating the position of a stationary transmitter based on TDOA measurements and analysed its performance.

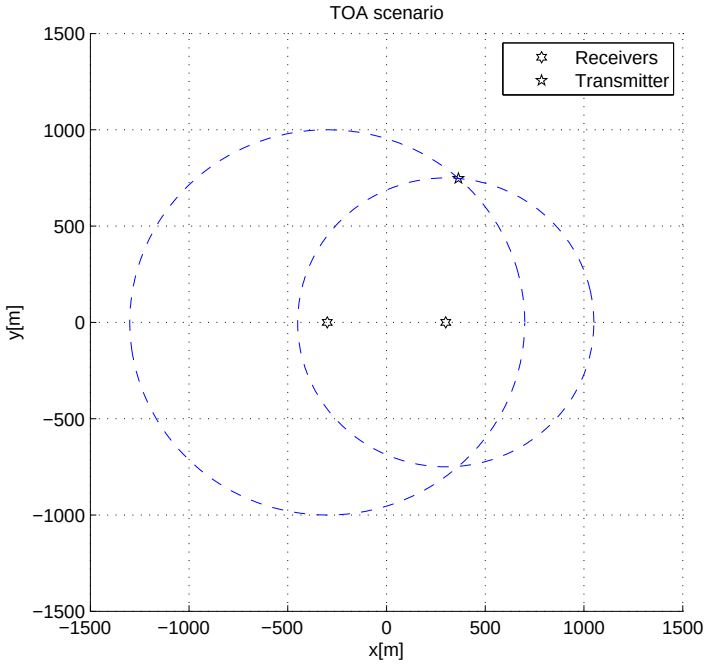

FIGURE 1.1: TOA Scenario. Two stationary receivers are located in (-300,0) and (300,0). The estimated TOA for each receiver forms a circle of possible transmitter locations around each receiver. The two circles intersect at two points that are the two possible transmitter locations. Using a-priori information regarding the position of the transmitter, the two possible transmitter positions can be reduced to a single estimated position.

Figure (1.2) shows an example of the TDOA based scenario: Two receivers are located at (-300,0) and (300,0). The TDOA measurement of this pair of receivers forms a hyperbola of possible transmitter positions. At least one more receiver is necessary in order to determine the position the transmitter.

It is interesting to mention that the TDOA estimated in a single interval contains no information regarding the velocity of the transmitter. Thus, the velocity of the transmitter cannot be estimated using the TDOA measurements.

There are many suggested methods for estimating the position of a transmitter based on TDOA measurements. We will shortly introduce the application of the Weighted-Least-Squares(WLS) method, because of its relative simplicity, and only to acquire some intuition.

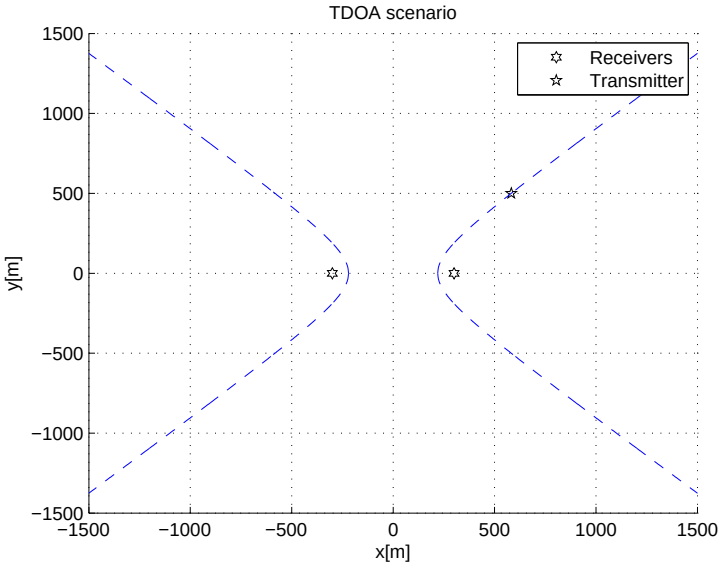

FIGURE 1.2: TDOA Scenario. Two receivers are located at (-300,0) and (300,0). The TDOA measurement of this pair of receivers forms a hyperbola of possible transmitter positions. At least one more receiver is necessary in order to determine the position the transmitter.

In the first step of the method introduced, the difference in the time-of-arrival is estimated for every pair of receivers, so that the matrix $\hat{\mathbf{T}}$ is estimated. The i,j-th element of the matrix $\hat{\mathbf{T}}$ is the time-of-arrival difference between the i-th and the j-th receivers.

For the transmitter position $\vec{p}$, and receivers positions $\vec{p_\ell}$, the expected $\mathbf{T}(\tilde{\mathbf{p}})$ matrix can be calculated:

$$T(\vec{p})_{i,j} = \frac{1}{C}\|\vec{p_i} - \vec{p}\| - \frac{1}{C}\|\vec{p_j} - \vec{p}\| \tag{1.5}$$

The i,j-th element of $\mathbf{T}(\tilde{\mathbf{p}})$ is the expected TDOA between the i-th and the j-th receivers, if the transmitter position is $\vec{p}$.

A WLS TDOA cost function can then be defined as:

$$C_{\text{TDOA}}(\vec{p}) = \sum_{i=1}^{L}\sum_{j=1}^{L} w_{i,j}(T(\vec{p})_{i,j} - \hat{T}_{i,j})^2 \tag{1.6}$$

Where $w_{i,j}$ is the i,j-th element of the weights matrix W.

The WLS estimator for the position is the position $\hat{\vec{p}}$ for which the value of the WLS cost function is minimal. Therefore:

$$\hat{\vec{p}} = \text{argmin}_{\vec{p}} C_{\text{TDOA}}(\vec{p}) \tag{1.7}$$

The Known-Signals FIM related to the TOA estimation of the ℓ-th signal is:

$$\text{FIM}_{\ell,\ell} = \frac{2}{\sigma_\ell^2} \left\| \frac{\partial \mathbf{m}_\ell}{\partial T_\ell} \right\|^2 \tag{1.8}$$

Where we assumed that the noise in the receivers is Gaussian i.i.d, independent between the receivers, with variance σ_ℓ^2 in each receiver. The data vector $\mathbf{m}_\ell$ is the time shifted known signal, as was received in the ℓ-th receiver if there was no noise.
Because $\mathbf{m_l}$ depends only on the time delay of the ℓ-th receiver, the FIM is diagonal. Thus:

$$\text{CRB}_\ell = \frac{\sigma_\ell^2}{2 \left\| \frac{\partial \mathbf{m}_\ell}{\partial T_\ell} \right\|^2} \tag{1.9}$$

So that:

$$\text{VAR}(\text{TOA}_\ell) \geq \frac{\sigma_\ell^2}{2 \left\| \frac{\partial \mathbf{m}_\ell}{\partial T_\ell} \right\|^2} \tag{1.10}$$

Assuming that the TOA measurements were taken using an efficient estimator, the CRB can be used to determine the weights matrix W.

1.1.3 FOA and FDOA Based Passive Geolocation

In the following subsection we discuss the methods to geolocate a transmitter using FOA and FDOA based methods.

When the transmitter is moving with a relative radial velocity to the receiver, a frequency shift of the transmitted signal is caused due to the Doppler effect.
Similarly to the TDOA based methods, the exact original transmitted frequency is usually unknown, and requires measurement of the FDOA between each pair of receivers.

The methods that use these measurements are sometimes also referred to as DD.

FOA and FDOA measurements contain information on both the position and velocity of the transmitter, unlike TDOA measurements that only contain information about the position of the transmitter.
Nevertheless, in order to acquire the FDOA measurements, a relative motion of the transmitter and the receivers is necessary, limiting the scenarios applicable for this method.

A simple, intuitive geometrical interpretation of the FDOA estimation methods is less direct, but is possible if we make a few assumptions and limit the discussion to simple scenarios. We present here two simple examples: Positioning of a stationary transmitter, transmitting a known frequency, using a moving receiver, and positioning of a stationary transmitter, transmitting an unknown frequency, using 2 moving receivers.

We start by describing the known transmitted frequency scenario: Consider a scenario in which the transmitter is stationary and a receiver is moving in a constant known velocity $\vec{v}$, transmitting a signal with a known frequency. The Doppler frequency shift will be proportional to the carrier frequency F_c and to the relative radial velocity $\|\vec{v}\|cos\theta$, where θ is the angle between the velocity and the line connecting the transmitter and the receiver, as can be seen in figure (1.3). Because the transmitted frequency is known, the Doppler shift can be easily estimated. Since $\vec{v}$ and F_c are known, $cos\theta$ can be estimated from the estimated Doppler shift, and 2 lines on which the transmitter is located are defined.
Additional receivers create additional lines that the transmitter lies in their spatial intersection.

In the case where the transmitted frequency is unknown, the Doppler shift cannot be estimated directly, and only the FDOA between pairs of receivers can be estimated. Figure (1.4) describes a scenario in which two receivers are moving in velocities $\vec{v_1}$ and $\vec{v_2}$, forming the angles θ_1 and θ_2 with the lines connecting their position and the position

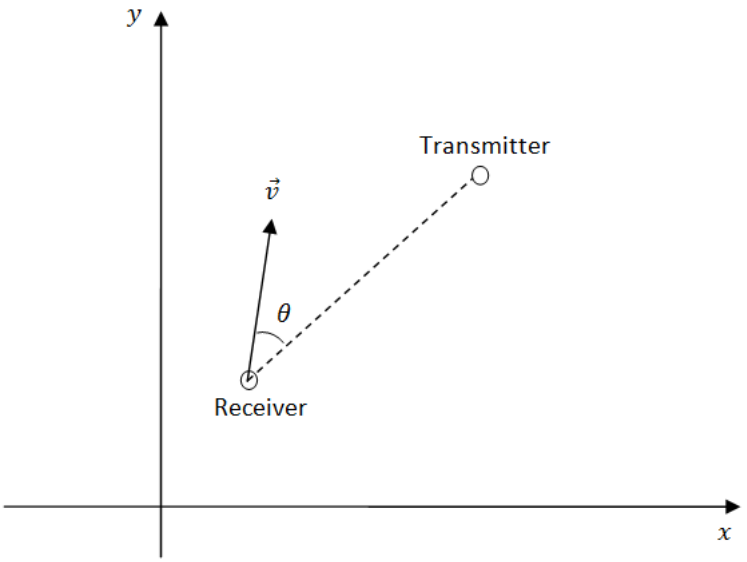

FIGURE 1.3: FOA based geolocation scenario. A receiver is moving at velocity $\vec{v}$, forming an angle θ with the line connecting the positions of the receiver and the transmitter.

of the transmitter. The lines connecting the position of the receivers and the position of the transmitter form the angles α_1 and α_2 with the x-axis. The FDOA between the two receivers is denoted by $\Delta f_{1,2}$.

We define the difference between the radial velocity of the receivers in relation to the transmitter by $\Delta v_{r,1,2}$ as follows:

$$\Delta v_{r,1,2} \triangleq \|\vec{v_1}\|\cos\theta_1 - \|\vec{v_2}\|\cos\theta_2 \tag{1.11}$$

And then $\Delta f_{1,2}$ can be expressed as:

$$\Delta f_{1,2} = \frac{F_c}{c}\Delta v_{r,1,2} \tag{1.12}$$

Assuming that θ_2 is known, by rearranging equation (1.11):

$$\cos\theta_1 = \frac{\Delta v_{r,1,2} + \|\vec{v_2}\|\cos\theta_2}{\|\vec{v_1}\|} \tag{1.13}$$

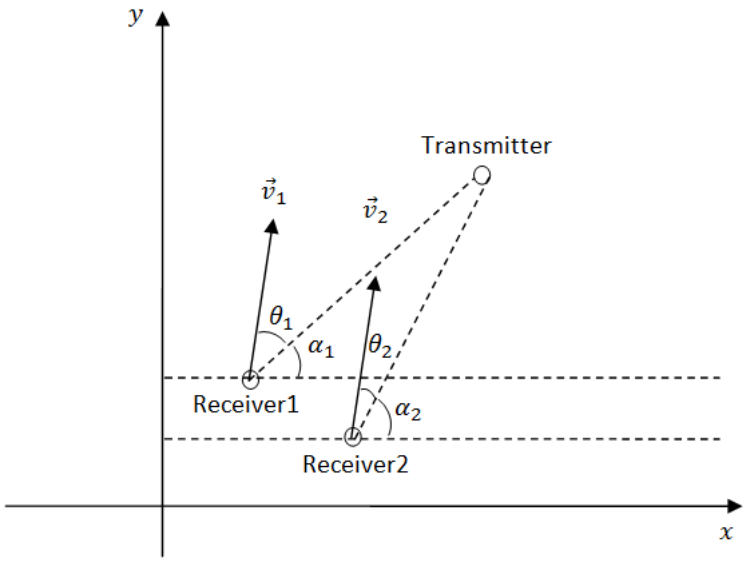

FIGURE 1.4: FDOA based geolocation scenario. Two receivers are moving in velocities $\vec{v_1}$ and $\vec{v_2}$, forming the angles θ_1 and θ_2 with the lines connecting their position and the position of the transmitter. The lines connecting the position of the receivers and the position of the transmitter form the angles α_1 and α_2 with the x-axis.

By rearranging equation (1.12) and substituting into (1.13) we get:

$$\cos\theta_1 = \frac{\frac{c}{F_c}\Delta f_{1,2} + \|\vec{v_2}\|\cos\theta_2}{\|\vec{v_1}\|} \tag{1.14}$$

And so θ_1 can be expressed as a function of θ_2:

$$\theta_1(\theta_2) = \arccos\frac{\frac{c}{F_c}\Delta f_{1,2} + \|\vec{v_2}\|\cos\theta_2}{\|\vec{v_1}\|} \tag{1.15}$$

Equation (1.15) above describes a constant FDOA curve. The curve is defined by the known receiver velocities, and by the estimated FDOA. Every point on the curve is a possible transmitter position. Adding another receiver creates two more constant FDOA curves that the receiver lies in their intersection.

Figure (1.5) shows an example of a constant FDOA curve. Two receivers are located at $(-300, 0)$ and $(300, 0)$ and moving with a $10[m/s]$ velocity in the positive x-axis direction, and the transmitter is located at $(1000, 500)$.

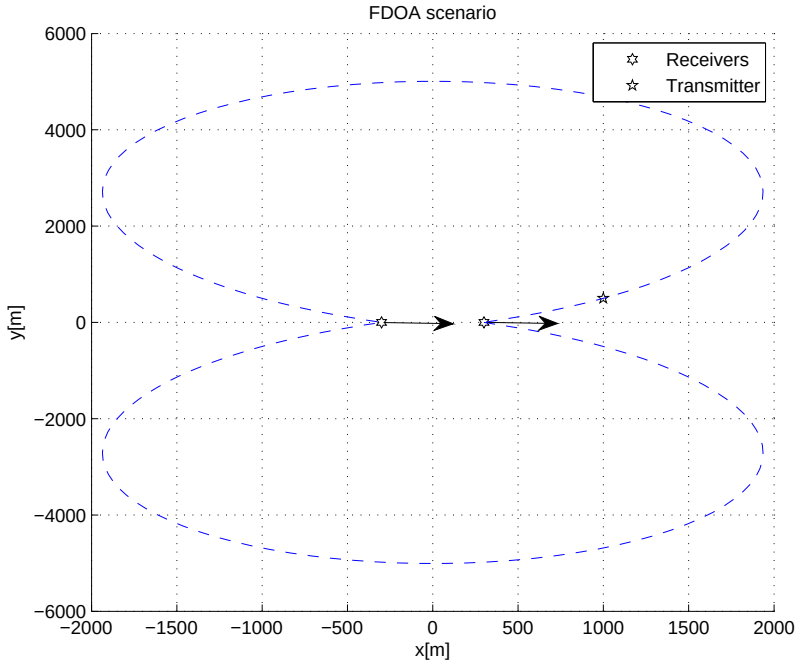

FIGURE 1.5: Constant FDOA curve example. Two receivers are located at $(-300, 0)$ and $(300, 0)$, moving with a $10[m/s]$ velocity in the positive x-axis direction. The transmitter is located at $(1000, 500)$.

Just in order to acquire some understanding of FDOA based geolocation methods, we introduce a simple WLS estimation method.

In the first step of the method introduced, the difference in the frequency-of-arrival is estimated for every pair of receivers, so that the matrix $\hat{F}$ is estimated. The i, j-th element of the matrix $\hat{F}$ is the frequency-of-arrival difference between the i-th and the j-th receiver.

For transmitter position and velocity $(\vec{p}, \vec{v})$, the expected $F(\vec{p}, \vec{v})$ matrix can be calculated:

$$F(\vec{p}, \vec{v})_{i,j} = -\frac{F_c}{c}\frac{(\vec{v} - \vec{v_i})(\vec{p} - \vec{p_i})}{|\vec{p} - \vec{p_i}|} + \frac{F_c}{c}\frac{(\vec{v} - \vec{v_j})(\vec{p} - \vec{p_j})}{|\vec{p} - \vec{p_j}|} \tag{1.16}$$

Where F_c is the carrier frequency of the signal, c is the propagation speed of the signal, $\vec{v}$ is the velocity of the transmitter and $\vec{v_i}$ is the velocity of the i-th receiver.

A WLS cost function can then be defined as:

$$C_{\text{FDOA}}(\vec{p},\vec{v}) = \sum_{i=1}^{L}\sum_{j=1}^{L} w_{i,j}(F(\vec{p},\vec{v})_{i,j} - \hat{F}_{i,j})^2 \tag{1.17}$$

Where $w_{i,j}$ is the i,j-th element of the weight matrix W. The WLS estimator for the position and velocity of the transmitter is the position and velocity that minimize the cost function:

$$(\hat{\vec{p}},\hat{\vec{v}}) = \text{argmin}_{(\vec{p},\vec{v})} C_{\text{FDOA}}(\vec{p},\vec{v}) \tag{1.18}$$

As opposed to the TDOA estimator, we can see that the FDOA estimate depends both on the position and on the velocity of the transmitter. Thus, both the position and velocity of the transmitter can be estimated using the FDOA measurements.

The Known-Signals Fischer information matrix related to the FDOA estimation of the ℓ-th signal is:

$$\text{FIM}_\ell = \frac{2}{\sigma_\ell^2}\left\|\frac{\partial \mathbf{m}_\ell}{\partial f_\ell}\right\|^2 \tag{1.19}$$

Where f_ℓ is the frequency shift caused by the Doppler effect. We used the assumption that the noise in the receivers is Gaussian i.i.d, independent between the receivers, with variance σ_ℓ^2 in each receiver. The data vector $\mathbf{m}_\ell$ is the frequency shifted known signal, as was received in the ℓ-th receiver if there was no noise.
Because $\mathbf{m_l}$ depends only on the frequency shift of the ℓ-th receiver, the FIM is diagonal. Thus:

$$\text{VAR}(\text{FOA}_\ell) \geq \text{CRB}_\ell = \frac{\sigma_\ell^2}{2\left\|\frac{\partial \mathbf{m}_\ell}{\partial f_\ell}\right\|^2} \tag{1.20}$$

Assuming that the FDOA measurements were taken using an efficient estimator, the CRB can be used to determine the weights matrix W.

1.1.4 TDOA-FDOA Based Passive Geolocation

We can easily combine the two methods suggested above using the weighted least squares (WLS) method. If we assume that the TDOA and FDOA estimations were performed by an efficient estimator, we can use the calculated CRB for TDOA and FDOA to define the weight matrices W_T and W_F for the TDOA measurements and for the FDOA measurements respectively. Then, the measurements can be combined in the following cost function:

$$C_{TF}(\vec{p},\vec{v}) = \sum_{i=1}^{L}\sum_{j=1}^{L} w_{T\,i,j}(T(\vec{p})_{i,j} - \hat{T}_{i,j})^2 + w_{F\,i,j}(F(\vec{p},\vec{v})_{i,j} - \hat{F}_{i,j})^2 \tag{1.21}$$

Where $w_{T\,i,j}$ and $w_{F\,i,j}$ are the i,j-th elments of the TDOA and FDOA weight matrices respectively. The estimated position and velocity are the position and velocity that minimize the cost function:

$$(\hat{\vec{p}},\hat{\vec{v}}) = \text{argmin}_{(\vec{p},\vec{v})} C_{TF}(\vec{p},\vec{v}) \tag{1.22}$$

1.2 DPD Algorithm Concepts

In this section we introduce the main ideas and concepts behind the DPD algorithm [11].

Most common methods consist of two steps. The first step is to estimate a certain parameter of the SOI, such as TDOA or FDOA.

The second step is to use the parameter estimated at each of the receivers, or receivers pairs, to estimate the location of the transmitter.

It is important to note that the estimation of the SOI parameters is done independently in each receiver or pair of receivers, so that the information used in each of the estimations is partial, consists only on the samples collected by its own antennas and does not

take into consideration that all of the received signals have a common origin.
The DPD algorithm uses exactly the same data used in conventional methods, but it skips the first step of parameter estimation. All of the samples are collected at a central base station, and the location of the transmitter is estimated using all of the samples at once, without making any intermediate estimations.

The DPD algorithm advantages are mainly better performance over conventional methods using the same data and conceptual simplicity. The DPD algorithm main drawbacks are its computational complexity and the need for high band-width communication between the receivers and the central processing station in order to transfer the entire sampled signals from the receivers to the processing station.

The original DPD algorithm[11] has been developed in recent years, and is now related to a family of algorithms, each of which related to a different scenario. The original DPD algorithm [11] assume a static scenario, in which both the transmitters and the receivers are stationary. The algorithm uses the time delays and the sensors spatial response function in order to locate multiple radio transmitters.

In [13] a direct algorithm for the location a stationary narrow-band transmitter using an array of moving receivers is presented. The algorithm assumes that the signal is narrow band, so that the envelope of the received signal is identical in all of the receivers. The different Doppler shifts observed by the receivers are used in order to localize the transmitter. A likelihood cost function is derived, and grid-search is suggested in order to find the maximum-likelihood estimation.

In [14] the direct algorithm is extended for locating a stationary wide-band transmitter using an array of moving receivers. This algorithm takes advantage on both the different Doppler shifts and time-delays observed by the different receivers.

All of the direct methods suggested above show better performance than conventional methods using the same data. The direct methods show better performance especially in low-SNR scenarios.

In this work, we present a direct passive location algorithm for a moving transmitter using a stationary array of receivers.

1.3 Outline

- **Chapter 1** (this chapter) consists of an introduction to this work and of a literature survey.
- **Chapter 2** presents the problem formulation and the derived ML estimator. The chapter handles the scenarios in which the transmitted signal is known or unknown, wide-band or narrow-band.
- **Chapter 3** explores the characteristics of the known-signals cost function L_2. The function is explored in order to acquire some intuition on its behaviour, and its derivatives are developed in order to be used by gradient-based search methods.
- **Chpater 4** suggests several possible location algorithms for different scenarios. Grid search algorithms and gradient-based algorithms are suggested. For the scenario in which the transmitter is tracked, a Kalman-filter based approach is suggested.
- **Chapter 5** develops the known-signals Cramer-Rao lower bound of the problem.
- **Chapter 6** presents the simulation results of several different scenarios. The results of the suggested algorithm are compared to the Cramer-Rao lower bound, and to conventional methods.

Chapter 2

Problem Formulation

2.1 General

Consider L stationary radio receivers and a moving transmitter. The receivers are synchronized in frequency and time. Let $\vec{p_\ell}$ $l \in \{1..L\}$ denote the positions of the stationary receivers. Let $\vec{v} = (v_x, v_y)$, $\vec{p} = (x, y)$ denote the velocity and position of the moving transmitter respectively, as can be seen in figure (2.1).

The complex signal observed by the l-th receiver at time t:

$$r_\ell(t) = b_\ell s(t - T_\ell) e^{j2\pi \tilde{f}_\ell t} + w_\ell(t), 0 \leq t \leq T \tag{2.1}$$

Where T is the observation time interval, $s(t)$ is the observed signal envelope, b_ℓ is an unknown complex path attenuation, $T_\ell \triangleq \frac{1}{c}\|\vec{p} - \vec{p_\ell}\|$ is the signal's delay where c is the signal's propagation speed, $w_\ell(t)$ is a wide sense stationary additive white zero mean complex Gaussian noise with flat spectrum and $\tilde{f}_\ell$ is given by:

The frequency received at the ℓ - th receiver:

$$\tilde{f}_\ell \triangleq [f_c + \nu][1 + \mu_\ell(\vec{p}, \vec{v})] \tag{2.2}$$

The frequency shift caused by the Doppler Effect:

$$\mu_\ell \triangleq -\frac{1}{c}\frac{\vec{v}(\vec{p}-\vec{p_\ell})}{\|\vec{p}-\vec{p_\ell}\|} \tag{2.3}$$

Where f_c is the known nominal carrier frequency of the transmitted signal, and ν is the unknown transmitted frequency shift due to the source instability during the interception interval. Since $\mu_\ell \ll 1$ and $\nu \ll f_c$, equation (2.2) can be approximated as $\tilde{f}_\ell \approx \nu + f_c[1+\mu_\ell(\vec{p},\vec{v})]$ where the term $\nu\mu_\ell(\vec{p},\vec{v})$, which is negligible with respect to all other terms, is omitted . Also, since f_c Is known to the receivers, each receiver performs a down conversion of the intercepted signal by f_c and (2.2) can be replaced by:

$$\tilde{f}_\ell \approx \nu + f_\ell(\vec{p},\vec{v}) \tag{2.4}$$

Where we defined the frequency shift caused by the Doppler effect f_ℓ as follows:

$$f_\ell(\vec{p},\vec{v}) \triangleq f_c\mu_\ell(\vec{p},\vec{v}) \tag{2.5}$$

2.2 Narrow-Band Time Domain Analysis

In the proceeding section we analyse the narrow-band signal scenario. In the narrow-band scenario we assume that the change rate of the envelope of the transmitted signal is sufficiently small, so that the signal envelopes seen in all of the receivers is identical.

The narrow-band scenario analysis is brought here because of its slight relative simplicity compared to the wide-band scenario, and because we use this formulation later in this work to derive lower complexity methods to solve the problem presented.

We start by introducing the assumptions and definitions of the narrow-band scenario and later introduce the ML estimator for the narrow-band scenario.

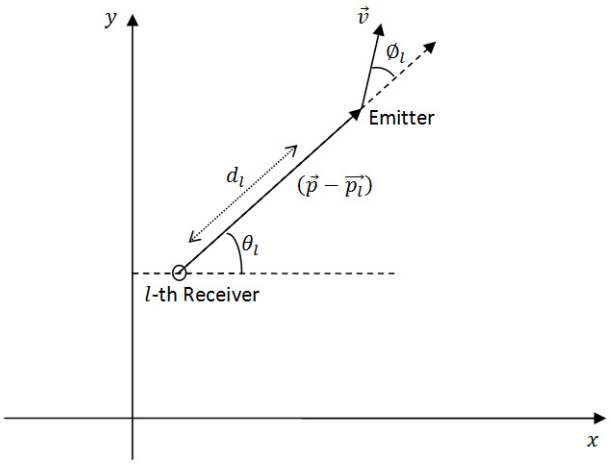

FIGURE 2.1: Scenario Geometry. $\vec{p}$ and $\vec{v}$ denote the transmitter's position and velocity respectively. $\vec{p_\ell}$ is the position of the ℓ-th receiver. d_ℓ is the distance between the transmitter and the ℓ-th receiver. Θ_ℓ is the angle between the line connecting the transmitter and the ℓ-th receiver and the x-axis. ϕ_ℓ is the angle between the transmitter's velocity and the line connecting the transmitter and the ℓ-th receiver

2.2.1 Definitions

We assume that the signal's bandwidth (change rate) is small compared to the inverse of the propagation time between the receivers. i.e. $B < c/d$, where d is a typical distance between the receivers. We can then assume that the signal's envelope is similar at all of the spatially separated receivers, meaning: $s(t - T_\ell) \approx s(t)$.

The down converted signal is sampled at times $t_n = nT_s$ where $n \in \{0..N-1\}$ and $T_s = \frac{T}{N-1}$. The signal at the interception interval is given as $r_\ell[n] = r_\ell(nT_s)$, and equation (2.1) can be written in a vector form as:

$$\mathbf{r}_\ell = b_\ell \mathbf{A}_\ell \mathbf{C}\mathbf{s} + \mathbf{w}_\ell \tag{2.6}$$

Where:

$$\mathbf{A}_\ell \triangleq diag\{1, e^{2\pi j f_\ell T_s}, \ldots, e^{2\pi j f_\ell (N-1) T_s}\} \tag{2.7}$$

$\mathbf{A}_\ell$ is a frequency shift operator, shifting the signal by the Doppler frequency shift related to the ℓ-th receiver f_ℓ.

$$\mathbf{C} \triangleq diag\{1, e^{2\pi j \nu T_s}, \ldots, e^{2\pi j \nu (N-1) T_s}\} \tag{2.8}$$

$\mathbf{C}$ is a frequency shift operator, shifting the signal by the unknown frequency shift caused by the transmitter instability ν.

$$s[n] \triangleq s(nT_s) \tag{2.9}$$

$s[n]$ is the original transmitted signal sampled at discrete times nT_s.

$$w_\ell[n] \triangleq w_\ell(nT_s) \tag{2.10}$$

$w_\ell[n]$ is the noise observed by the ℓ-th receiver, sampled at times nT_s.

Note that $\mathbf{A}_\ell$ is a function of the unknown emitter position and velocity while $\mathbf{C}$ is a function of the unknown transmitted frequency. Here we assume that the signal's envelope is the same in all of the receivers.

2.2.2 ML Estimator

The log-likelihood function of the observation vectors is given (up to an additive constant) by:

$$L_1 = -\frac{1}{\sigma 2} \sum_{l=1}^{L} \|\mathbf{r}_\ell - b_\ell A_\ell C \mathbf{s}\|^2 \tag{2.11}$$

The path attenuation factors that maximize Eq. (2.11) are given by:

$$b_\ell = [(A_\ell C \mathbf{s})^H A_\ell C \mathbf{s}]^{-1} (A_\ell C \mathbf{s})^H \mathbf{r}_\ell = (A_\ell C \mathbf{s})^H \mathbf{r}_\ell \tag{2.12}$$

Where we assume, without loss of generality, that $\|s\|^2 = 1$ and use the special structure of A_ℓ and C.

Substitution of Eq. (2.12) into Eq. (2.11) yields:

$$L_1 = -\frac{1}{\sigma^2}[\sum_{l=1}^{L} \|\mathbf{r}_\ell\|^2 - \|(A_\ell C\mathbf{s})^H \mathbf{r}_\ell\|^2] \tag{2.13}$$

Since r_ℓ is independent of the parameters, then instead of maximizing Eq. (2.13), we can now maximize:

$$L_2 = \sum_{l=1}^{L} \|(A_\ell C\mathbf{s})^H \mathbf{r}_\ell\|^2 = \mathbf{u}^H Q\mathbf{u} \tag{2.14}$$

Where we defined:

$$\mathbf{u} \triangleq C\mathbf{s} \tag{2.15}$$

$$V \triangleq [A_1^H \mathbf{r_1}, \ldots, A_L^H \mathbf{r_L}] \tag{2.16}$$

$$Q \triangleq VV^H \tag{2.17}$$

If the original transmitted is known, L_2 can be used as the known-signals cost function. The maximum likelihood estimation of the position and velocity for the known signals scenario is the maximum of the L_2 cost function:

$$(\hat{\vec{p}}, \hat{\vec{v}}) = \text{argmax}_{(\vec{p},\vec{v})} L_2(\vec{p}, \vec{v}) \tag{2.18}$$

If the original signal is unknown, in order to maximize the cost function, $\mathbf{u}$ should be selected as the eigenvector corresponding to the largest eigenvalue of the matrix Q.

Therefore, the cost function L_2 reduces to

$$L_3 = \lambda_{max}\{Q\} \tag{2.19}$$

Notice that Q is a $N \times N$ Matrix. In certain applications N, which is the length of the sampled signals, can be quite large and finding the largest eigenvalue of a $N \times N$ matrix can create a high computational load. By using the known theorem that given a matrix X, the non zero eigenvalues of XX^H and X^HX are identical, we can replace the $N \times N$ matrix with a $L \times L$ matrix:

$$\tilde{Q} \triangleq V^H V \tag{2.20}$$

So that:

$$L_3 = \lambda_{max}\{Q\} = \lambda_{max}\{\tilde{Q}\} \tag{2.21}$$

The maximum likelihood estimation of the position and velocity for the unknown signals scenario is the maximum of the L_3 cost function:

$$(\hat{\vec{p}}, \hat{\vec{v}}) = \text{argmax}_{(\vec{p},\vec{v})} L_3(\vec{p}, \vec{v}) \tag{2.22}$$

Because the cost functions are non linear, deriving an explicit solution for the problem is not possible and employing various search methods is necessary in order to find its maximum.

2.3 Wide-Band Time Domain Analysis

In the following section we introduce the analysis of the scenario in which the signal is wide-band. Although we do not make any further simplifying assumptions, the problem formulation and ML estimator derivation is similar to the narrow-band scenario.

We start by introducing the assumptions and definitions of the wide-band scenario, and later derive the ML estimator for the wide-band scenario.

2.3.1 Definitions

The down converted signal is sampled at times $t_n = nT_s$ where $n \in \{0..N-1\}$ and $T_s = \frac{T}{N-1}$. The signal at the interception interval is given as $r_\ell[n] = r_\ell(nT_s)$, and equation (2.1) can be written in a vector form as:

$$\mathbf{r}_\ell = b_\ell A_\ell F_\ell C\mathbf{s} + \mathbf{w}_\ell \tag{2.23}$$

Where:

$$A_\ell \triangleq diag\{1, e^{2\pi j f_\ell T_s}, \ldots, e^{2\pi j f_\ell (N-1)T_s}\} \tag{2.24}$$

A_ℓ is a frequency shift operator, shifting the signal by the Doppler frequency shift related to the ℓ-th receiver f_ℓ.

$$C \triangleq diag\{1, e^{2\pi j \nu T_s}, \ldots, e^{2\pi j \nu (N-1)T_s}\} \tag{2.25}$$

C is a frequency shift operator, shifting the signal by the unknown frequency shift caused by the transmitter instability ν.

$$s[n] \triangleq s(nT_s) \tag{2.26}$$

$s[n]$ is the original transmitted signal sampled at discrete times nT_s.

$$w_\ell[n] \triangleq w_\ell(nT_s) \tag{2.27}$$

$w_\ell[n]$ is the noise observed by the ℓ-th receiver, sampled at times nT_s.

F_ℓ is a downshift operator. The product F_ℓ shifts the vector $\mathbf{s}$ by $\lfloor {}^{T_\ell}/_{T_s} \rfloor$ indices. Note that A_ℓ is a function of the unknown emitter position and velocity, F_ℓ is a function of the unknown emitter position, while C is a function of the unknown transmitted frequency.

2.3.2 ML estimator

The log-likelihood function of the observation vectors is given (up to an additive constant) by:

$$L_1 = -\frac{1}{\sigma 2}\sum_{l=1}^{L}\|\mathbf{r}_\ell - b_\ell A_\ell F_\ell C\mathbf{s}\|^2 \tag{2.28}$$

The path attenuation factors that maximize Eq. (2.28) are given by:

$$b_\ell = [(A_\ell F_\ell C\mathbf{s})^H A_\ell F_\ell C\mathbf{s}]^{-1}(A_\ell F_\ell C\mathbf{s})^H\mathbf{r}_\ell = (A_\ell F_\ell C\mathbf{s})^H\mathbf{r}_\ell \tag{2.29}$$

Where we assume, without loss of generality that $\|\mathbf{s}\|^2 = 1$ and use the special structure of A_ℓ and C. Substitution of Eq. (2.29) into Eq. (2.28) yields:

$$L_1 = -\frac{1}{\sigma^2}[\sum_{(l=1)}^{L}\|\mathbf{r}_\ell\|^2 - \|(A_\ell F_\ell C\mathbf{s})^H\mathbf{r}_\ell\|^2] \tag{2.30}$$

Since $\mathbf{r}_\ell$ is independent of the parameters, then instead of maximizing Eq. (2.30), we can now maximize:

$$L_2 = \sum_{(l=1)}^{L}\|(A_\ell F_\ell C\mathbf{s})^H\mathbf{r}_\ell\|^2 = \mathbf{u}^H Q\mathbf{u} \tag{2.31}$$

Where:

$$u \triangleq C\mathbf{s} \tag{2.32}$$

$$Q \triangleq VV^H \tag{2.33}$$

$$V \triangleq [F_1^H A_1^H\mathbf{r_1}, \ldots, F_L^H A_L^H\mathbf{r_L}] \tag{2.34}$$

If the original transmitted is known, L_2 can be used as the wide-band known-signals cost function. The maximum likelihood estimation of the position and velocity for the known signals scenario is the maximum of the L_2 cost function:

$$(\hat{\vec{p}}, \hat{\vec{v}}) = \text{argmax}_{(\vec{p},\vec{v})} L_2(\vec{p}, \vec{v}) \tag{2.35}$$

If the original signal is unknown, in order to maximize the cost function, **u** should be selected as the eigenvector corresponding to the largest eigenvalue of the matrix Q.

Therefore, the cost function L_2 reduces to

$$L_3 = \lambda_{max}\{Q\} \tag{2.36}$$

Notice that Q is a $N \times N$ Matrix. In certain applications N, which is the length of the sampled signals, can be quite large and finding the largest eigenvalue of a $N \times N$ matrix can create a high computational load. By using the known theorem that given a matrix X, the non zero eigenvalues of XX^H and X^HX are identical, we can replace the $N \times N$ matrix with an $L \times L$ matrix.

$$\tilde{Q} \triangleq V^H V \tag{2.37}$$

So that:

$$L_3 = \lambda_{max}\{Q\} = \lambda_{max}\{\tilde{Q}\} \tag{2.38}$$

The maximum likelihood estimation of the position and velocity for the unknown signals scenario is the maximum of the L_3 cost function:

$$(\hat{\vec{p}}, \hat{\vec{v}}) = \text{argmax}_{(\vec{p},\vec{v})} L_3(\vec{p}, \vec{v}) \tag{2.39}$$

Because the cost functions are non linear, deriving an explicit solution for the problem is not possible and employing various search methods is necessary in order to find its maximum.

Section (6.5) presents several simulation results that demonstrate the behaviour of the cost function for various scenarios and for various signals. The simulation results provide some understanding on the behaviour of the cost function and its complexities, and could provide some intuition to the discussed problem.

Chapter 3

Exploring the cost function L_2

In this section, we will try to analyse the cost function L_2, in order to get some insight about its behaviour. We will also develop the derivatives of $L2$ by the position and velocity in order to use them in gradient based search methods for finding its maximum. Because L_2 requires the knowledge of the transmitted signal, it is mainly useful for the case in which the transmitted signal is known.

It is important to remember that given a received signal, L_2 is a function of the evaluated transmitter's position and velocity estimates, meaning $L_2(\vec{p}, \vec{v})$. The dependency of the cost function in these parameters is expressed by A_ℓ that depends on the relative speed and position between the transmitter and the receiver, and by F_ℓ that depends on the relative distance between the transmitter and the receiver.

3.1 Zero Noise Analysis - Simplified Scenario

In order to simplify the analysis, we will use a few assumptions in the proceeding subsection. We will assume that $b_\ell = 1 \ \forall l \in \{1 \dots L\}$, that there is no source instability, meaning $\nu = 0$ so that $C = I$,and that the signal is narrow-band, meaning $F_\ell = I$ $\forall l \in \{1 \dots L\}$.

Remembering that (from (2.23)):

$$\mathbf{r}_\ell = b_\ell A_\ell F_\ell C\mathbf{s} + \mathbf{w}_\ell$$

We can write:

$$\mathbf{r}_\ell = A_\ell^{(0)}\mathbf{s} \tag{3.1}$$

Where we used the assumptions that $b_\ell = 1$, $C = I$, $F_\ell = I$, $\mathbf{w}_\ell = 0$. $A_\ell^{(0)}$, represents the true Doppler frequency shift caused by the relative speed of the transmitter and the emitters.

Thus:

$$(A_\ell\mathbf{s})^H\mathbf{r}_\ell = (A_\ell\mathbf{s})^H(A_\ell^{(0)}\mathbf{s}) \tag{3.2}$$

Therefore:

$$\|(A_\ell\mathbf{s})^H\mathbf{r}_\ell\|^2 = \|(A_\ell\mathbf{s})^H(A_\ell^{(0)}\mathbf{s})\|^2 = \|\mathbf{s}^H A_\ell^H A_\ell^{(0)}\mathbf{s}\|^2 \tag{3.3}$$

Defining:

$$D_\ell = A_\ell^H A_\ell^{(0)} \tag{3.4}$$

Where D_ℓ is a frequency shift operator, shifting the signal by $f_\ell^{(0)} - f_\ell$ where $f_\ell^{(0)}$ is the true Doppler shift of the signal received by the ℓ-th receiver and f_ℓ is the expected doppler shift for a transmitter in the evaluated position and velocity $(\vec{p}, \vec{v})$.
We can see that:

$$\|(A_\ell\mathbf{s})^H\mathbf{r}_\ell\|^2 = \|\mathbf{s}^H D_\ell\mathbf{s}\|^2 \tag{3.5}$$

Which is the squared absolute value of the correlation between the signal shifted by $f_\ell^{(0)} - f_\ell$ and the original signal.

$$L_2 = \sum_{l=1}^{L} \|(A_\ell \mathbf{s})^H \mathbf{r}_\ell\|^2 = \sum_{l=1}^{L} \|\mathbf{s}^H D_\ell \mathbf{s}\|^2 \tag{3.6}$$

Which is the sum of squared absolute value of the correlation between the signal shifted by $f_\ell^{(0)} - f_\ell$ and the original signal. We can easily see that the maximum of the simplified L_2 function will occur when $\forall l \in \{1 \dots L\}$, $\mathbf{D}_\ell = I$, meaning that $\forall l \in \{1 \dots L\}$, $f_\ell = f_\ell^{(0)}$. Notice that if the location of the receivers is known with infinite accuracy, the maximum of the simplified cost function L_2 occurs at the true position of the transmitter.

If the there is an error in the known position of the receivers, there might not be a transmitter position and velocity $(\vec{p}, \vec{v})$ for which $\forall l \in \{1 \dots L\}$, $\mathbf{D}_\ell(\vec{p}, \vec{v}) = I$ and there is no guarantee that the maximum of the cost function occurs at the true transmitter position. We can notice that for the simplified scenario $\mathbf{D}_\ell(\vec{p}, \vec{v})$ is actually a function of $(\|\vec{v}\| cos\phi_\ell)$, and it can be written as $\mathbf{D}_\ell(\|\vec{v}\| cos\phi_\ell)$.

3.2 Noisy Analysis - Simplified Scenario

In this subsection we will try to analyse the effect of the noise in the receiver on the cost function.

If we consider the noise, we can write:

$$\mathbf{r}_\ell = A_\ell^{(0)} \mathbf{s} + \mathbf{w}_\ell$$

Then (3.2) becomes:

$$(A_\ell \mathbf{s})^H \mathbf{r}_\ell = (A_\ell \mathbf{s})^H (A_\ell^{(0)} \mathbf{s} + \mathbf{w}_\ell) = \mathbf{s}^H D_\ell \mathbf{s} + \mathbf{s}^H A_\ell^H \mathbf{w}_\ell \tag{3.7}$$

So:

$$
\begin{aligned}
L_2^{(\ell)} = & \qquad (3.8)\\
&= \|(A_\ell \mathbf{s})^H \mathbf{r}_\ell\|^2 = \\
&= \|\mathbf{s}^H D_\ell \mathbf{s}\|^2 + \|\mathbf{s}^H A_\ell^H \mathbf{w}_\ell\|^2 + \mathbf{s}^H D_\ell \mathbf{s} (\mathbf{s}^H A_\ell^H \mathbf{w}_\ell)^H + \mathbf{s}^H A_\ell^H \mathbf{w}_\ell (\mathbf{s}^H D_\ell \mathbf{s})^H = \\
&= \|\mathbf{s}^H D_\ell \mathbf{s}\|^2 + \|\mathbf{s}^H A_\ell^H \mathbf{w}_\ell\|^2 + \mathbf{s}^H D_\ell \mathbf{s} \mathbf{w}_\ell{}^H A_\ell \mathbf{s} + \mathbf{s}^H A_\ell^H \mathbf{w}_\ell \mathbf{s}^H D_\ell^H \mathbf{s}
\end{aligned}
$$

Because $\mathbf{w}_\ell$ is stochastic, L_2 is also a stochastic variable and we can look at its stochastic properties such as expectation and variance.

$$
\begin{aligned}
\|\mathbf{s}^H A_\ell^H \mathbf{w}_\ell\|^2 = & \qquad (3.9)\\
&= \| \sum_{m=1}^{N} s[m]^H a_\ell^H[m] w_\ell[m] \|^2 = \\
&= \sum_{m=1}^{N} \sum_{n=1}^{N} s[m]^H s[n] a_\ell^H[m] a_\ell[n] w_\ell[m] w_\ell^H[n]
\end{aligned}
$$

Where we denoted $a_\ell[n]$ as the n-th element on the diagonal of A_ℓ and used the diagonal property of A_ℓ.

Taking the expectation of the above expression we get:

$$
\begin{aligned}
E\{\|\mathbf{s}^H A_\ell^H \mathbf{w}_\ell\|^2\} = & \qquad (3.10)\\
&= E\left\{ \sum_{m=1}^{N} \sum_{n=1}^{N} s[m]^H s[n] a_\ell^H[m] a_\ell[n] w_\ell[m] w_\ell^H[n] \right\} = \\
&= \sum_{m=1}^{N} \sigma_\ell^2 |a_\ell[m]|^2 |s[m]|^2 = \\
&= \sigma_\ell^2 \|\mathbf{s}\|^2
\end{aligned}
$$

By taking the expectation of (3.8) and substituting the result from (3.10)):

$$
E\{L_2^{(\ell)}\} = E\{\|(A_\ell \mathbf{s})^H \mathbf{r}_\ell\|^2\} = \|\mathbf{s}^H D_\ell \mathbf{s}\|^2 + \sigma_\ell^2 \|\mathbf{s}\|^2 \qquad (3.11)
$$

Where we used the assumptions that $\mathbf{w}_\ell$ is a zero mean, i.i.d process with σ_ℓ^2 variance.

Thus:

$$\begin{aligned} E\{L_2\} &= E\{\sum_{\ell=1}^{L} L_2^{(\ell)}\} = \\ &= \sum_{\ell=1}^{L} E\{\|(A_\ell \mathbf{s})^H \mathbf{r}_\ell\|^2\} = \sum_{\ell=1}^{L} \|\mathbf{s}^H D_\ell \mathbf{s}\|^2 + \sum_{\ell=1}^{L} \sigma_\ell^2 \|\mathbf{s}\|^2 \end{aligned} \tag{3.12}$$

From the above result we learn that adding noise affects the expectation of the cost function by adding a constant to the cost function, that does not depend on the geometry. Thus, the maximum of the expectation of the cost function is at the same position and velocity as the cost function without any noise.

$$\begin{aligned} VAR\{L_2^{(\ell)}\} = & \\ &= VAR\{\mathbf{s}^H D_\ell \mathbf{s} {\mathbf{w}_\ell}^H A_\ell \mathbf{s} + \mathbf{s}^H A_\ell^H \mathbf{w}_\ell \mathbf{s}^H D_\ell^H \mathbf{s}\} = \\ &= 2E\{\|\mathbf{s}^H D_\ell \mathbf{s} {\mathbf{w}_\ell}^H A_\ell \mathbf{s}\|^2\} + 2\Re\{E\{(\mathbf{s}^H D_\ell \mathbf{s} {\mathbf{w}_\ell}^H A_\ell \mathbf{s})^2\}\} = \\ &= 2\|\mathbf{s}^H D_\ell \mathbf{s}\|^2 \sigma_\ell^2 \|\mathbf{s}\|^2 + 2\Re\left\{(\mathbf{s}^H D_\ell \mathbf{s})^2 E\left\{({\mathbf{w}_\ell}^H A_\ell \mathbf{s})^2\right\}\right\} \end{aligned} \tag{3.13}$$

If we notice that for an arbitary complex Gaussian variable $a + bj$:

$$\begin{aligned} E\{(a+jb)^2\} = & \\ &= E\{a^2 - b^2 + 2abj\} = E\{a^2\} - E\{b^2\} + 2jE\{ab\} = \\ &= \sigma^2 - \sigma^2 + 0 = 0 \end{aligned}$$

Where we assumed that $VAR\{a\} = VAR\{b\} = \sigma^2$ and that a and b have zero mean and are uncorrelated.

We can see that $E\left\{({\mathbf{w}_\ell}^H A_\ell \mathbf{s})^2\right\} = 0$ and (3.13) becomes:

$$VAR\{L_2^{(\ell)}\} = 2\|\mathbf{s}^H D_\ell \mathbf{s}\|^2 \sigma_\ell^2 \|\mathbf{s}\|^2 \tag{3.14}$$

Thus:

$$VAR\{L_2\} = \sum_{l=1}^{L} 2\|\mathbf{s}^H D_\ell \mathbf{s}\|^2 \sigma_\ell^2 \|\mathbf{s}\|^2 \tag{3.15}$$

Where we used the assumption that the noise in all of the receivers is independent. Therefore, the variance of the sum becomes the sum of variances.

3.3 Zero Noise Analysis - Full scenario

In the proceeding section we will not use the assumptions used above, in the simplified scenario sections. We will express L_2 using the complete signal model presented.

Remembering that (from (2.23)):

$$\mathbf{r}_\ell = b_\ell A_\ell F_\ell C \mathbf{s} + \mathbf{w}_\ell$$

We can write:

$$\mathbf{r}_\ell = b_\ell A_\ell^{(0)} F_\ell^{(0)} C^{(0)} \mathbf{s} \tag{3.16}$$

Where we used the assumption that $\mathbf{w}_\ell = 0$.

$A_\ell^{(0)}$, $F_\ell^{(0)}$, $C^{(0)}$ represent the true Doppler frequency shift caused by the relative speed of the transmitter and the receivers, the true delay caused by the relative distance of the transmitter and the receivers and the true transmitter frequency instability respectively.

Thus:

$$(A_\ell F_\ell C \mathbf{s})^H \mathbf{r}_\ell = (A_\ell F_\ell C \mathbf{s})^H (b_\ell A_\ell^{(0)} F_\ell^{(0)} C^{(0)} \mathbf{s}) \tag{3.17}$$

Therefore:

$$\begin{aligned} \|(A_\ell \mathbf{s})^H \mathbf{r}_\ell\|^2 = & \\ &= \|(A_\ell F_\ell C\mathbf{s})^H (b_\ell A_\ell^{(0)} F_\ell^{(0)} C^{(0)}\mathbf{s})\|^2 = \\ &= \|\mathbf{s}^H C^H F_\ell^H A_\ell^H b_\ell A_\ell^{(0)} F_\ell^{(0)} C^{(0)}\mathbf{s}\|^2 \end{aligned} \tag{3.18}$$

Defining:

$$D_\ell \triangleq F_\ell^H F_\ell^{(0)} A_\ell^H A_\ell^{(0)} C^H C^{(0)} \tag{3.19}$$

Where D_ℓ is a frequency and time shift operator, shifting the signal frequency by $(f_\ell^{(0)} - f_\ell) + (\nu^{(0)} - \nu)$ and shifting the signal by $\lfloor {}^{T_\ell^{(0)}}/_{T_s} \rfloor - \lfloor {}^{T_\ell}/_{T_s} \rfloor$ indices. $f_\ell^{(0)}$ is the true Doppler shift of the signal received by the ℓ-th receiver, $\nu^{(0)}$ is the true frequency instability of the transmitter and $T_\ell^{(0)}$ is the delay caused by the true distance between the transmitter and the ℓ-the receiver.

If we notice that if A is a general frequency-shift matrix, F is a general time shift operator and $\mathbf{s}$ is an arbitrary signal, then $\|\mathbf{s}^H AF\mathbf{s}\|^2 = \|\mathbf{s}^H FA\mathbf{s}\|^2$, then we can write by commutating the operators in (3.18):

$$\|(A_\ell \mathbf{s})^H \mathbf{r}_\ell\|^2 = \|b_\ell\|^2 \|\mathbf{s}^H D_\ell \mathbf{s}\|^2 \tag{3.20}$$

We can see that the expression above is the correlation between the signal shifted by $\lfloor {}^{T_\ell^{(0)}}/_{T_s} \rfloor - \lfloor {}^{T_\ell}/_{T_s} \rfloor$ indices and by $(f_\ell^{(0)} - f_\ell) + (\nu^{(0)} - \nu)$ in frequency and the original signal.

And eventually:

$$L_2 = \sum_{l=1}^{L} \|(A_\ell \mathbf{s})^H \mathbf{r}_\ell\|^2 = \sum_{l=1}^{L} \|\mathbf{s}^H D_\ell \mathbf{s}\|^2 \tag{3.21}$$

Which is the sum of squared absolute value of the correlation between the time and frequency shifted signal and the original signal.

3.4 Noisy Analysis - Full Scenario

In this subsection we will try to analyse the effect of the noise in the receiver on the cost function.

If we consider the noise, (3.17) becomes:

$$(A_\ell F_\ell C\mathbf{s})^H \mathbf{r}_\ell = (A_\ell F_\ell C\mathbf{s})^H (b_\ell A_\ell^{(0)} F_\ell^{(0)} C^{(0)}\mathbf{s} + \mathbf{w_l}) = b_\ell \mathbf{s}^H D_\ell \mathbf{s} + \mathbf{s}^H C^H F_\ell^H A_\ell^H \mathbf{w}_\ell \quad (3.22)$$

So:

$$\begin{aligned} L_2^{(\ell)} = & \qquad (3.23)\\ &= \|(A_\ell F_\ell C\mathbf{s})^H \mathbf{r}_\ell\|^2 = \\ &= |b_\ell|^2 \|\mathbf{s}^H D_\ell \mathbf{s}\|^2 + \|\mathbf{s}^H C^H F_\ell^H A_\ell^H \mathbf{w}_\ell\|^2 + \dots \\ \dots &+ b_\ell \mathbf{s}^H D_\ell \mathbf{s} (\mathbf{s}^H C^H F_\ell^H A_\ell^H \mathbf{w}_\ell)^H + \mathbf{s}^H C^H F_\ell^H A_\ell^H \mathbf{w}_\ell (b_\ell \mathbf{s}^H D_\ell \mathbf{s})^H = \end{aligned}$$

Because $\mathbf{w}_\ell$ is stochastic, L_2 is also a stochastic variable and we can look at its stochastic properties such as expectation and variance.

Similarly to (3.10) we can show that:

$$E\{\|\mathbf{s}^H C^H F_\ell^H A_\ell^H \mathbf{w}_\ell\|^2\} = \sigma_\ell^2 \|\mathbf{s}\|^2$$

Thus:

$$E\{L_2^{(\ell)}\} = E\{\|(A_\ell F_\ell C\mathbf{s})^H \mathbf{r}_\ell\|^2\} = |b_\ell|^2 \|\mathbf{s}^H D_\ell \mathbf{s}\|^2 + \sigma_\ell^2 \|\mathbf{s}\|^2 \quad (3.24)$$

Where we used the assumptions that $\mathbf{w}_\ell$ is a zero mean, i.i.d process with σ_ℓ^2 variance.

Also, similarly to the simplified scenario, we can show that:

$$VAR\{L_2\} = \sum_{l=1}^{L} 2|b_\ell|^2 \|\mathbf{s}^H D_\ell \mathbf{s}\|^2 \sigma_\ell^2 \|\mathbf{s}\|^2 \quad (3.25)$$

3.5 Expression For $\frac{\partial L_2}{\partial v_x}$ and $\frac{\partial L_2}{\partial v_y}$

In the following section, we develop the derivatives of the known signals cost function L_2 by the components of the velocity v_x and v_y. This derivation allows us to perform gradient-based search in the velocity subspace for finding the maximum of the cost function.

Defining:

$$L_2^{(\ell)} \triangleq \| \left(A_\ell F_\ell C\mathbf{s}\right)^H \mathbf{r}_\ell \|^2 \tag{3.26}$$

The cost function L_2 can be expressed as:

$$L_2 = \sum_{l=1}^{L} L_2^{(\ell)} \tag{3.27}$$

For further simplicity along the derivation we define:

$$\mathbf{u}_\ell \triangleq F_\ell C\mathbf{s} \tag{3.28}$$

By substituting (3.28) into (3.26) we get:

$$L_2^{(\ell)} = \|(A_\ell \mathbf{u}_\ell)^H \mathbf{r}_\ell\|^2 \tag{3.29}$$

Notice that for an arbitrary vector $\mathbf{x}$, if $y = \|\mathbf{x}\|^2 = \mathbf{x}^H\mathbf{x}$ then

$$\frac{\partial y}{\partial z} = \frac{\partial \mathbf{x}}{\partial z}^H \mathbf{x} + \mathbf{x}^H \frac{\partial \mathbf{x}}{\partial z} = 2\Re\left\{\frac{\partial \mathbf{x}}{\partial z}^H \mathbf{x}\right\}$$

Using the above statement for the derivative of $L_2^{(\ell)}$ by v_x:

$$\frac{\partial}{\partial v_x} L_2^{(\ell)} = 2\Re\left\{\left[\frac{\partial}{\partial v_x}(Al\mathbf{u}_\ell)^H \mathbf{r}_\ell\right]^H (Al\mathbf{u}_\ell)^H \mathbf{r}_\ell\right\} \tag{3.30}$$

By using the chain rule, we can see that:

$$\frac{\partial}{\partial v_x}\left((Al\mathbf{u}_\ell)^H\mathbf{r}_\ell\right) = \frac{\partial}{\partial f_\ell}\left((Al\mathbf{u}_\ell)^H\mathbf{r}_\ell\right)\frac{\partial f_\ell}{\partial v_x} \tag{3.31}$$

We notice that:

$$\begin{aligned}\frac{\partial}{\partial f_\ell}\left((Al\mathbf{u}_\ell)^H\mathbf{r}_\ell\right) = & \\ &= \frac{\partial}{\partial f_\ell}\left(\sum_{n=0}^{N-1} e^{-2\pi f_\ell T_s n}u_\ell^*[n]r_\ell[n]\right) = \\ &= -2\pi jT_s\sum_{n=0}^{N-1} ne^{-2\pi f_\ell T_s n}u_\ell^*[n]r_\ell[n] = \\ &= -2\pi jT_s\left((\tilde{N}Al\mathbf{u}_\ell)^H\mathbf{r}_\ell\right)\end{aligned} \tag{3.32}$$

Where we used the matrix $\tilde{N}$ defined:

$$\tilde{N} \triangleq diag\{0,1,\ldots,N-1\} \tag{3.33}$$

By substituting (3.32) into (3.31), using the derivation of $\frac{\partial f_\ell}{\partial v_x}$ and looking at the hermitian conjugate we get:

$$\left[\frac{\partial}{\partial v_x}(Al\mathbf{u}_\ell)^H\mathbf{r}_\ell\right]^H = -2\pi jT_s\frac{f_c}{c}cos\theta_\ell\mathbf{r}_\ell{}^H(\tilde{N}A_\ell\mathbf{u}_\ell) \tag{3.34}$$

Hence, by substituting the result in (3.34) into (3.30) we get:

$$\frac{\partial L_2}{\partial v_x} = \sum_{l=1}^{L}(4\pi T_s\frac{f_c}{c}cos\theta_\ell)\Im\left\{(A_\ell\mathbf{u}_\ell)^H\mathbf{r}_\ell\mathbf{r}_\ell{}^H(\tilde{N}A_\ell\mathbf{u}_\ell)\right\} \tag{3.35}$$

And after substituting $\mathbf{u}_\ell$:

$$\frac{\partial L_2}{\partial v_x} = \sum_{l=1}^{L}(4\pi T_s\frac{f_c}{c}cos\theta_\ell)\Im\left\{(A_\ell F_\ell C\mathbf{s})^H\mathbf{r}_\ell\mathbf{r}_\ell{}^H(\tilde{N}A_\ell F_\ell C\mathbf{s})\right\} \tag{3.36}$$

And similarly:

$$\frac{\partial L_2}{\partial v_y} = \sum_{l=1}^{L}(4\pi T_s \frac{f_c}{c} sin\theta_\ell)\Im\left\{(A_\ell F_\ell C\mathbf{s})^H \mathbf{r}_\ell {\mathbf{r}_\ell}^H(\tilde{N}A_\ell F_\ell C\mathbf{s})\right\} \tag{3.37}$$

To demonstrate that the expressions above give the exact location when there is no noise, we will try to show that the derivatives of L_2 by the velocity components zeros for the true position of the transmitter when there is no noise.
For the demonstration, we take $F_\ell = I$, $C = I$ (narrow-band case, no transmitter frequency instability, for ease).

The signal received at the ℓ-th receiver is then:

$$\mathbf{r}_\ell = A_\ell^{(0)}\mathbf{s} \tag{3.38}$$

When evaluating A_ℓ at the true transmitter position we get:

$$A_\ell = A_\ell^{(0)} \tag{3.39}$$

Using the above definitions, we can easily see that:

$$(A_\ell F_\ell C\mathbf{s})^H \mathbf{r}_\ell = \mathbf{s}^H C^{(0)H} A_\ell^{(0)H} A_\ell^{(0)} C^{(0)}\mathbf{s} = \|\mathbf{s}\|^2 \tag{3.40}$$

And that:

$${\mathbf{r}_\ell}^H(\tilde{N}A_\ell F_\ell C\mathbf{s}) = \mathbf{s}^H C^{(0)H} A_\ell^{(0)H} \tilde{N} A_\ell^{(0)} C^{(0)}\mathbf{s} = \mathbf{s}^H\tilde{N}\mathbf{s} = \sum_{n=1}^{N} n\|s[n]\|^2 \tag{3.41}$$

We can clearly see that the above expressions are real. Therefore, Substituting in (3.36) and in (3.37) we can see that the true transmitter position $\vec{p_0}, \vec{v_0}$ is an extremum point

of the cost function:

$$\begin{aligned}\frac{\partial L_2}{\partial v_x}|_{\vec{p_0},\vec{v_0}} &= 0 \\ \frac{\partial L_2}{\partial v_y}|_{\vec{p_0},\vec{v_0}} &= 0\end{aligned} \tag{3.42}$$

We can also easily show that the derivative of the cost function zeros when $F_\ell \neq I$ because the above expressions are also real.

3.6 Expression For $\frac{\partial L_2}{\partial x}$ and $\frac{\partial L_2}{\partial y}$ for Narrow-Band signals

In the following section, we develop the derivatives of the known signals cost function L_2 by the components of the position x and y for the narrow-band scenario. This derivation allows us to perform gradient-based search in the position subspace for finding the maximum of the cost function.

We start by analysing the narrow-band scenario because the derivation and the received expressions are simpler for this scenario. In the next section we also develop these expressions for the general wide-band scenario.

For narrow-band signals, we assume that $F_\ell = I$, thus similarly to (3.31), by using the chain rule, we get:

$$\frac{\partial}{\partial x}\left((Al\mathbf{u}_\ell)^H\mathbf{r}_\ell\right) = \frac{\partial}{\partial f_\ell}\left((Al\mathbf{u}_\ell)^H\mathbf{r}_\ell\right)\frac{\partial f_\ell}{\partial x} \tag{3.43}$$

Using the result of (3.32) and the expression for $\frac{\partial f_\ell}{\partial x}$ we get:

$$\frac{\partial}{\partial x}((A_\ell\mathbf{u}_\ell)^H\mathbf{r}_\ell) = -2\pi jT_s((\tilde{N}A_\ell\mathbf{u}_\ell)^H\mathbf{r}_\ell)\frac{f_c}{c}\frac{\|\vec{v}\|}{d_\ell}\sin\phi_\ell\sin\theta_\ell \tag{3.44}$$

Therefore, similarly to (3.35):

$$\frac{\partial L_2}{\partial x} = -\sum_{l=1}^{L}(4\pi T_s\frac{f_c}{c}\frac{\|\vec{v}\|}{d_\ell}\sin\phi_\ell\sin\theta_\ell)\Im\left\{(A_\ell C\mathbf{s}_\ell)^H\mathbf{r}_\ell\mathbf{r}_\ell{}^H(\tilde{N}A_\ell C\mathbf{s}_\ell)\right\} \tag{3.45}$$

And similarly:

$$\frac{\partial L_2}{\partial y} = \sum_{l=1}^{L}(4\pi T_s \frac{f_c}{c}\frac{\|\vec{v}\|}{d_\ell}\sin\phi_\ell\cos\theta_\ell)\Im\left\{(A_\ell C\mathbf{s}_\ell)^H\mathbf{r}_\ell\mathbf{r}_\ell{}^H(\tilde{N}A_\ell C\mathbf{s}_\ell)\right\} \tag{3.46}$$

To demonstrate that when there is no noise, there is an extremum point in the true position of the transmitter, we can see that the expression inside the $\Im\{\dots\}$ operator is identical to the one in the expression for $\frac{\partial L_2}{\partial v_x}$. So, for the true position of the transmitter, the expression inside the $\Im\{\dots\}$ operator is real, and we get:

$$\begin{aligned}\frac{\partial L_2}{\partial x}|_{\vec{p_0},\vec{v_0}} &= 0 \\ \frac{\partial L_2}{\partial y}|_{\vec{p_0},\vec{v_0}} &= 0\end{aligned} \tag{3.47}$$

3.7 Expression For $\frac{\partial L_2}{\partial x}$ and $\frac{\partial L_2}{\partial y}$ for Wide-Band signals

In the following section, we develop the derivatives of the known signals cost function L_2 by the components of the position x and y for the general wide-band scenario. This derivation allows us to perform gradient-based search in the position subspace for finding the maximum of the cost function.

In order to derive an expression for $\frac{\partial L_2}{\partial x}$ and $\frac{\partial L_2}{\partial y}$ for wide-band signals, we can relate to F_ℓ as a continuous time-shift operator.

We can write:

$$L_2^{(\ell)} = \|(A_\ell F_\ell C\mathbf{s})^H\mathbf{r}_\ell\|^2 = \|(A_\ell C F_\ell\mathbf{s})^H\mathbf{r}_\ell\|^2 = \|(A_\ell C\mathbf{s}_\ell)^H\mathbf{r}_\ell\|^2 \tag{3.48}$$

Where we denote:

$$\mathbf{s}_\ell \triangleq [s(t_1 - T_\ell)\dots s(t_N - T_\ell)]^T \tag{3.49}$$

By using the chain rule, we know that:

$$\frac{\partial L_2}{\partial x} = \sum_{l=1}^{L} \frac{\partial L_2^{(\ell)}}{\partial x} = \sum_{l=1}^{L} \frac{\partial L_2^{(\ell)}}{\partial T_\ell} \frac{\partial T_\ell}{\partial x} + \frac{\partial L_2^{(\ell)}}{\partial f_\ell} \frac{\partial f_\ell}{\partial x} \tag{3.50}$$

Looking at:

$$\frac{\partial L_2^{(\ell)}}{\partial T_\ell} = \frac{\partial}{\partial T_\ell} \|(A_\ell C \mathbf{s}_\ell)^H \mathbf{r}_\ell\|^2 \tag{3.51}$$

We notice that:

$$\frac{\partial}{\partial T_\ell} (AlC\mathbf{s}_\ell)^H \mathbf{r}_\ell = -(AlC\dot{\mathbf{s}}_\ell)^H \mathbf{r}_\ell \tag{3.52}$$

Thus:

$$\begin{aligned} \frac{\partial L_2^{(\ell)}}{\partial T_\ell} = & \\ &= 2\Re\{(-(AlC\dot{\mathbf{s}}_\ell)^H \mathbf{r}_\ell)^H (AlC\mathbf{s}_\ell)^H \mathbf{r}_\ell\} \\ &= -2\Re\{(AlC\mathbf{s}_\ell)^H \mathbf{r}_\ell \mathbf{r}_\ell{}^H (A_\ell C\dot{\mathbf{s}}_\ell)\} \end{aligned} \tag{3.53}$$

Subtituting the expressions for $\frac{\partial L_2^{(\ell)}}{\partial T_\ell}$, $\frac{\partial L_2^{(\ell)}}{\partial f_\ell}$, $\frac{\partial T_\ell}{\partial x}$ and $\frac{\partial f_\ell}{\partial x}$ into (3.50) we get:

$$\begin{aligned} \frac{\partial L_2}{\partial x} = & \\ &= \sum_{l=1}^{L} -2\Re\left\{(A_\ell C\mathbf{s}_\ell)^H \mathbf{r}_\ell \mathbf{r}_\ell{}^H (A_\ell C\dot{\mathbf{s}}_\ell)\right\} \frac{1}{c} \cos\theta_\ell - \\ &- 4\pi T_s \frac{F_c}{c} \frac{\|\vec{v}\|}{d_\ell} \sin\phi_\ell \sin\theta_\ell \Im\left\{(A_\ell C\mathbf{s}_\ell)^H \mathbf{r}_\ell \mathbf{r}_\ell{}^H (\tilde{N} A_\ell C\mathbf{s}_\ell)\right\} \end{aligned} \tag{3.54}$$

And similarly for $\frac{\partial L_2}{\partial y}$:

$$\begin{aligned} \frac{\partial L_2}{\partial y} = & \\ &= \sum_{l=1}^{L} -2\Re\left\{(A_\ell C\mathbf{s}_\ell)^H \mathbf{r}_\ell \mathbf{r}_\ell{}^H (A_\ell C\dot{\mathbf{s}}_\ell)\right\} \frac{1}{c} \sin\theta_\ell + \\ &+ 4\pi T_s \frac{F_c}{c} \frac{\|\vec{v}\|}{d_\ell} \sin\phi_\ell \cos\theta_\ell \Im\left\{(A_\ell C\mathbf{s}_\ell)^H \mathbf{r}_\ell \mathbf{r}_\ell{}^H (\tilde{N} A_\ell C\mathbf{s}_\ell)\right\} \end{aligned} \tag{3.55}$$

And now we can go ahead and use these expressions in order to preform a gradient-based search in the position subspace for the maximum of the cost-function.

3.8 Peak Size Approximation

As we saw before, the one-step cost function is not necessarily convex, and is usually not convex outside the area of its maximum. Only in a small area around the maximum, whose dimensions vary from scenario to scenario, the cost function is convex, and all of the gradient based methods that introduce lower computational complexity than grid search based methods could be used.

In fact, in the scenario where there is no a priori information regarding the location of the transmitter, and the search area is wide, a proposed method would be to perform a rough grid search, up to the resolution of the peak size, and then perform a fine gradient-based search to find the location of the peak in high accuracy and in low-complexity.

It is rather complicated to deduce a general expression for the size of the peak, since it depends on the exact transmitted signal and on the scenario's geometry, but by following a few simplifying assumptions we are able to derive a rough approximation of the peak's magnitude.

The first assumption that we make, is regarding the auto ambiguity function of the transmitted signal. We assume that the auto ambiguity function of the transmitted signal has a peak with a width of δt in time and δf in frequency, as can be seen in figure (3.1). Although the ambiguity function of most signals is not actually bounded in time or frequency, we are usually able to determine an estimate of the magnitude of the ambiguity function's peak size - an area that contains most of the "energy" of the ambiguity function. As we saw in (3.21) L_2 is a superposition of the $L_2^{(\ell)}$ cost functions generated by each of the receivers. Each one of the $L_2^{(\ell)}$ cost functions is actually a mapping between the ambiguity function, and the estimated position and velocity of the transmitter. The value of the cost function in each point in position and velocity space is the value of the ambiguity function for the difference in time and frequency between the time and frequency shift for the real position and velocity of the transmitter, and

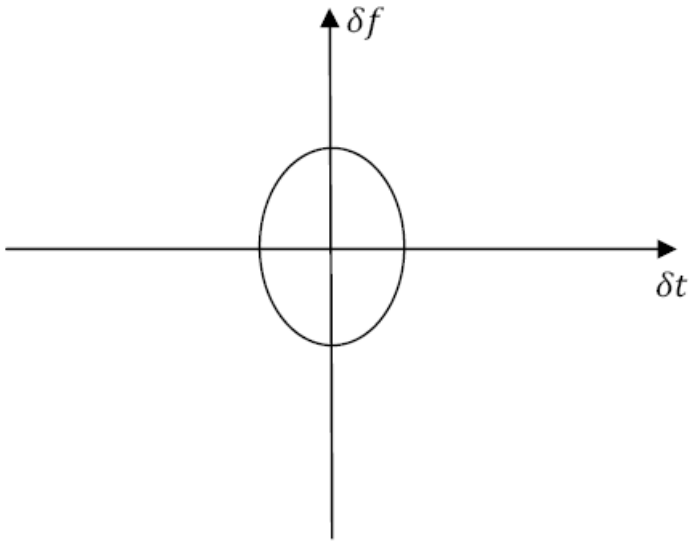

FIGURE 3.1: In order to simplify the peak size approximation we assume that the auto ambiguity function of the signal has a peak with a width of δt in time and δf in frequency.

the time and frequency shift for the estimated position and velocity of the transmitter, as can be seen here:

$$\delta t = \frac{\sqrt{(x-x_0)^2+(y-y_0)^2}}{C} - \frac{\sqrt{(x-x_r)^2+(y-y_r)^2}}{C} \tag{3.56}$$

$$\delta f = -\frac{f_c}{C}\frac{\vec{v_0}(\vec{p_0}-\vec{p_r})}{\|\vec{p_0}-\vec{p_r}\|} + \frac{f_c}{C}\frac{\vec{v}(\vec{p}-\vec{p_r})}{\|\vec{p}-\vec{p_r}\|} \tag{3.57}$$

where x_0,y_0,$\vec{p_0}$,$\vec{v_0}$ represent the real position and velocity of the transmitter, and x_r,y_r,$\vec{p_r}$ represent the position of the ℓ-th receiver.

From (3.56) we notice that every δt in the ambiguity function translates to a circle in the position space around the receiver with a radius of $C(t_0+\delta t)$, where t_0 is the real time delay of the received signal. Thus, a peak of the ambiguity function with a δt width would be found on a circular strip with a width of $C\delta t$ as can be seen in figure (3.2).

From (3.57) we notice that every δf translates to a line that originates in the position of the receiver, since every δf determines a value for $\vec{v}(\vec{p}-\vec{p_r})$. Thus, a peak of the

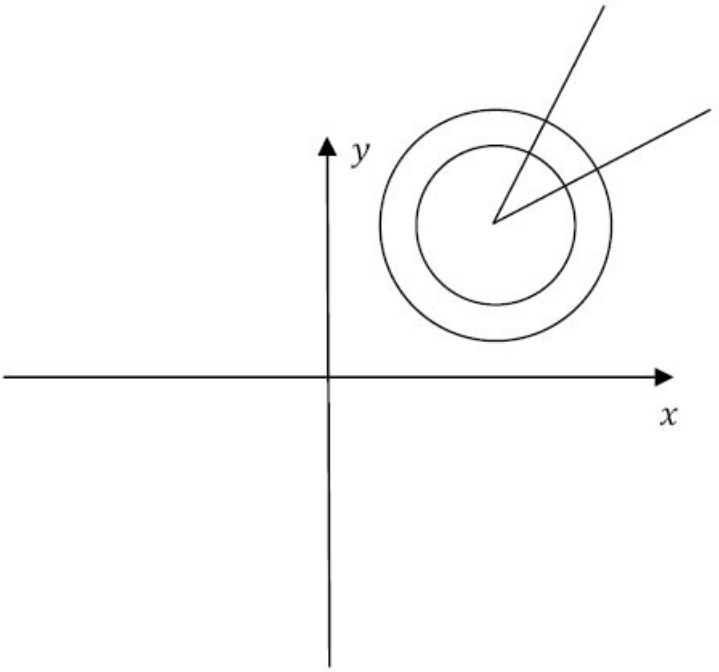

FIGURE 3.2: Every δt in the ambiguity function translates to a circle in the position space around the receiver with a radius of $C(t_0 + \delta t)$, where t_0 is the real time delay of the received signal. Every δf translates to a line that originates in the position of the receiver, since every δf determines a value for $\vec{v}(\vec{p} - \vec{p_r})$.

ambiguity function with a δf width would be found on a sector with an origin in the position of the receiver. In order to derive an approximate expression of the width of the sector in the area of the peak in the position space, we can use the expressions for the derivatives of f_ℓ in x and in y to perform a first order approximation.

We know that:

$$\begin{aligned} \frac{\partial f_\ell}{\partial x} &= \frac{f_c}{C}\frac{\|\vec{v_0}\|}{d_\ell}\sin\phi_\ell \sin\theta_\ell \\ \frac{\partial f_\ell}{\partial y} &= -\frac{f_c}{C}\frac{\|\vec{v_0}\|}{d_\ell}\sin\phi_\ell \cos\theta_\ell \end{aligned}$$

Assuming the the distance from the receiver is much larger the the width of the peak we can assume that ϕ_ℓ and θ_ℓ are constant, and then for a tangent change in position

δl we get a frequency shift of:

$$\delta f = \frac{f_c}{C}\frac{\|\vec{v_0}\|}{d_\ell}\sin\phi_\ell \delta l \tag{3.58}$$

To summarize, as can be seen in figure (3.4), we can approximate the width of the peak in the position space in the radial and tangent directions by:

$$\begin{aligned} \delta r &= C\delta t \\ \delta l &= \frac{C}{f_c}\frac{d_\ell}{\|\vec{v_0}\|}\frac{1}{\sin\phi_\ell}\delta f \end{aligned}$$

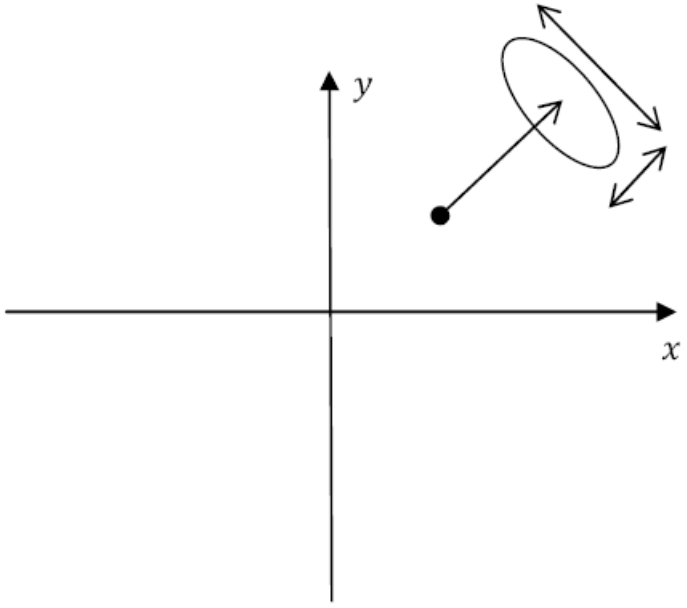

FIGURE 3.3: We approximate the width of the peak in the position space in the radial and tangent directions.

Of course, what we have developed so far only relates to the cost function for an individual receiver $L_2^{(\ell)}$. It has to be taken into consideration that the L_2 cost function is a super position of all the individual $L_2^{(\ell)}$ cost functions, as can be seen in figure (**??**).

In the velocity space, all the points with the same $\|\vec{v}\|\cos\phi_\ell$ have the same Doppler shift. Thus, as can be seen in figure (**??**), an auto ambiguity function with a width of δf would be translated to a strip with a radial width of $\delta\|\vec{v}\| = \frac{f_C}{C}\delta f$.

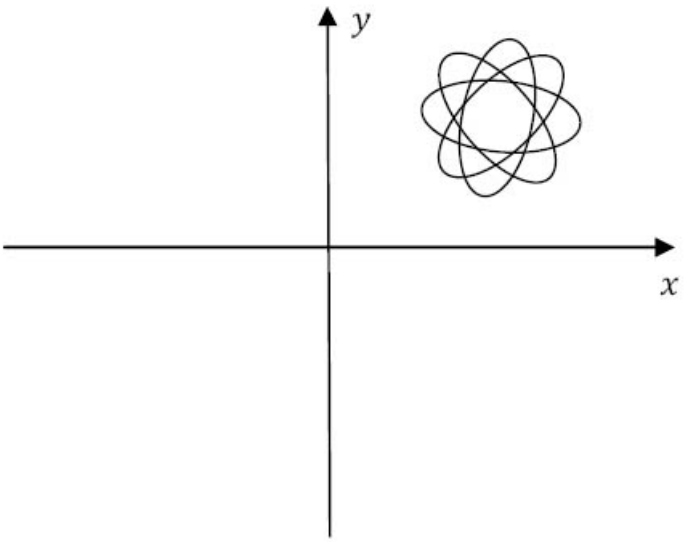

FIGURE 3.4: It has to be taken into consideration that the L_2 cost function is a super position of all the individual $L_2^{(\ell)}$ cost functions.

Similarly to the position space, since the L_2 cost function is a super position of all of the individual $L_2^{(\ell)}$ cost functions, the width of the peak would be determined by the geometry of the particular scenario. Assuming that the receivers are evenly spread around the transmitter, we can assume that the peak's width in the velocity space is $\frac{f_c}{C}\delta f$.

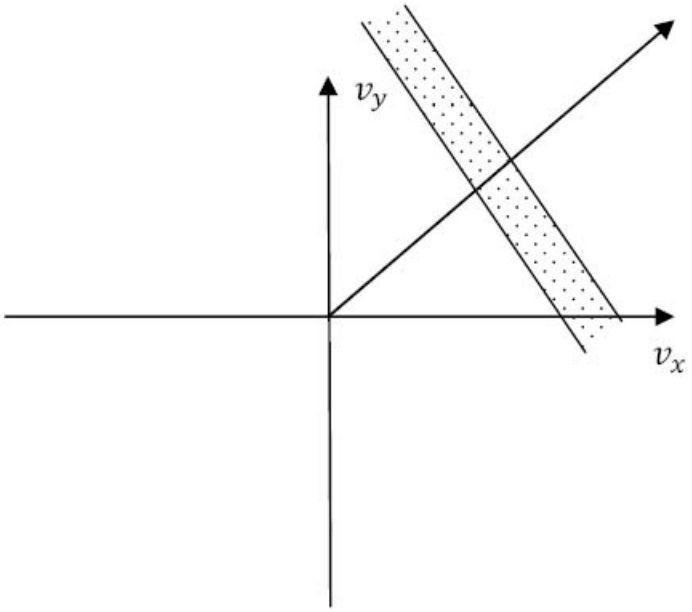

FIGURE 3.5: In the velocity space, all the points with the same $\|\vec{v}\| \cos \phi_\ell$ have the same Doppler shift. Thus, an auto ambiguity function with a width of δf would be translated to a strip with a radial width of $\delta \|\vec{v}\| = \frac{f_C}{C} \delta f$.

Chapter 4

Location Algorithms

4.1 General

The aim of this study is to develop a localization method for moving RF transmitters that will have superior performance without significantly raising the algorithm complexity.

While conventional algorithms estimate the TDOA and FDOA parameters from which they obtain the transmitter location, the suggested algorithm finds the location and velocity directly, without intermediate estimations and by applying a search that involves the complete data gathered from all of the base stations simultaneously.

In this sense, it is an extension of the DPD algorithm, that was developed for the static transmitter and moving receivers scenario.

The proposed method performs localization of a moving RF transmitter and an estimation of its velocity.

The unknown velocity adds to the unknown parameters of the problem, thus, increasing its complexity. Applying the conventional grid-search method requires a 4-dimensional grid-search for every estimation, drastically increasing the complexity.

In the following sections, we will suggest algorithms for different scenarios, allowing to reduce the problem's complexity using gradient based methods, in the cases in which it

was possible to differentiate the cost function.

The scenarios for which we will be able to reduce complexity are mainly the scenarios in which the signals are known. We employ our knowledge on the cost function L_2 and its derivatives in order to perform gradient based methods in the position and velocity space to find the maximum of the cost function.

In the scenario where the signal is both known and narrow band, we are able to easily preform gradient based methods in the position sub-space, in addition to the velocity sub-space. In all of the gradient based methods we will assume that the function is convex in the search area. The cost function is generally not convex, it is only approximately convex in a small area around its maximum.

Therefore, in each of the suggested algorithms employing gradient-based methods we will have to assume that the start point for the algorithm is close enough to the maximum, so that it is found within the global maximum's convex area so that the algorithm is guaranteed to find the global maximum. At the last section of the chapter, we will try to handle the dynamic scenario where the transmitter's position is estimated in a number of lags along its trajectory. For this purpose we employ a simple dynamic model for the transmitter and use an extended Kalman filter for the dynamic estimation.

4.2 Known Narrow Band Signals

In the case where the signals are known and are narrow-band, we can use our knowledge of L_2 and its derivatives to perform gradient-based methods to avoid performing a grid-search. Of course, to employ the gradient-based methods we need a good initial guess on the position and velocity of the transmitter, which can be acquired by a rough initial grid-search, or, as we will later see in section (4.5), from the prediction of the Kalman filter.

4.2.1 Steepest Descent Method

A simple implementation of gradient based steepest descent search can be employed using the results of sections (3.5) and (3.6). A starting point

$$\mathbf{x}^{(0)} = [x^{(0)}, y^{(0)}, v_x^{(0)}, v_y^{(0)}]^T$$

has to be chosen using an initial guess, a-priori information about the location and velocity of the transmitter or using a rough grid-search. At the k-th step we can choose:

$$\mathbf{x}^{k+1} = \mathbf{x}^k + \alpha \nabla L_2|_{\mathbf{x}^k} \tag{4.1}$$

Where:

$$\nabla L_2 = [\frac{\partial L_2}{x}, \frac{\partial L_2}{y}, \frac{\partial L_2}{v_x}, \frac{\partial L_2}{v_y}]^T \tag{4.2}$$

We represent the stepsize with α. There are many methods to determine the optimal stepsize, and usually there is a trade-off between optimality and complexity. The simplest choice is the constant stepsize. However, choosing a constant stepsize should be done carefully. If the stepsize is too large, divergence will occur, if the stepsize is too small, the rate of convergence may be very slow. Other common methods are the minimization rule, the Armijo rule, the Goldstein rule and the diminishing stepsize method. The steepest descent search is very simple to derive and implement, but often leads to slow convergence rates.

4.2.2 Gauss-Newton Method

In order to achieve higher convergence rates, we can employ the Gauss-Newton method, described in [19], trying to minimize the least squares cost $\frac{1}{2}\|g(\mathbf{x})\|^2$. Small adjustments need to be made in order to use the method to effectively find a maximum of the above cost function, rather than its minimum. We define $\mathbf{x}$ as the unknown parameters vector:

$$\mathbf{x} \triangleq [x, y, v_x, v_y]^T$$

And therefore:

$$\nabla \triangleq \left[\frac{\partial}{\partial x}, \frac{\partial}{\partial y}, \frac{\partial}{\partial v_x}, \frac{\partial}{\partial v_y}\right]$$

In order to use the notation in (2.14) we choose: $g(\mathbf{x}) = \sqrt{2}\begin{pmatrix} Re\{V^H\mathbf{u}\} \\ Im\{V^H\mathbf{u}\} \end{pmatrix}$ notice that $\mathbf{u}$ is the known transmitted signal. we get:

$$\frac{1}{2}\|g(\mathbf{x})\|^2 = \|\Re\{V^H\mathbf{u}\}\|^2 + \|\Im\{V^H\mathbf{u}\}\|^2 = \|V^H\mathbf{u}\|^2 = L_2 \tag{4.3}$$

Thus, we can use the iterative method proposed:

$$\mathbf{x}^{k+1} = \mathbf{x}^k + \left(\nabla g(\mathbf{x}^k)\nabla g(\mathbf{x}^k)^T\right)^{-1}\nabla g(\mathbf{x}^k)g(\mathbf{x}^k) \tag{4.4}$$

Where:

$$\nabla g(\mathbf{x^k}) = \sqrt{2}\begin{pmatrix} \nabla Re\{V^H\mathbf{u}\} \\ \nabla Im\{V^H\mathbf{u}\} \end{pmatrix} = \sqrt{2}\begin{pmatrix} Re\{\nabla(V^H\mathbf{u})\} \\ Im\{\nabla(V^H\mathbf{u})\} \end{pmatrix} \tag{4.5}$$

And:

$$\nabla V^H\mathbf{u} = -2\pi j T_s \frac{f_c}{c}\begin{pmatrix} \tilde{\Theta}_x V^H\tilde{N}\mathbf{u} & \tilde{\Theta}_y V^H\tilde{N}\mathbf{u} & \tilde{\Theta}_{v_x} V^H\tilde{N}\mathbf{u} & \tilde{\Theta}_{v_y} V^H\tilde{N}\mathbf{u} \end{pmatrix} \tag{4.6}$$

Where:

$$\tilde{\Theta}_x = diag\left[-\frac{\|\vec{v}\|}{d_1}\sin\phi_1\sin\theta_1, \ldots, -\frac{\|\vec{v}\|}{d_L}\sin\phi_L\sin\theta_L\right] \tag{4.7}$$

$$\tilde{\Theta}_y = diag\left[\frac{\|\vec{v}\|}{d_1}\sin\phi_1\cos\theta_1, \ldots, \frac{\|\vec{v}\|}{d_L}\sin\phi_L\cos\theta_L\right] \tag{4.8}$$

$$\tilde{\Theta}_{v_x} = diag\left[cos\theta_1, \ldots, cos\theta_L\right] \tag{4.9}$$

$$\tilde{\Theta}_{v_y} = diag\left[sin\theta_1, \ldots, sin\theta_L\right] \tag{4.10}$$

Note that the direction used in the above iteration is a climb direction since $\nabla g(\mathbf{x}^k)g(\mathbf{x}^k)$ is the gradient at $\mathbf{x}^k$ of the cost function $\frac{1}{2}\|g(\mathbf{x})\|^2$ and $\left(\nabla g(\mathbf{x}^k)\nabla g(\mathbf{x}^k)^T\right)^{-1}$ is a positive

definite matrix.

4.3 Known Wide Band Signals

4.3.1 Steepest Descent Method

Implementing the steepest descent gradient based search method is very similar to the known narrow band signals scenario. The only difference is that the derivatives $\frac{\partial L_2}{\partial x}$ and $\frac{\partial L_2}{\partial y}$ that need to be used are the ones derived for the wide band known signals scenario in section (3.7).

4.3.2 Gauss-Newton Method

In the wide-band known signals scenario, the derivatives $\frac{\partial L_2}{\partial x}$ and $\frac{\partial L_2}{\partial y}$ are more complex, and the expressions for the Gauss-Newton method in the entire position and velocity space are much less elegant.

Therefore, we can suggest to perform a grid search, or a steepest descent search in the position subspace, and employ the Gauss-Newton method in the velocity sub-space as follows.

Exactly like the at previous section, we have:

$$g(\mathbf{x}) = \sqrt{2} \begin{pmatrix} Re\{V^H \mathbf{u}\} \\ Im\{V^H \mathbf{u}\} \end{pmatrix} \tag{4.11}$$

only that $\mathbf{x}$ contains only the velocity unknown parameters, meaning:

$$\mathbf{x} \triangleq [v_x, v_y]^T \tag{4.12}$$

And therefore:

$$\nabla \triangleq \left[\frac{\partial}{\partial v_x}, \frac{\partial}{\partial v_y} \right] \tag{4.13}$$

We can see that:

$$\frac{1}{2}\|g(\mathbf{x})\|^2 = \|Re\{V^H\mathbf{u}\}\|^2 + \|Im\{V^H\mathbf{u}\}\|^2 = \|V^H\mathbf{u}\|^2 = L_2 \tag{4.14}$$

We can use the iterative method suggested:

$$\mathbf{x}^{k+1} = \mathbf{x}^k + \left(\nabla g(\mathbf{x}^k)\nabla g(\mathbf{x}^k)^T\right)^{-1}\nabla g(\mathbf{x}^k)g(\mathbf{x}^k) \tag{4.15}$$

Where:

$$\nabla g(\mathbf{x}^k) = \begin{pmatrix} \nabla Re\{V^H\mathbf{u}\} \\ \nabla Im\{V^H\mathbf{u}\} \end{pmatrix} = \begin{pmatrix} Re\{\nabla V^H\mathbf{u}\} \\ Im\{\nabla V^H\mathbf{u}\} \end{pmatrix} \tag{4.16}$$

And:

$$\nabla V^H\mathbf{u} \ = -2\pi j T_s \frac{f_c}{c}\begin{pmatrix} \tilde{\Theta}_{v_x}V^H\tilde{N}\mathbf{u} & \tilde{\Theta}_{v_y}V^H\tilde{N}\mathbf{u} \end{pmatrix} \tag{4.17}$$

Where:

$$\tilde{\Theta}_{v_x} = diag\left[cos\theta_1, \ldots, cos\theta_L\right] \tag{4.18}$$

$$\tilde{\Theta}_{v_y} = diag\left[sin\theta_1, \ldots, sin\theta_L\right] \tag{4.19}$$

4.4 Unknown Signals

In the case of unknown signals, we do not have explicit expressions for the derivatives of the cost function L_3 in the position subspace or in the velocity subspace. Therefore, we need to perform a grid search both in the velocity subspace and in the position subspace or we can perform a gradient search based method, where the gradient is derived numerically.

4.5 Applying the Extended Kalman Filter

So far, we handled the semi-static scenario in which we did not take into consideration the dynamic motion model of the transmitter. In the semi-static scenario we estimated

the position and velocity of the transmitter in one observation interval.

In this section, we will use a simple constant velocity dynamic motion model, together with the extended Kalman filter, to take into consideration the motion of the transmitter and to improve the position and velocity estimation of the transmitter over time.

We call this method - The Extnded Kalman Filter - because the measurement noise is not necessarily Gaussian, although we assume it is.

In our scenario, the state vector is:

$$\mathbf{x} = \begin{pmatrix} x \\ v_x \\ y \\ v_y \end{pmatrix} \tag{4.20}$$

We assume that between each step the transmitter undergoes a constant acceleration of $\mathbf{a_k}$ that is normally distributed, with zero mean and covariance matrix:

$$R = \begin{pmatrix} \sigma_{a_x}^2 & 0 \\ 0 & \sigma_{a_y}^2 \end{pmatrix} \tag{4.21}$$

From Newton's Law:

$$\mathbf{x}_k = F\mathbf{x}_{k-1} + G\mathbf{a}_k \tag{4.22}$$

Where:

$$F = \begin{pmatrix} 1 & \Delta t & 0 & 0 \\ 0 & 1 & 0 & 0 \\ 0 & 0 & 1 & \Delta t \\ 0 & 0 & 0 & 1 \end{pmatrix} \tag{4.23}$$

And:

$$G = \begin{pmatrix} \frac{\Delta t^2}{2} & 0 \\ \Delta t & 0 \\ 0 & \frac{\Delta t^2}{2} \\ 0 & \Delta t \end{pmatrix} \tag{4.24}$$

So that:

$$\mathbf{x}_k = F\mathbf{x}_{k-1} + \mathbf{w}_k \tag{4.25}$$

Where $\mathbf{w}_k \sim N(0, Q)$

$$\begin{aligned} Q = GRG^T = & \qquad (4.26) \\ = & \begin{pmatrix} \frac{\Delta t^2}{2} & 0 \\ \Delta t & 0 \\ 0 & \frac{\Delta t^2}{2} \\ 0 & \Delta t \end{pmatrix} \begin{pmatrix} \sigma_{a_x}^2 & 0 \\ 0 & \sigma_{a_y}^2 \end{pmatrix} \begin{pmatrix} \frac{\Delta t^2}{2} & 0 \\ \Delta t & 0 \\ 0 & \frac{\Delta t^2}{2} \\ 0 & \Delta t \end{pmatrix}^T = \\ = & \begin{pmatrix} \frac{\Delta t^2}{4}\sigma_{a_x}^2 & \frac{\Delta t^3}{2}\sigma_{a_x}^2 & 0 & 0 \\ \frac{\Delta t^3}{2}\sigma_{a_x}^2 & \Delta t^2\sigma_{a_x}^2 & 0 & 0 \\ 0 & 0 & \frac{\Delta t^2}{4}\sigma_{a_y}^2 & \frac{\Delta t^3}{2}\sigma_{a_y}^2 \\ 0 & 0 & \frac{\Delta t^3}{2}\sigma_{a_y}^2 & \Delta t^2\sigma_{a_y}^2 \end{pmatrix} \end{aligned}$$

At each time step, using one of the semi-static algorithm suggested in the previous sections, a measurement of the position and velocity of the transmitter is made.
Let us assume that measurement noise, caused by our estimation error, ν_k is zero mean, with covariance matrix R_z. We can use the CRB as an estimation for the measurement noise covariance matrix R_z.

Thus, our measurement model takes the form:

$$\mathbf{z}_k = H\mathbf{x}_k + \nu_k \tag{4.27}$$

Where:

$$H = I \tag{4.28}$$

Using the definitions above we can use the standard Kalman filter algorithm:

Prediction for the state vector and variance:

$$\hat{\mathbf{x}}_{k|k-1} = F\hat{\mathbf{x}}_{k-1|k-1} \tag{4.29}$$

$$\hat{P}_{k|k-1} = F\hat{P}_{k-1|k-1}F^T + Q \tag{4.30}$$

The Kalman gain factor:

$$K_k = \hat{P}_{k|k-1}H^T(H\hat{P}_{k|k-1}H^T + R_z)^{-1} \tag{4.31}$$

Correction based on observation:

$$\hat{\mathbf{x}}_{k|k} = \hat{\mathbf{x}}_{k|k-1} + K_k(\mathbf{z}_k - H\hat{\mathbf{x}}_{k|k-1}) \tag{4.32}$$

$$\hat{P}_{k|k} = (I - K_kH)\hat{P}_{k|k-1} \tag{4.33}$$

For Initialization we can choose:

$$\hat{\mathbf{x}}_{0|0} = \mathbf{z}_0$$

$$P_{0|0} = CRB$$

Where we use the first measurement as the best estimate for the position and velocity, and the Cramer-Rao lower bound as a good estimate for the estimator accuracy.

Chapter 5

CRAMER-RAO Lower Bound

The Cramer-Rao Lower Bound (CRB) is a lower bound on the covariance of any unbiased estimator. The bound is given by the inverse of the Fisher Information Matrix (FIM).

Because we are using a ML estimator in our work, the CRB also helps us in evaluating the performance of our estimator. It can be shown, that for small-errors(low noise scenarios) the ML estimator's performance is asymptotic to the CRB. Therefore, by evaluating the CRB of our scenario, we also evaluate the performance of our ML estimator.

In this work, we derive the CRB for the known signals scenario in which we assume that the only unknown parameters are the position and the velocity of the transmitter. This bound still serve as a lower bound, but not necessarily as a tight lower bound for the unknown signals scenario.

5.1 General CRAMER-RAO Lower Bound Formulation

For complex Gaussian data vectors $\mathbf{r} \sim N(\mathbf{m}, R)$ the elements of the Fischer Information Matrix are given by:

$$[J]_{ij} = tr\{R^{-1}\frac{\partial R}{\partial \psi_i}R^{-1}\frac{\partial R}{\partial \psi_j}\} + 2Re\{\frac{\partial \mathbf{m}^H}{\partial \psi_i}R^{-1}\frac{\partial \mathbf{m}}{\partial \psi_j}\} \tag{5.1}$$

Where ψ is the unknown parameters vector and R is the covariance matrix. in our case:

$$\psi = \begin{pmatrix} x \\ y \\ v_x \\ v_y \end{pmatrix}$$

$$R = diag\{\sigma_1^2 \cdot I, \ldots, \sigma_L^2 \cdot I\}$$

If we consider the signals as non-random variables, the data covariance is equal to the noise covariance which is independent of the unknown parameters, under the assumption that the noise covariance is known.
Thus, we get:

$$[J]_{ij} = 2Re\{\frac{\partial \mathbf{m}^H}{\partial \psi_i}R^{-1}\frac{\partial \mathbf{m}}{\partial \psi_j}\} \tag{5.2}$$

The data vector is given by:

$$\mathbf{m} \triangleq [\mathbf{m_1}^T, \ldots, \mathbf{m}_\ell{}^T]^T \tag{5.3}$$

where:

$$\mathbf{m}_\ell = b_\ell A_\ell F_\ell C\mathbf{s} = b_\ell A_\ell C F_\ell \mathbf{s} = b_\ell A_\ell C\mathbf{s}_\ell \tag{5.4}$$

and:

$$\mathbf{s}_\ell \triangleq [s(t_1 - T_\ell) \dots s(t_N - T_\ell)]^T \tag{5.5}$$

Taking into account the structure of R and $\mathbf{m}_\ell$ we get:

$$\frac{\partial \mathbf{m}^H}{\partial \psi_i} R^{-1} \frac{\partial \mathbf{m}}{\partial \psi_j} = \sum_{l=1}^{L} \frac{1}{\sigma_\ell^2} \frac{\partial \mathbf{m}_\ell}{\partial \psi_i}^H \frac{\partial \mathbf{m}_\ell}{\partial \psi_j} \tag{5.6}$$

We are interested in the derivatives of $\mathbf{m}$ with respect to the target coordinates and velocity. Using the chain rule we can write:

$$\frac{\partial \mathbf{m}_\ell}{\partial \psi_i} = \frac{\partial \mathbf{m}_\ell}{\partial f_\ell} \frac{\partial f_\ell}{\partial \psi_i} + \frac{\partial \mathbf{m}_\ell}{\partial T_\ell} \frac{\partial T_\ell}{\partial \psi_i} \tag{5.7}$$

5.1.1 $\frac{\partial \mathbf{m}_\ell}{\partial f_\ell}$ derivation:

$$\frac{\partial \mathbf{m}_\ell}{\partial f_\ell} = \frac{\partial}{\partial f_\ell} b_\ell A_\ell C \mathbf{s}_\ell = b_\ell (\frac{\partial}{\partial f_\ell} A_\ell) C \mathbf{s}_\ell \tag{5.8}$$

Note that:

$$\frac{\partial}{\partial f_\ell} A_\ell = 2\pi j T_s \tilde{N} A_\ell \tag{5.9}$$

Where:

$$\tilde{N} \triangleq diag\{0, 1, 2, \dots, N-1\} \tag{5.10}$$

So that:

$$\frac{\partial \mathbf{m}_\ell}{\partial f_\ell} = 2\pi j T_s b_\ell \tilde{N} A_\ell C \mathbf{s}_\ell \tag{5.11}$$

5.1.2 $\frac{\partial \mathbf{m}_\ell}{\partial T_\ell}$ derivation:

$$\frac{\partial \mathbf{m}_\ell}{\partial T_\ell} = \frac{\partial}{\partial T_\ell} b_\ell A_\ell C \mathbf{s}_\ell = b_\ell A_\ell C \frac{\partial}{\partial T_\ell} \mathbf{s}_\ell \tag{5.12}$$

Where:

$$\frac{\partial}{\partial T_\ell}\mathbf{s}_\ell = \frac{\partial}{\partial T_\ell}[s(t_1 - T_\ell)\dots s(t_N - T_\ell)]^T = -[\dot{s}(t_1 - T_\ell)\dots \dot{s}(t_N - T_\ell)]^T = -\dot{\mathbf{s}}_\ell \quad (5.13)$$

$\dot{s(t)}$ represents the temporal derivative of the signal envelope $\frac{\partial s(t)}{\partial t}$ and we defined:

$$\dot{s_\ell}[n] \triangleq \frac{\partial}{\partial t}s(t)|_{t=nTs-T_\ell} \quad (5.14)$$

So that:

$$\frac{\partial \mathbf{m}_\ell}{\partial T_\ell} = -b_\ell A_\ell C\dot{\mathbf{s}}_\ell \quad (5.15)$$

5.1.3 $\frac{\partial f_\ell}{\partial x}$, $\frac{\partial f_\ell}{\partial y}$, $\frac{\partial f_\ell}{\partial v_x}$, $\frac{\partial f_\ell}{\partial v_y}$ derivation:

Notice that:

$$\frac{\partial f_\ell}{\partial \psi_i} = \frac{\partial}{\partial \psi_i}f_c\mu_\ell(\vec{p},\vec{v}) \quad (5.16)$$

And that:

$$(\frac{-c}{f_c})\frac{\partial}{\partial \psi_i}f_c\mu_\ell(\vec{p},\vec{v}) = \frac{\partial}{\partial \psi_i}(\frac{\vec{v}(\vec{p}-\vec{p_\ell})}{\|\vec{p}-\vec{p_\ell}\|}) \quad (5.17)$$

$$\frac{\partial}{\partial x}(\frac{\vec{v}(\vec{p}-\vec{p_\ell})}{\|\vec{p}-\vec{p_\ell}\|}) = \frac{\partial}{\partial x}(\frac{v_x(x-x_\ell)+v_y(y-y_\ell)}{\sqrt{(x-x_\ell)^2+(y-y_\ell)^2}}) = -\frac{\|\vec{v}\|}{d_\ell}sin\phi_\ell sin\theta_\ell \quad (5.18)$$

$$\frac{\partial}{\partial y}(\frac{\vec{v}(\vec{p}-\vec{p_\ell})}{\|\vec{p}-\vec{p_\ell}\|}) = \frac{\|\vec{v}\|}{d_\ell}sin\phi_\ell cos\theta_\ell \quad (5.19)$$

$$\frac{\partial}{\partial v_x}(\frac{\vec{v}(\vec{p}-\vec{p_\ell})}{\|\vec{p}-\vec{p_\ell}\|}) = \frac{\partial}{\partial v_x}\frac{v_x(x-x_\ell)+v_y(y-y_\ell)}{\sqrt{(x-x_\ell)^2+(y-y_\ell)^2}} = \frac{x-x_\ell}{\sqrt{(x-x_\ell)^2+(y-y_\ell)^2}} = cos\theta_\ell \quad (5.20)$$

$$\frac{\partial}{\partial v_y}\frac{\vec{v}(\vec{p}-\vec{p_\ell})}{\|\vec{p}-\vec{p_\ell}\|} = \frac{\partial}{\partial v_y}\frac{v_x(x-x_\ell)+v_y(y-y_\ell)}{\sqrt{(x-x_\ell)^2+(y-y_\ell)^2)}} = \frac{y-y_\ell}{\sqrt{(x-x_\ell)^2+(y-y_\ell)^2}} = sin\theta_\ell \tag{5.21}$$

Where d_ℓ denotes the distance between the emitter and the ℓ-th receiver, ϕ_ℓ is the angle between the emitter velocity and the line connecting the ℓ-th receiver and the emitter. θ_ℓ is the angle between the line connecting the ℓ-th receiver and the emitter and the x-axis.

5.1.4 $\frac{\partial T_\ell}{\partial x}$, $\frac{\partial T_\ell}{\partial y}$, $\frac{\partial T_\ell}{\partial v_x}$, $\frac{\partial T_\ell}{\partial v_y}$ derivation:

Remember that:

$$T_\ell = \frac{1}{c}\|\vec{p}-\vec{p_\ell}\| \tag{5.22}$$

$$\frac{\partial}{\partial x}T_\ell = \frac{1}{c}\frac{\partial}{\partial x}\sqrt{(x-x_\ell)^2+(y-y_\ell)^2} = \frac{1}{c}\frac{x-x_\ell}{\sqrt{(x-x_\ell)^2+(y-y_\ell)^2}} = \frac{1}{c}cos\theta_\ell \tag{5.23}$$

$$\frac{\partial}{\partial y}T_\ell = \frac{1}{c}\frac{\partial}{\partial y}\sqrt{(x-x_\ell)^2+(y-y_\ell)^2} = \frac{1}{c}\frac{y-y_\ell}{\sqrt{(x-x_\ell)^2+(y-y_\ell)^2}} = \frac{1}{c}sin\theta_\ell \tag{5.24}$$

Since T_ℓ is independent of v_x,v_y:

$$\frac{\partial}{\partial v_x}T_\ell = \frac{\partial}{\partial v_y}T_\ell = 0 \tag{5.25}$$

For summary:

$$\frac{\partial f_\ell}{\partial x} = \frac{f_c}{c}\frac{\|\vec{v}\|}{d_\ell}sin\phi_\ell sin\theta_\ell \tag{5.26}$$

$$\frac{\partial f_\ell}{\partial y} = -\frac{f_c}{c}\frac{\|\vec{v}\|}{d_\ell}sin\phi_\ell cos\theta_\ell \tag{5.27}$$

$$\frac{\partial f_\ell}{\partial v_x} = -\frac{f_c}{c} cos\theta_\ell \tag{5.28}$$

$$\frac{\partial f_\ell}{\partial v_y} = -\frac{f_c}{c} sin\theta_\ell \tag{5.29}$$

$$\frac{\partial}{\partial x} T_\ell = \frac{1}{c} cos\theta_\ell \tag{5.30}$$

$$\frac{\partial}{\partial y} T_\ell = \frac{1}{c} sin\theta_\ell \tag{5.31}$$

$$\frac{\partial}{\partial v_x} T_\ell = 0 \tag{5.32}$$

$$\frac{\partial}{\partial v_y} T_\ell = 0 \tag{5.33}$$

5.1.5 $\frac{\partial \mathbf{m}_\ell}{\partial v_x}, \frac{\partial \mathbf{m}_\ell}{\partial v_y}$ derivation

Remembering that: $\frac{\partial \mathbf{m}_\ell}{\partial v_x} = \frac{\partial \mathbf{m}_\ell}{\partial f_\ell} \frac{\partial f_\ell}{\partial v_x} + \frac{\partial \mathbf{m}_\ell}{\partial T_\ell} \frac{\partial T_\ell}{\partial v_x}$ we get:

$$\frac{\partial \mathbf{m}_\ell}{\partial v_x} = -(2\pi j \frac{f_c}{c} cos\theta_\ell) T_s b_\ell \tilde{N} A_\ell C \mathbf{s}_\ell \tag{5.34}$$

And in the same manner, for v_y we get:

$$\frac{\partial \mathbf{m}_\ell}{\partial v_y} = -(2\pi j \frac{f_c}{c} sin\theta_\ell) T_s b_\ell \tilde{N} A_\ell C \mathbf{s}_\ell \tag{5.35}$$

5.1.6 $\frac{\partial \mathbf{m}_\ell}{\partial x}, \frac{\partial \mathbf{m}_\ell}{\partial y}$ derivation

Remembering that $\frac{\partial \mathbf{m}_\ell}{\partial x} = \frac{\partial \mathbf{m}_\ell}{\partial f_\ell} \frac{\partial f_\ell}{\partial x} + \frac{\partial \mathbf{m}_\ell}{\partial T_\ell} \frac{\partial T_\ell}{\partial x}$ we get:

$$\frac{\partial \mathbf{m}_\ell}{\partial x} = (2\pi j T_s \frac{f_c}{c} \frac{\|\vec{v}\|}{d_\ell} sin\phi_\ell sin\theta_\ell) b_\ell \tilde{N} A_\ell C \mathbf{s}_\ell - \frac{1}{c} cos\theta_\ell b_\ell A_\ell C \dot{\mathbf{s}}_\ell \tag{5.36}$$

And in the same manner, for y we get:

$$\frac{\partial \mathbf{m}_\ell}{\partial y} = -(2\pi j T_s \frac{f_c}{c} \frac{\|\vec{v}\|}{d_\ell} sin\phi_\ell cos\theta_\ell) b_\ell \tilde{N} A_\ell C \mathbf{s}_\ell - \frac{1}{c} sin\theta_\ell b_\ell A_\ell C \dot{\mathbf{s}}_\ell \tag{5.37}$$

5.2 Expression for $[J]_{v_x v_x}$ and $[J]_{v_y v_y}$

Substituting in the expression for $[J]_{v_x v_x}$ we get:

$$[J]_{v_x v_x} = 2\sum_{l=1}^{L} \frac{1}{\sigma_\ell^2} \left\| \frac{\partial \mathbf{m}_\ell}{\partial v_x} \right\|^2 \tag{5.38}$$

Hence:

$$\begin{aligned} [J]_{v_x v_x} = & \qquad (5.39) \\ &= 2\sum_{l=1}^{L} \frac{1}{\sigma_\ell^2} (2\pi T_s \frac{f_c}{c} cos\theta_\ell)^2 \|b_\ell\|^2 \mathbf{s}_\ell{}^H C^H A_\ell^H \tilde{N}^H \tilde{N} A_\ell C \mathbf{s}_\ell = \\ &= 2\sum_{l=1}^{L} \frac{1}{\sigma_\ell^2} (2\pi T_s \frac{f_c}{c} cos\theta_\ell)^2 \|b_\ell\|^2 \mathbf{s}_\ell{}^H \tilde{N}^H \tilde{N} \mathbf{s}_\ell = \\ &= 2\sum_{l=1}^{L} \frac{1}{\sigma_\ell^2} (2\pi T_s \frac{f_c}{c} cos\theta_\ell)^2 \|b_\ell\|^2 \|\tilde{N}\mathbf{s}_\ell\|^2 = \\ &= 2\sum_{l=1}^{L} \frac{\|b_\ell\|^2 \|\mathbf{s}_\ell\|^2}{N\sigma_\ell^2} N (2\pi T_s \frac{f_c}{c} cos\theta_\ell)^2 \frac{\|\tilde{N}\mathbf{s}_\ell\|^2}{\|\mathbf{s}_\ell\|^2} \qquad (5.40) \end{aligned}$$

If we denote B as the signal's bandwidth, and assume that $B = \frac{F_s}{2}$. Thus, $T_s = \frac{1}{2B}$ and $N = \frac{T}{T_s} = 2BT$.

Substituting in (5.39) we get:

$$\begin{aligned} [J]_{v_x v_x} = & \qquad (5.41) \\ &= 2\sum_{l=1}^{L} \frac{\|b_\ell\|^2 \|\mathbf{s}_\ell\|^2}{N\sigma_\ell^2} 2BT (2\pi \frac{1}{2B} \frac{f_c}{c} cos\theta_\ell)^2 \frac{\|\tilde{N}\mathbf{s}_\ell\|^2}{\|\mathbf{s}_\ell\|^2} = \\ &= 4\left(\pi \frac{f_c}{c}\right)^2 \frac{T}{B} \sum_{l=1}^{L} SNR_\ell cos^2\theta_\ell \frac{\|\tilde{N}\mathbf{s}_\ell\|^2}{\|\mathbf{s}_\ell\|^2} \qquad (5.42) \end{aligned}$$

And similarly:

$$[J]_{v_y v_y} = 4\left(\pi \frac{f_c}{c}\right)^2 \frac{T}{B} \sum_{l=1}^{L} SNR_\ell sin^2\theta_\ell \frac{\|\tilde{N}\mathbf{s}_\ell\|^2}{\|\mathbf{s}_\ell\|^2} \tag{5.43}$$

5.3 Expression for $[J]_{xx}$ and $[J]_{yy}$

Substituting in the expression for $[J]_{xx}$ we get:

$$[J]_{xx} = 2\sum_{l=1}^{L} \frac{1}{\sigma_\ell^2} \left\| \frac{\partial \mathbf{m}_\ell}{\partial x} \right\|^2 \tag{5.44}$$

Hence:

$$[J]_{xx} = \tag{5.45}$$
$$= 2\sum_{l=1}^{L} \frac{1}{\sigma_\ell^2} \left[\left(2\pi T_s \frac{f_c}{c} \frac{\|\vec{v}\|}{d_\ell} sin\phi_\ell sin\theta_\ell \right)^2 \|b_\ell\|^2 \|\tilde{N}\mathbf{s}_\ell\|^2 + \left(\frac{1}{c} cos\theta_\ell \right)^2 \|b_\ell\|^2 \|\dot{\mathbf{s}_\ell}\|^2 - (*) - (*)^H \right]$$

Where:

$$(*) = \tag{5.46}$$
$$= \left[\left(2\pi j T_s \frac{f_c}{c} \frac{\|\vec{v}\|}{d_\ell} sin\phi_\ell sin\theta_\ell \right) b_\ell \tilde{N} A_\ell C \mathbf{s}_\ell \right]^H \left[\frac{1}{c} cos\theta_\ell b_\ell A_\ell C \dot{\mathbf{s}_\ell} \right]$$
$$= -2\pi j T_s \frac{f_c}{c^2} \frac{\|\vec{v}\|}{d_\ell} sin\phi_\ell sin\theta_\ell cos\theta_\ell \|b_\ell\|^2 \mathbf{s}_\ell{}^H \tilde{N} \dot{\mathbf{s}_\ell}$$

And therefore:

$$(*) + (*)^H = \tag{5.47}$$
$$= -2\pi T_s \frac{f_c}{c^2} \frac{\|\vec{v}\|}{d_\ell} sin\phi_\ell sin\theta_\ell cos\theta_\ell \|b_\ell\|^2 (j\mathbf{s}_\ell{}^H \tilde{N} \dot{\mathbf{s}_\ell} - j\dot{\mathbf{s}_\ell}{}^H \tilde{N}^H \mathbf{s}_\ell) =$$
$$= 4\pi T_s \frac{f_c}{c^2} \frac{\|\vec{v}\|}{d_\ell} sin\phi_\ell sin\theta_\ell cos\theta_\ell \|b_\ell\|^2 IM\{\mathbf{s}_\ell{}^H \tilde{N} \dot{\mathbf{s}_\ell}\}$$

Hence:

$$[J]_{xx} = \tag{5.48}$$
$$= 2\sum_{l=1}^{L} \frac{1}{\sigma_\ell^2} [\left(2\pi T_s \frac{f_c}{c} \frac{\|\vec{v}\|}{d_\ell} sin\phi_\ell sin\theta_\ell \right)^2 \|b_\ell\|^2 \|\tilde{N}\mathbf{s}_\ell\|^2 + \dots$$
$$\dots + \left(\frac{1}{c} cos\theta_\ell \right)^2 \|b_\ell\|^2 \|\dot{\mathbf{s}_\ell}\|^2 - \dots$$
$$\dots - 4\pi T_s \frac{f_c}{c^2} \frac{\|\vec{v}\|}{d_\ell} sin\phi_\ell sin\theta_\ell cos\theta_\ell \|b_\ell\|^2 \Im\{\mathbf{s}_\ell{}^H \tilde{N} \dot{\mathbf{s}_\ell}\}]$$

And so:

$$[J]_{xx} = \tag{5.49}$$
$$= 2\sum_{l=1}^{L} \frac{\|b_\ell\|^2\|\mathbf{s}_\ell\|^2}{N\sigma_\ell^2} N[\ \left(2\pi T_s \frac{f_c}{c}\frac{\|\vec{v}\|}{d_\ell} sin\phi_\ell sin\theta_\ell\right)^2 \frac{\|\tilde{N}\mathbf{s}_\ell\|^2}{\|\mathbf{s}_\ell\|^2} + \dots$$
$$\cdots + \left(\frac{1}{c}cos\theta_\ell\right)^2 \frac{\|\dot{\mathbf{s}_\ell}\|^2}{\|\mathbf{s}_\ell\|^2} - \dots$$
$$\cdots - 4\pi T_s \frac{f_c}{c^2}\frac{\|\vec{v}\|}{d_\ell} sin\phi_\ell sin\theta_\ell cos\theta_\ell \frac{\Im\{\mathbf{s}_\ell{}^H \tilde{N}\dot{\mathbf{s}_\ell}\}}{\|\mathbf{s}_\ell\|^2}]$$

Thus:

$$[J]_{xx} = \tag{5.50}$$
$$= 2\sum_{l=1}^{L} SNR_\ell 2BT[\ \left(2\pi \frac{1}{2B}\frac{f_c}{c}\frac{\|\vec{v}\|}{d_\ell} sin\phi_\ell sin\theta_\ell\right)^2 \frac{\|\tilde{N}\mathbf{s}_\ell\|^2}{\|\mathbf{s}_\ell\|^2} + \dots$$
$$\cdots + \left(\frac{1}{c}cos\theta_\ell\right)^2 \frac{\|\dot{\mathbf{s}_\ell}\|^2}{\|\mathbf{s}_\ell\|^2} - \dots$$
$$\cdots - 4\pi \frac{1}{2B}\frac{f_c}{c^2}\frac{\|\vec{v}\|}{d_\ell} sin\phi_\ell sin\theta_\ell cos\theta_\ell \frac{\Im\{\mathbf{s}_\ell{}^H \tilde{N}\dot{\mathbf{s}_\ell}\}}{\|\mathbf{s}_\ell\|^2}]$$

$$[J]_{xx} = \tag{5.51}$$
$$= 4\frac{T}{B}\sum_{l=1}^{L} SNR_\ell[\ \left(\pi \frac{f_c}{c}\frac{\|\vec{v}\|}{d_\ell} sin\phi_\ell sin\theta_\ell\right)^2 \frac{\|\tilde{N}\mathbf{s}_\ell\|^2}{\|\mathbf{s}_\ell\|^2} + \dots$$
$$\cdots + B^2\left(\frac{1}{c}cos\theta_\ell\right)^2 \frac{\|\dot{\mathbf{s}_\ell}\|^2}{\|\mathbf{s}_\ell\|^2} - \dots$$
$$\cdots - 2\pi B \frac{f_c}{c^2}\frac{\|\vec{v}\|}{d_\ell} sin\phi_\ell sin\theta_\ell cos\theta_\ell \frac{\Im\{\mathbf{s}_\ell{}^H \tilde{N}\dot{\mathbf{s}_\ell}\}}{\|\mathbf{s}_\ell\|^2}]$$

Similarly:

$$[J]_{yy} = \tag{5.52}$$
$$= 4\frac{T}{B}\sum_{l=1}^{L} SNR_\ell[\ \left(\pi \frac{f_c}{c}\frac{\|\vec{v}\|}{d_\ell} sin\phi_\ell cos\theta_\ell\right)^2 \frac{\|\tilde{N}\mathbf{s}_\ell\|^2}{\|\mathbf{s}_\ell\|^2} + \dots$$
$$\cdots + B^2\left(\frac{1}{c}sin\theta_\ell\right)^2 \frac{\|\dot{\mathbf{s}_\ell}\|^2}{\|\mathbf{s}_\ell\|^2} + \dots$$
$$\cdots + 2\pi B \frac{f_c}{c^2}\frac{\|\vec{v}\|}{d_\ell} sin\phi_\ell sin\theta_\ell cos\theta_\ell \frac{\Im\{\mathbf{s}_\ell{}^H \tilde{N}\dot{\mathbf{s}_\ell}\}}{\|\mathbf{s}_\ell\|^2}]$$

5.4 Expression for $[J]_{xv_x}$,$[J]_{yv_y}$,$[J]_{xv_y}$ and $[J]_{yv_x}$

$$\left(\frac{\partial \mathbf{m}_\ell}{\partial x}\right)^H \left(\frac{\partial \mathbf{m}_\ell}{\partial v_x}\right) = \tag{5.53}$$

$$\begin{aligned} &= \left[(2\pi j T_s \frac{f_c}{c}\frac{\|\vec{v}\|}{d_\ell} sin\phi_\ell sin\theta_\ell) b_\ell \tilde{N} A_\ell C \mathbf{s}_\ell - \frac{1}{c} cos\theta_\ell b_\ell A_\ell C \dot{\mathbf{s}_\ell}\right]^H \cdot \\ &\cdot \quad \left[-(2\pi j \frac{f_c}{c} cos\theta_\ell) T_s b_\ell \tilde{N} A_\ell C \mathbf{s}_\ell\right] = \\ &= \|b_\ell\|^2 \|s_\ell\|^2 [-\left(2\pi T_s \frac{f_c}{c}\right)^2 \left(\frac{\|\vec{v}\|}{d_\ell} sin\phi_\ell sin\theta_\ell cos\theta_\ell\right) \frac{\|\tilde{N}\mathbf{s}_\ell\|^2}{\|\mathbf{s}_\ell\|2} + \dots \\ &\quad \cdots + \left(\frac{1}{c} cos\theta_\ell\right)^2 (2\pi f_c T_s) j \frac{\dot{\mathbf{s}_\ell}^H \tilde{N} \mathbf{s}_\ell}{\|\mathbf{s}_\ell\|^2}] \end{aligned}$$

Hence:

$$[J]_{xv_x} = \tag{5.54}$$

$$\begin{aligned} &= 2\sum_{l=1}^{L} \frac{\|b_\ell\|^2 \|s_\ell\|^2}{N\sigma_\ell^2} N[-\left(2\pi T_s \frac{f_c}{c}\right)^2 \left(\frac{\|\vec{v}\|}{d_\ell} sin\phi_\ell sin\theta_\ell cos\theta_\ell\right) \frac{\|\tilde{N}\mathbf{s}_\ell\|^2}{\|\mathbf{s}_\ell\|2} - \dots \\ &\quad \cdots - \left(\frac{1}{c} cos\theta_\ell\right)^2 (2\pi f_c T_s) \Im\left\{\frac{\dot{\mathbf{s}_\ell}^H \tilde{N} \mathbf{s}_\ell}{\|\mathbf{s}_\ell\|^2}\right\}] \\ &= 4\frac{T}{B}\sum_{l=1}^{L} SNR_\ell [-\left(\pi \frac{f_c}{c}\right)^2 \left(\frac{\|\vec{v}\|}{d_\ell} sin\phi_\ell sin\theta_\ell cos\theta_\ell\right) \frac{\|\tilde{N}\mathbf{s}_\ell\|^2}{\|\mathbf{s}_\ell\|2} - \dots \\ &\quad \cdots - \left(\frac{1}{c} cos\theta_\ell\right)^2 (\pi f_c B) \Im\left\{\frac{\dot{\mathbf{s}_\ell}^H \tilde{N} \mathbf{s}_\ell}{\|\mathbf{s}_\ell\|^2}\right\}] \end{aligned}$$

And similarly:

$$[J]_{yv_y} = \tag{5.55}$$

$$\begin{aligned} &4\frac{T}{B}\sum_{l=1}^{L} SNR_\ell [\left(\pi \frac{f_c}{c}\right)^2 \left(\frac{\|\vec{v}\|}{d_\ell} sin\phi_\ell sin\theta_\ell cos\theta_\ell\right) \frac{\|\tilde{N}\mathbf{s}_\ell\|^2}{\|\mathbf{s}_\ell\|2} - \dots \\ &\cdots - \left(\frac{1}{c} sin\theta_\ell\right)^2 (\pi f_c B) \Im\{\frac{\dot{\mathbf{s}_\ell}^H \tilde{N} \mathbf{s}_\ell}{\|\mathbf{s}_\ell\|^2}\}] \end{aligned}$$

$$[J]_{xv_y} = \tag{5.56}$$
$$= 4\frac{T}{B}\sum_{l=1}^{L} SNR_\ell[-\left(\pi\frac{f_c}{c}\right)^2\left(\frac{\|\vec{v}\|}{d_\ell}sin\phi_\ell sin^2\theta_\ell\right)\frac{\|\tilde{N}\mathbf{s}_\ell\|^2}{\|\mathbf{s}_\ell\|2} - \dots$$
$$\cdots - \left(\frac{1}{c}\right)^2 sin\theta_\ell cos\theta_\ell(\pi f_c B)\Im\{\frac{\dot{\mathbf{s}}_\ell{}^H\tilde{N}\mathbf{s}_\ell}{\|\mathbf{s}_\ell\|^2}\}]$$

$$[J]_{yv_x} = \tag{5.57}$$
$$= 4\frac{T}{B}\sum_{l=1}^{L} SNR_\ell[\left(\pi\frac{f_c}{c}\right)^2\left(\frac{\|\vec{v}\|}{d_\ell}sin\phi_\ell cos^2\theta_\ell\right)\frac{\|\tilde{N}\mathbf{s}_\ell\|^2}{\|\mathbf{s}_\ell\|2} - \dots$$
$$\cdots - \left(\frac{1}{c}\right)^2 sin\theta_\ell cos\theta_\ell(\pi f_c B)\Im\{\frac{\dot{\mathbf{s}}_\ell{}^H\tilde{N}\mathbf{s}_\ell}{\|\mathbf{s}_\ell\|^2}\}]$$

5.5 Expression for $[J]_{xy}$ and $[J]_{v_xv_y}$

Similarly to the previous sections:

$$\left(\frac{\partial\mathbf{m}_\ell}{\partial x}\right)^H\left(\frac{\partial\mathbf{m}_\ell}{\partial y}\right) = \tag{5.58}$$
$$= -(2\pi T_s\frac{f_c}{c}\frac{\|\vec{v}\|}{d_\ell}sin\phi_\ell)^2 sin\theta_\ell cos\theta_\ell|b_\ell|^2\|\tilde{N}\mathbf{s}_\ell\|^2 + \dots$$
$$\cdots + \frac{1}{c^2}sin\theta_\ell cos\theta_\ell|b_\ell|^2\|\dot{\mathbf{s}}_\ell\|^2 + \dots$$
$$\cdots + (2\pi T_s\frac{f_c}{c^2}\frac{\|\vec{v}\|}{d_\ell}sin\phi_\ell)(j + 2sin^2\theta_\ell\Im\{\dot{\mathbf{s}}_\ell{}^H\tilde{N}\mathbf{s}_\ell\})$$

Thus:

$$[J]_{xy} = \tag{5.59}$$
$$= 2\sum_{l=1}^{L}\frac{|b_\ell|^2\|\mathbf{s}_\ell\|^2}{N\sigma_\ell^2}N[-(2\pi T_s\frac{f_c}{c}\frac{\|\vec{v}\|}{d_\ell}sin\phi_\ell)^2 sin\theta_\ell cos\theta_\ell|b_\ell|^2\|\tilde{N}\mathbf{s}_\ell\|^2 + \dots$$
$$\cdots + \frac{1}{c^2}sin\theta_\ell cos\theta_\ell|b_\ell|^2\|\dot{\mathbf{s}}_\ell\|^2 + \dots$$
$$\cdots + 4\pi T_s\frac{f_c}{c^2}\frac{\|\vec{v}\|}{d_\ell}sin\phi_\ell sin^2\theta_\ell\Im\{\dot{\mathbf{s}}_\ell{}^H\tilde{N}\mathbf{s}_\ell\}]$$

And:

$$\left(\frac{\partial \mathbf{m}_\ell}{\partial v_x}\right)^H \left(\frac{\partial \mathbf{m}_\ell}{\partial v_y}\right) = -(2\pi \frac{f_c}{c} T_s)^2 sin\theta_\ell cos\theta_\ell |b_\ell|^2 \|\tilde{N}\mathbf{s}_\ell\|^2 \tag{5.60}$$

Thus:

$$[J]_{v_x v_y} = -4\frac{T}{B}(\pi \frac{f_c}{c})^2 \sum_{l=1}^{L} SNR_\ell sin\theta_\ell cos\theta_\ell \frac{\|\tilde{N}\mathbf{s}_\ell\|^2}{\|\mathbf{s}_\ell\|^2} \tag{5.61}$$

Chapter 6

Numerical Results

6.1 General

In the following chapter we present the results of several simulations of the discussed scenarios and algorithms.

We start by comparing the performance of the suggested method to the conventional method and to the CRB in various SNR. We present the results of the simulation for a circular array of receivers and for a linear array of receivers, and for a pulse transmitted signal, and a random transmitted signal.

Later, we present an experimental study of the various cost functions. In that section we present contour plots of the cost function for various signals and for various receiver geometries. The cost functions are presented in order to acquire some intuition regarding their behaviour, and in order to understand the challenges of finding their global maximum.

Finally, we present an experimental study of the relation between the performance of the suggested method and the geometry of the scenario. We perform the analysis using the CRB that gives a good estimation of the performance of the ML estimator for small error scenarios(i.e. high SNR scenarios).

6.2 Performance vs. SNR - Circular Receivers Array, Pulse Signal

In this scenario, 6 receivers are evenly spaced on a circle with a radius of 1[km] around the origin. The transmitter is located 100[m] away from the origin on the x-axis, and 300[m] away from the origin on the y-axis, as can be seen in figure (6.1). The transmitter's velocity is 200[m/s] in the x direction and 200[m/s] in the y direction.

The transmitted signal is a pulse signal with a carrier frequency of 1[GHz]. The signal is sampled with a sampling frequency of 2^{23}[hz]$\simeq$ 8.4 [MHz]. The length of the sampling interval in each receiver is 512 [samples]$\simeq 60[\mu$ Sec]. The simulated transmitted signal is a band-limited pulse signal, so that only the main lobe of the spectrum of the signal is not filtered. Figure (6.2) shows the signal in the time-domain, while the power spectrum of the original transmitted signal is shown in figure (6.3).

For every point on the graphs of the performance simulation , an average of 10 estimations is taken. Since the discussed problem requires the estimation of both the position and velocity of the transmitter, two parameters are calculated and presented in two different graphs for each SNR: The RMS of the positioning error, and the RMS of the velocity estimation error.

In this scenario, we compare the performance of the direct unknown signals method, the direct known signals method, and the conventional two-step unknown signals method. For known signals we use the $L2$ cost function in order to estimate the position and velocity of the transmitter. For unknown signals we use the $L3$ cost function.

For the evaluation of the performance of the conventional method, we use the two step method. At the first step the TDOA and FDOA are estimated between each pair of receivers, and later used in a WLS cost function at the second step. We determine the optimal weights of the measurements using the known signals CRB for TOA and FOA measurements, as explained in subsection (1.1.4).

The CRLB for known signals is presented on the graphs as well for reference.

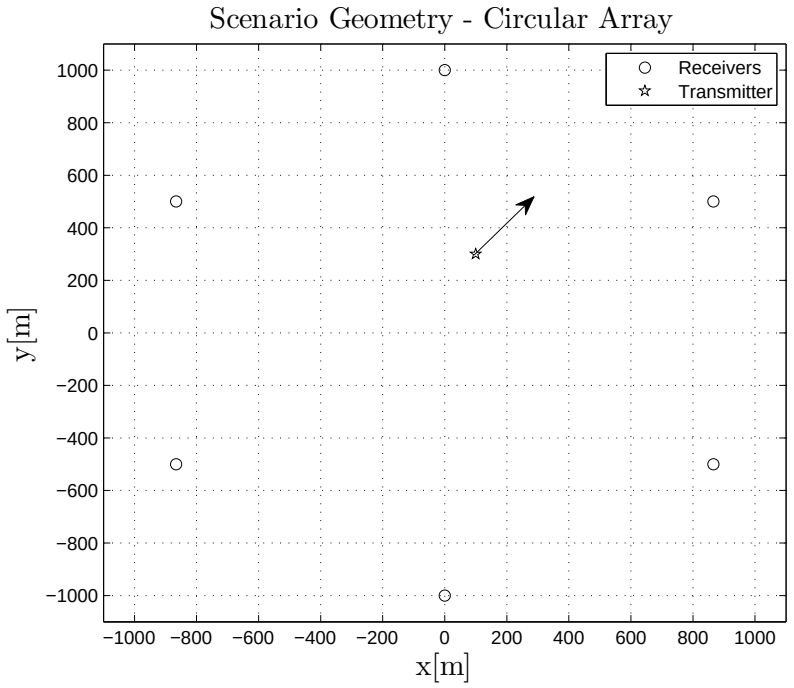

FIGURE 6.1: Scenario Geometry: The 6 receivers are evenly spread on a circle with a radius of $1[km]$ around the origin. The transmitter is located at $(100, 300)[m, m]$ with velocity $(200, 200)[m/s, m/s]$.

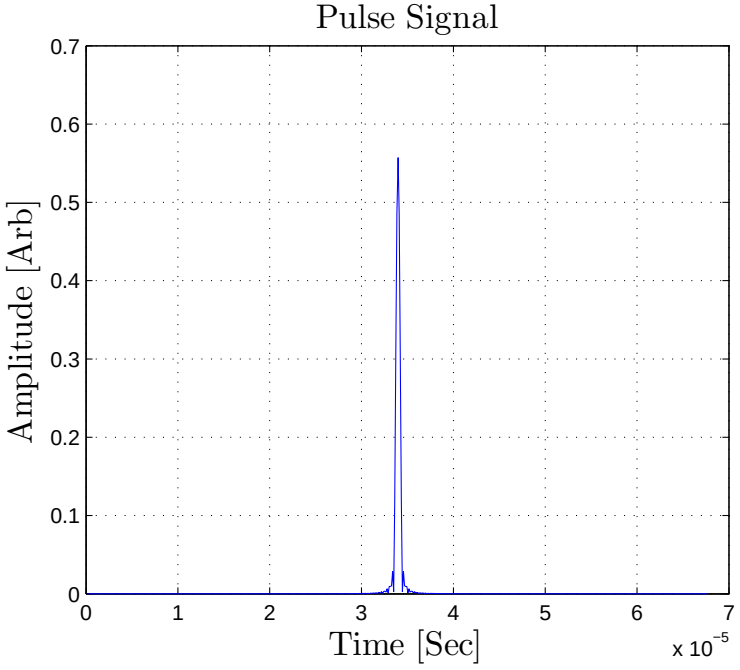

FIGURE 6.2: Time domain plot of the transmitted pulse signal

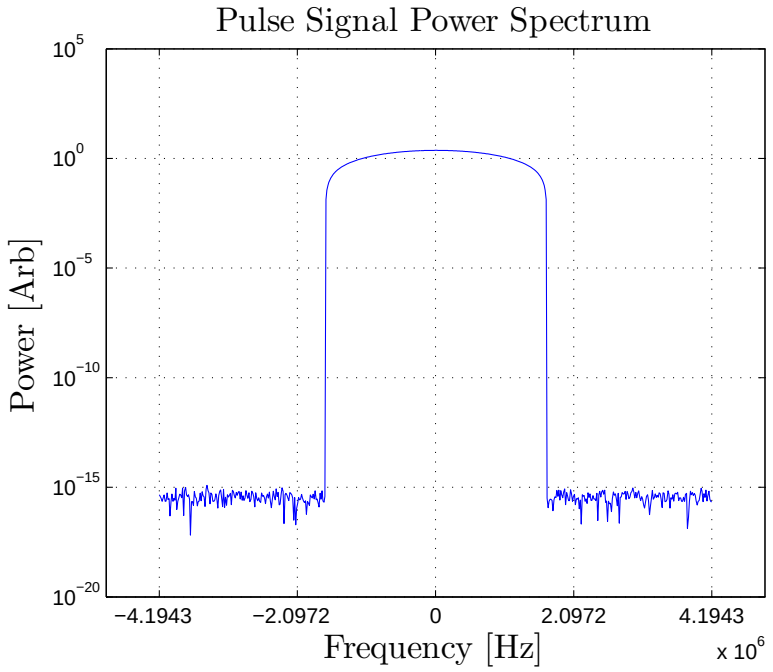

FIGURE 6.3: Power spectrum plot of the transmitted pulse signal

Results

As can be seen in figure (6.4) and figure (6.5) the direct one-step methods achieve better results than the conventional method.

Looking at figure (6.4) we can see that in the examined SNRs, in the presented scenario, the known signals direct method achieves the position estimation CRLB for all of the examined SNR range.

Both the conventional two-step method and the direct unknown signals method achieve the bound at high SNR, but it is obvious that at lower SNR, the direct method shows better performance.

It is interesting to mention that both the known signals method, and the unknown signals methods achieve the known signals CRLB at high SNR. We would expect that only the known signals methods would achieve the known signals CRLB while the unknown signals methods would achieve the unknown signals CRLB, which is outside the scope of this work. Apparently, in this scenario, the unknown signals and the known signals CRLB are close enough so we are not able to distinct their asymptotic performance.

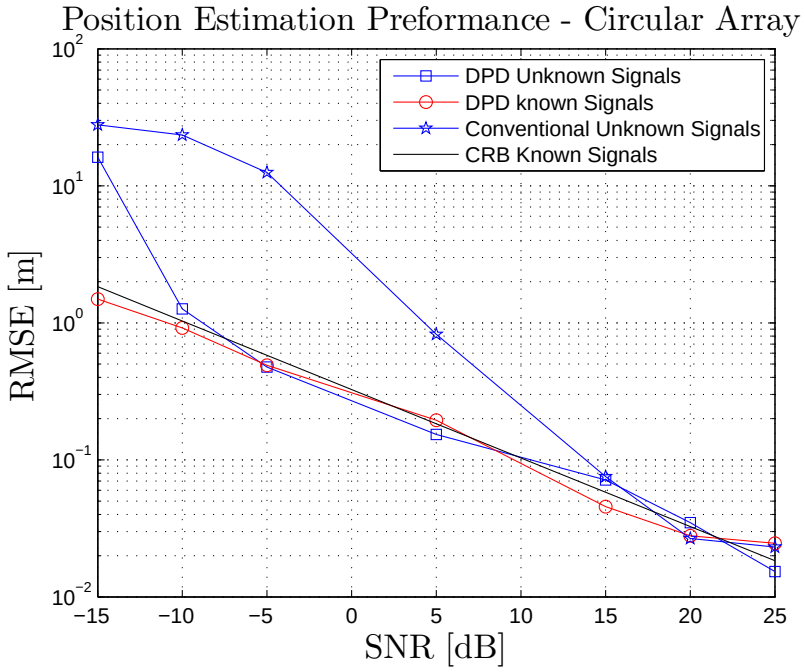

FIGURE 6.4: Position Estimation Performance Vs. SNR - Circular Receivers Array

The superiority of the direct methods is less obvious in the results of the velocity estimation, as can be seen in figure (6.5). Nevertheless, in spite of the noisy velocity estimations, it can be seen from figure (6.5) that the direct methods show better performance than the conventional method, and that the known signals direct method shows better performance than the unknown signals method in lower SNRs.

It is interesting to notice that none of the velocity estimation methods reach the CRLB at any of the examined SNRs. A possible explanation is that the frequency shift caused by the Doppler effect in this scenario is extremely small compared to the sampling frequency divided by the number of samples, so that quantization errors in the simulation raise the effective noise level, and do not allow the performance achieve the CRLB.

6.3 Performance vs. SNR - Circular Receivers Array, Random Signal

In this scenario, we used the same circular array geometry as in section (6.2), and the same transmitter position and velocity.

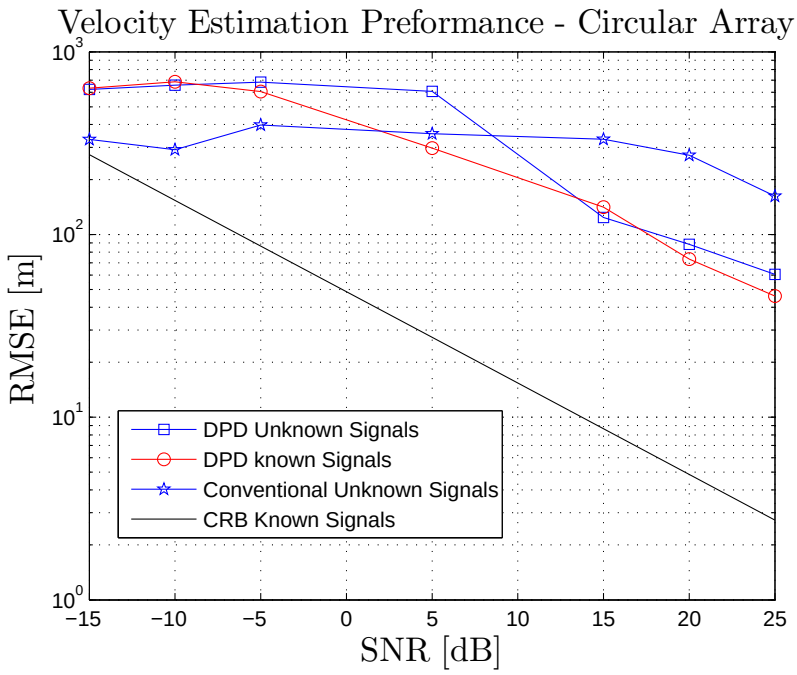

FIGURE 6.5: Velocity Estimation Performance Vs. SNR - Circular Receivers Array

The transmitted signal is a random signal with a carrier frequency of 1[GHz]. The signal is sampled with a sampling frequency of 2^{20}[hz]$\simeq$ 1 [MHz]. The length of the sampling interval in each receiver is 512 [samples]$\simeq$ 488[μ Sec].
The simulated transmitted signal is a band-limited random signal. Figure (6.6) shows random signal in the time domain. The power spectrum of the signal is shown in figure (6.7).

For every point on the graph, an average of 10 estimations is taken. Since the discussed problem requires the estimation of both the position and velocity of the transmitter, two parameters are calculated and presented in two different graphs for each SNR: The RMS of the positioning error, and the RMS of the velocity estimation error.

In this scenario, we compare the performance of the direct unknown signals method and the conventional two-step unknown signals method.

For the evaluation of the performance of the direct unknown signals method we use the $L3$ cost function.

For the evaluation of the performance of the conventional method, we use the two step method. At the first step the TDOA and FDOA are estimated between each pair of

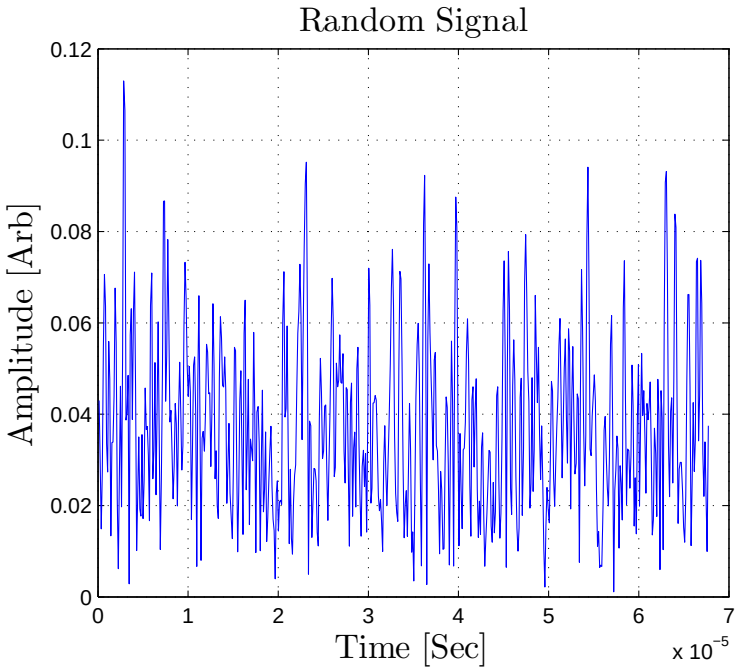

FIGURE 6.6: Time domain plot of the transmitted random signal

receivers, and later used in a WLS cost function at the second step. We determine the optimal weights of the measurements using the known signals CRB for TOA and FOA measurements, as explained in subsection (1.1.4).

The CRLB for known signals is presented on the graphs as well for reference.

Results

As can be seen in figure (6.8) and figure (6.9) the direct one-step method achieves better results than the conventional two-step method.

Looking at figure (6.8) we can see that in the examined SNRs, in the presented scenario, the known signals direct method achieves the position estimation CRLB for almost all of the examined SNR range.

Both the conventional two-step method and the direct unknown signals method achieve the bound at high SNR, but it is obvious that at lower SNR, the direct method shows better performance.

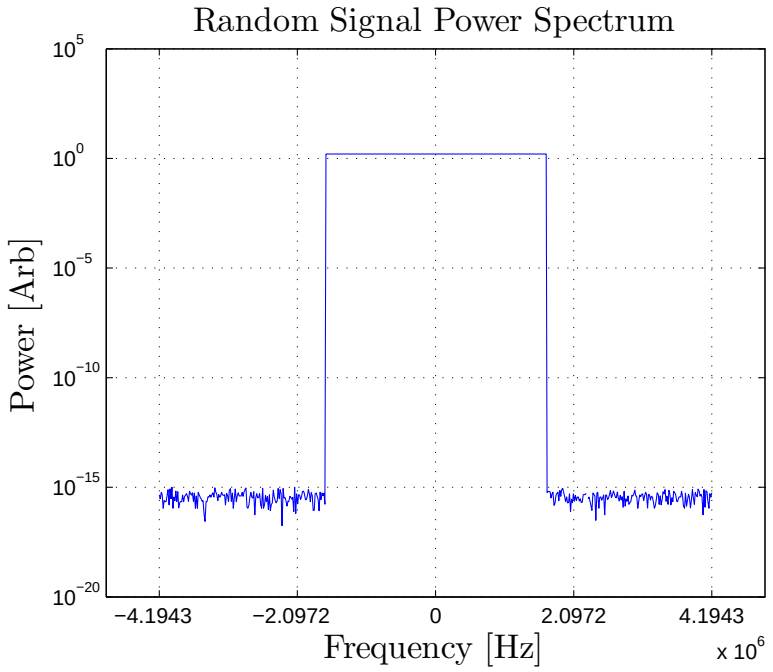

FIGURE 6.7: Power spectrum plot of the transmitted random signal

It is interesting to mention that both methods, which are both unknown signals methods, achieve the known signals CRLB at high SNR. We would expect that the unknown signals method would not achieve the known signals CRLB, whose derivation is outside the scope of this work. Apparently, in this scenario, the unknown signals and the known signals CRLB are close enough so we are not able to distinct between them.

The superiority of the suggested direct method is a little less obvious in the results of the velocity estimation, as can be seen in figure (6.9). Nevertheless, in spite of the noisy velocity estimations, it can be seen from figure (6.9) that both methods achieve the known-signals CRLB for almost all of the examined SNR range. Due to the noisy velocity estimations, it is hard to determine whether there is an advantage in the performance of the direct one-step method over the conventional two-step method.

Similarly to the position estimation performance, we note that although the two methods are unknown-signals methods, they achieve the known-signals CRLB for the velocity estimation performance as well.

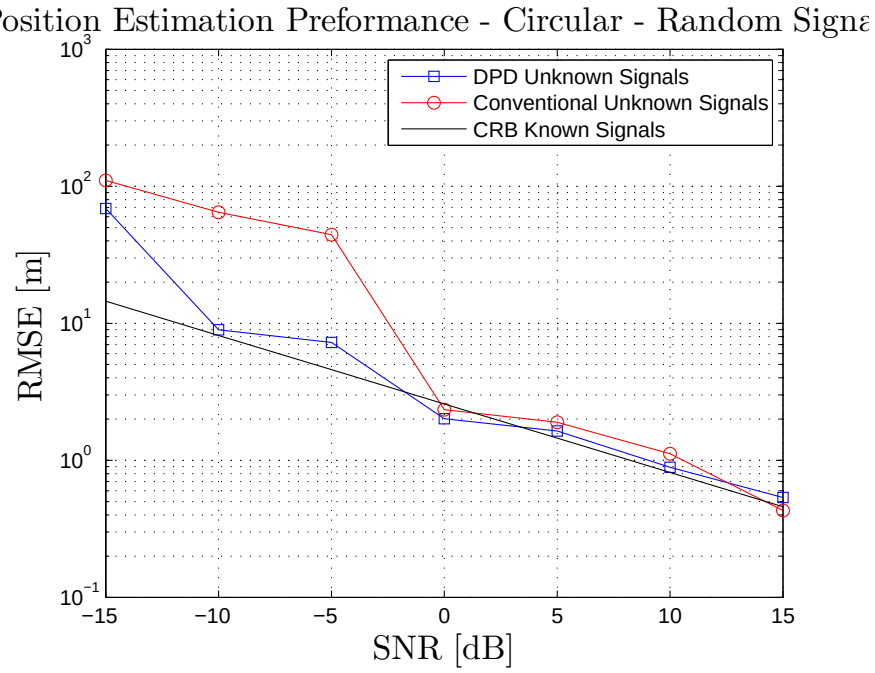

FIGURE 6.8: Position Estimation Performance Vs. SNR - Circular Receivers Array, Random Signal

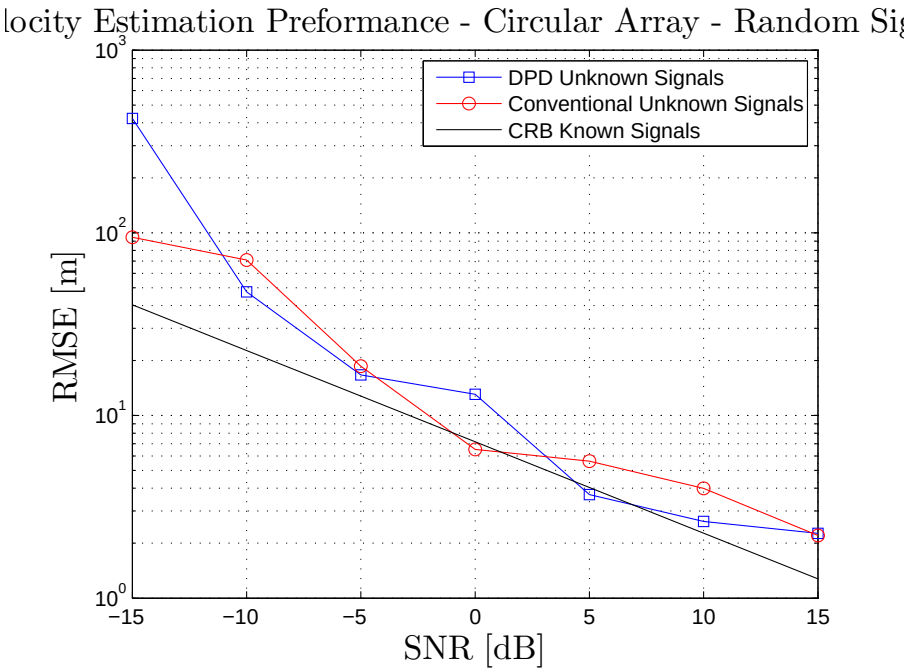

FIGURE 6.9: Velocity Estimation Performance Vs. SNR - Circular Receivers Array, Random Signal

6.4 Performance vs. SNR - Linear Receivers Array, Pulse Signal

In this scenario, 6 receivers are evenly spaced on the x-axis in a 2[km] long linear array around the origin. The transmitter is located 100[m] away from the origin on the x-axis, and 1000[m] away from the origin on the y-axis, as can be seen in figure (6.10). The transmitter's velocity is 200[m/s] in the x direction and 200[m/s] in the y direction.

The transmitted signal is a pulse signal with a carrier frequency of $1[GHz]$. The signal is sampled with a sampling frequency of 2^{23}[Hz]$\simeq$ 8.4 [MHz]. The length of the sampling interval in each receiver is 512 [samples]$\simeq 60[\mu$ Sec]. The simulated transmitted signal is the same band-limited pulse signal that we used in section(6.2). Figure (6.2) shows the signal in the time-domain, while the power spectrum of the original transmitted signal is shown in figure (6.3).

For every point on the graph, an average of 10 estimations is taken. Since the discussed problem requires the estimation of both the position and the velocity of the transmitter, two parameters are calculated and presented in two different graphs for each SNR: The RMS of the positioning error, and the RMS of the velocity estimation error.

In this scenario, we compare the performance of the direct unknown signals method, the direct known signals method, and the conventional two-step method. For known signals we use the $L2$ cost function in order to estimate the position and velocity of the transmitter. For unknown signals we use the $L3$ cost function.

For the evaluation of the performance of the conventional method, we use the two step method. At the first step the TDOA and FDOA are estimated between each pair of receivers, and later used in a WLS cost function at the second step. We determine the optimal weights of the measurements using the known signals CRB for TOA and FOA measurements, as explained in subsection (1.1.4).

The CRLB for known signals is presented on the graphs as well for reference.

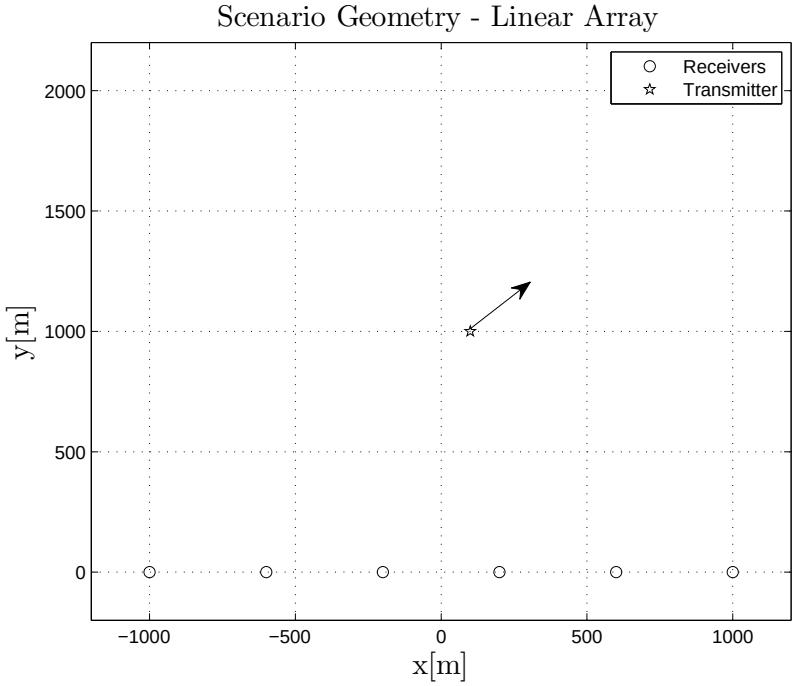

FIGURE 6.10: Scenario Geometry: The 6 receivers are evenly spread on a the x-axis in a $2[km]$ long linear array around the origin. The transmitter is located at $(100, 1000)$[m,m] with velocity $(200, 200)$[m/s,m/s].

Results

As can be seen in figure (6.11) and figure (6.12) the direct one-step methods achieve better results than the conventional two-step method.

In figure (6.11) we can see that in the examined SNRs, in the presented scenario, the known signals direct one-step method achieves the position estimation CRLB for all of the examined SNR range.

Both the conventional two-step method and the direct unknown signals method do not achieve the known signals CRLB, but show a different kind of asymptotic behaviour. Because the derivation of the unknown signals CRLB is out of the scope of this work, we can only assume that both methods mentioned above achieve the unknown signals CRLB in high SNR.

Nevertheless, although both methods show similar asymptotic behaviour in high SNR, it is clear that the direct unknown signals achieves better performance than the conventional method in low SNR scenarios.

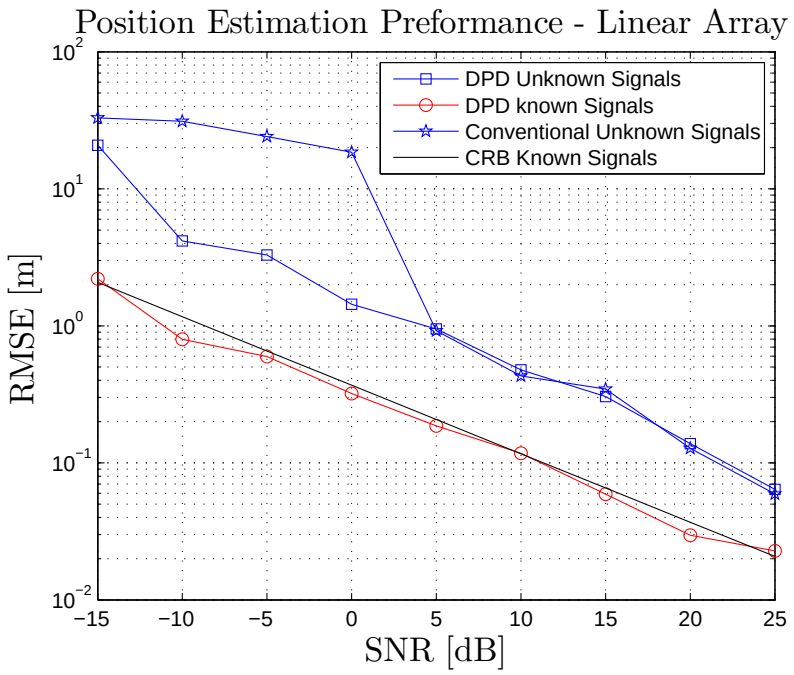

FIGURE 6.11: Position Estimation Performance Vs. SNR - Linear Receivers Array, Pulse Signal

The superiority of the suggested direct method is less obvious in the results of the velocity estimation, as can be seen in figure (6.12). Nevertheless, in spite of the noisy velocity estimations, it can be seen from figure (6.12) that the direct methods show better performance than the conventional method, and that the known signals direct method shows slightly better performance than the unknown signals method in lower SNRs.

It is interesting to notice that none of the velocity estimation methods achieve the CRLB at any of the examined SNRs. A possible explanation is that the frequency shift caused by the Doppler effect in this scenario is extremely small compared to the sampling frequency divided by the number of samples, so that quantization errors in the simulation raise the effective noise level, and do not allow the performance achieve the CRLB.

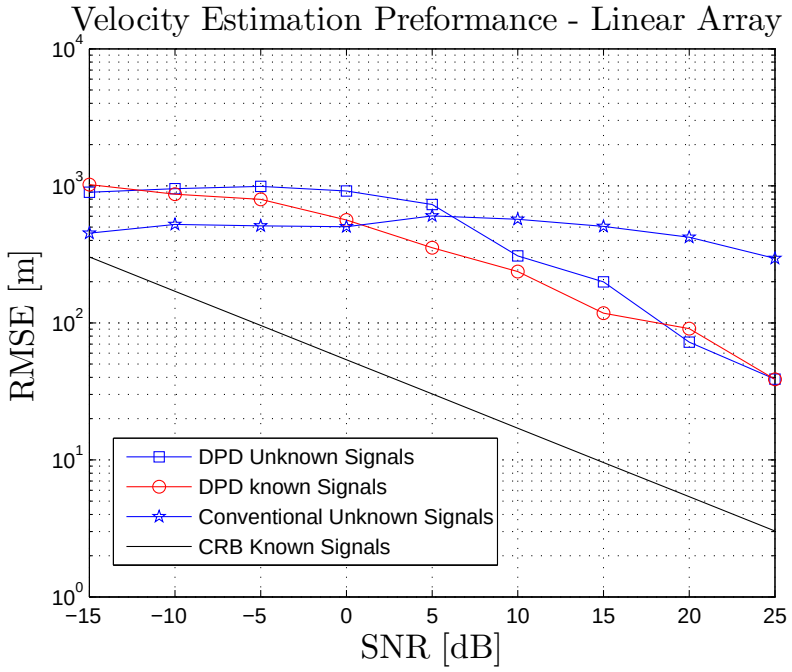

FIGURE 6.12: Velocity Estimation Performance Vs. SNR - Linear Receivers Array, Pulse Signal

6.5 Experimental Study Of The Cost Function

6.5.1 General

In the following section we present an experimental study, in which we show a few examples of the cost function. We present several contour plots to demonstrate the behaviour of the different cost functions, for several different geometries, and for different signal types.

We present the contour plots of the unknown signals, the known signals and the conventional cost functions, for pulse signals and for random signals, and for a linear array of receivers and for a circular array of receivers.

We present the different plots in order to provide a better understanding of the problem presented in this work and some intuition for it.

For creating the contour plots of the cost function we simulated a signal with a carrier frequency of 1[GHz] sampled at a sampling frequency of $2^{23} \simeq 8.4$[MHz]. The sampled signals we used were 512 samples long. The velocity of the transmitter was $(200, 200)$

[m/s] in all of the simulated scenarios. Wherever a circular receivers array is mentioned, the circular array presented in figure (6.1) is used, and whenever a linear receivers array is mentioned, the circular array presented in figure (6.10)

The cost functions presented were simulated in a noiseless environment with an infinite SNR, in order to demonstrate the behaviour of the cost function without the effect of noise.

The cost functions in this work are four-dimensional, they are evaluated in the two-dimensional position space and in the two-dimensional velocity space. Therefore, they are difficult to visualize. In this experimental study, we chose to demonstrate the behaviour of the cost functions in the two-dimensional position space, where the cost functions are evaluated at the true value of the velocity of the transmitter.

6.5.2 Pulse Signals

We start by examining the contour plots of the various cost functions for pulse signals. In this subsection, we use the same pulse signal described by figure (6.2) and figure (6.3), with the transmitter parameters described above.

Circular Array of Receivers

Figure (6.13) presents the contour plot of the unknown signals one-step cost function for a circular array of receivers, figure (6.14) presents the contour plot of the known signals one-step cost function and figure (6.15) presents the contour plot of the conventional two-step cost function.

We notice that the one-step cost functions show mild apparent difference, as seen in figure (6.13) and (6.14). We notice that for this scenario geometry, where the transmitter is located near the center of the circular array of receivers, the peak of the one-step cost functions is circular.

We notice that the width of the peak around the transmitter is rather small. In order to find the peak for performing the position estimation, a high resolution grid is required.

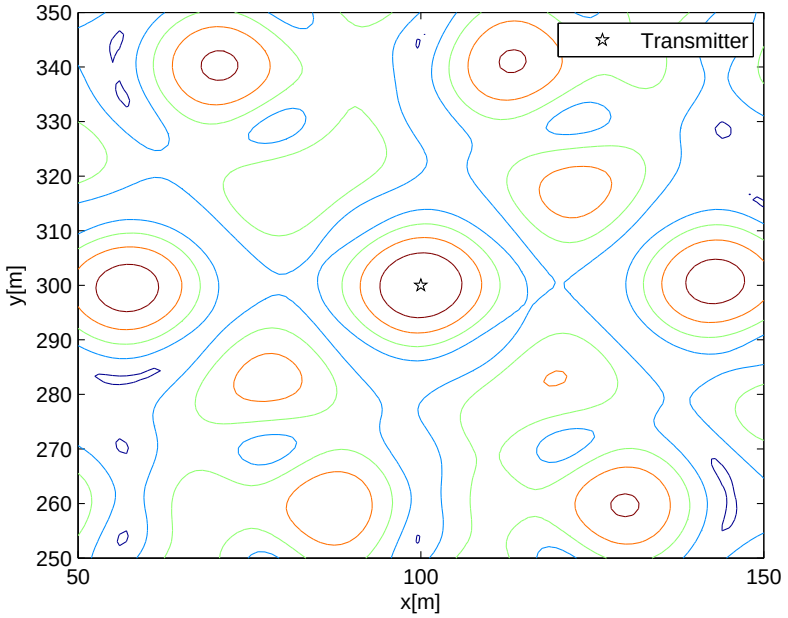

FIGURE 6.13: Contour plot of the unknown signals cost function, for a circular receivers array and a pulse signal

The cost function is clearly not convex outside of the area of the peak, so gradient based search methods can be used only for performing fine tuning once the peak was found, and cannot be used in order to find the peak.

We notice that there is some ambiguity in the cost function of the one-step methods, and some secondary peaks could be seen around the main peak. Although the value of the cost function at the real position of the transmitter is higher than its value at the secondary peaks, these peaks might prevent the algorithm from finding the real position of the transmitter, if the resolution of the grid search is not high enough.

As can be seen in figure (6.15), the peak around the real position of the transmitter is rather wide, there are no apparent ambiguities, and the cost-function is convex for a wide area. As can be seen further in a wider view of the conventional cost function in figure (6.16), the cost-function maintains its convexity for a much wider area than the one-step methods. Thus, using gradient based methods, and avoiding grid search is possible with the conventional cost function.

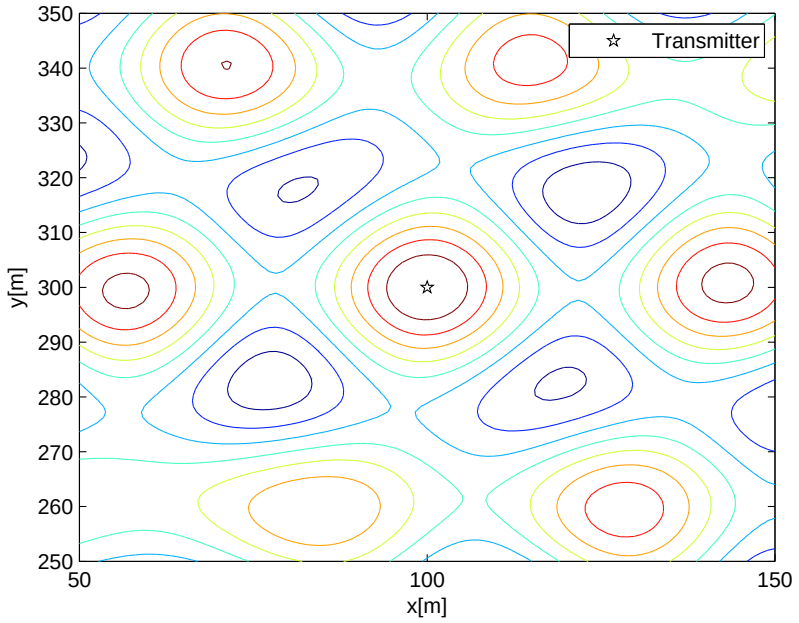

FIGURE 6.14: Contour plot of the known signals cost function, for a circular receivers array and a pulse signal

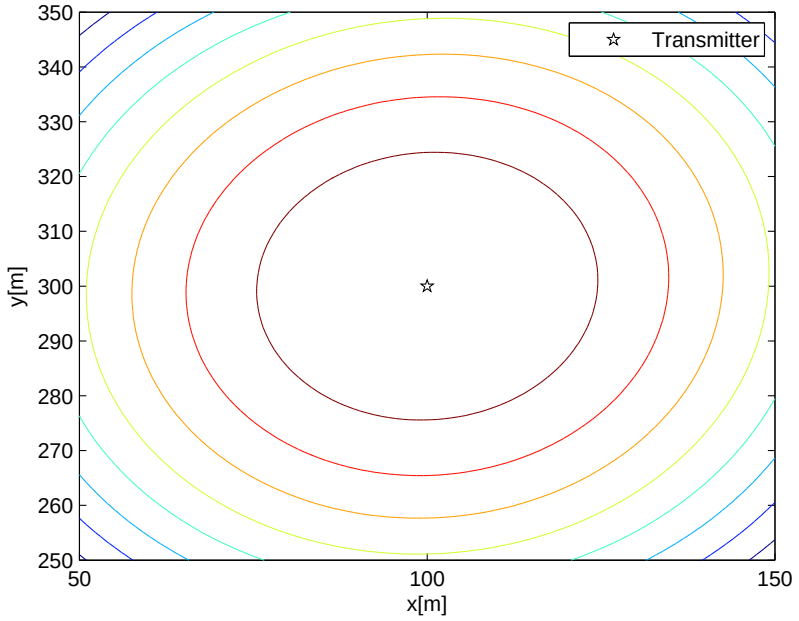

FIGURE 6.15: Contour plot of the conventional two-step cost function, for a circular receivers array and a pulse signal

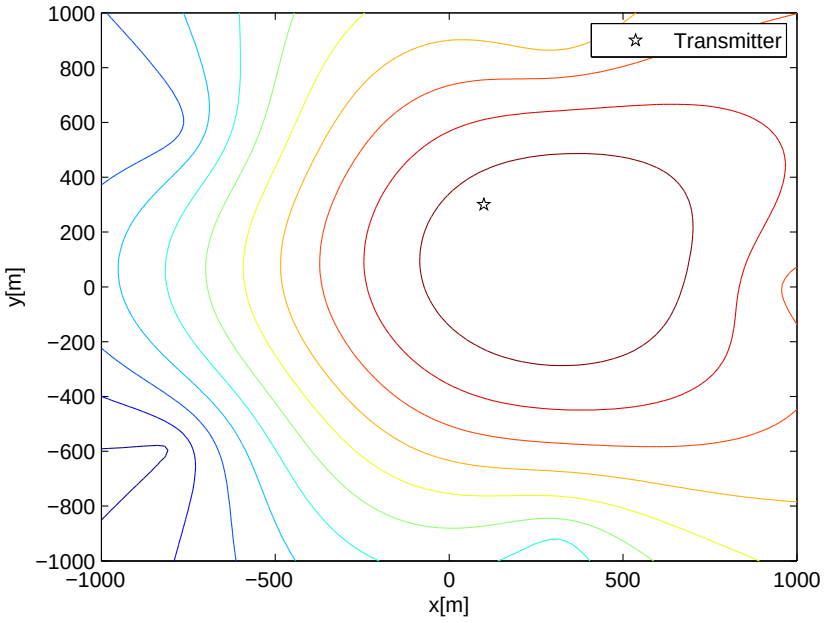

FIGURE 6.16: Wide view contour plot of the conventional two-step cost function, for a circular receivers array and a pulse signal

Linear Array of Receivers

Figure (6.17) presents the contour plot of the unknown signals one-step cost function for a linear array of receivers, figure (6.18) presents the contour plot of the known signals one-step cost function and figure (6.19) presents the contour plot of the conventional two-step cost function.

We notice that contrary to the previous scenario, in this scenario there is a significant difference between all of the cost functions.

In figure (6.17) we can see that in this scenario the peak of the cost function around the position of the transmitter is no longer circular, but rather elliptical.

The known signals cost function, on the other hand, keeps the same peak characteristics as in the circular array of receivers scenario, as can be seen in figure (6.18).

We notice that in the cost function of both one-step methods, the width of the peak around the transmitter is rather small. In order to find the peak for performing the position estimation, a high resolution grid is required.

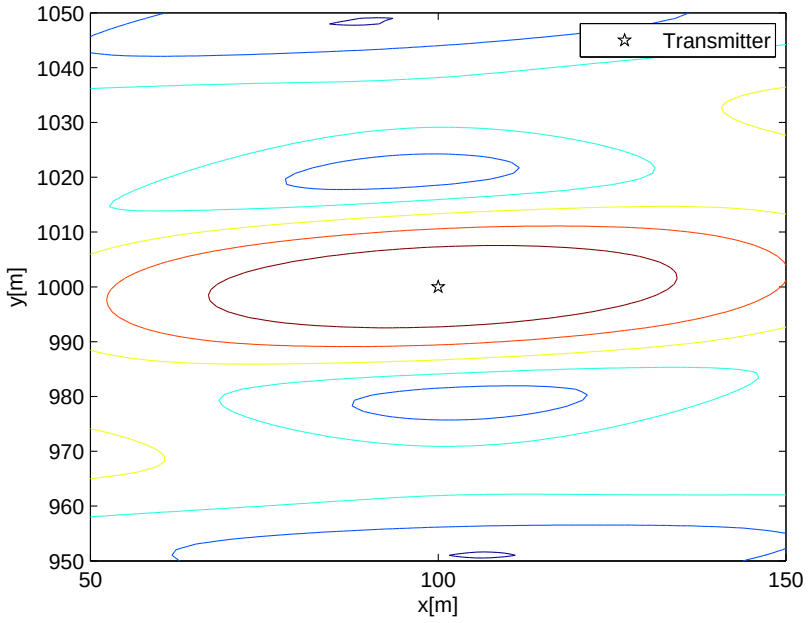

FIGURE 6.17: Contour plot of the unknown signals cost function, for a linear receivers array and a pulse signal

The cost function of both one-step methods is clearly not convex outside of the area of the peak, so gradient based search methods can be used only for performing fine tuning once the peak was found, and cannot be used in order to find the peak.

We notice that there is some ambiguity in the cost function of the one-step methods, and some secondary peaks could be seen around the main peak. Although the value of the cost function at the real position of the transmitter is higher than its value at the secondary peaks, these peaks might prevent the algorithm from finding the real position of the transmitter, if the resolution of the grid search is not high enough.

As can be seen in figure (6.19), the peak around the real position of the transmitter is rather wide, there are no apparent ambiguities, and the cost-function is convex for a wide area. As can be seen further in a wider view of the conventional cost function in figure (6.20), the cost-function maintains its convexity for a much wider area than the one-step methods. Thus, using gradient based methods, and avoiding grid search is possible with the conventional cost function.

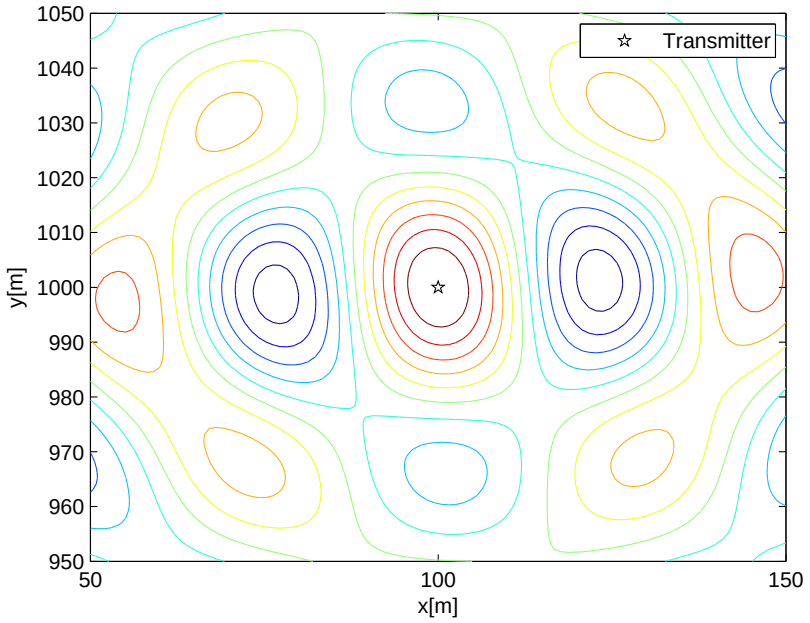

FIGURE 6.18: Contour plot of the known signals cost function, for a linear receivers array and a pulse signal

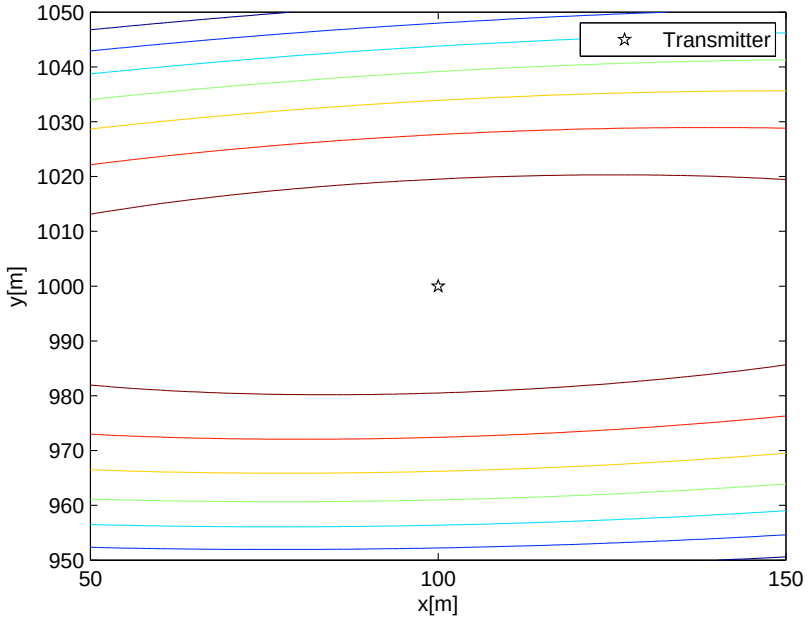

FIGURE 6.19: Contour plot of the conventional two-step cost function, for a linear receivers array and a pulse signal

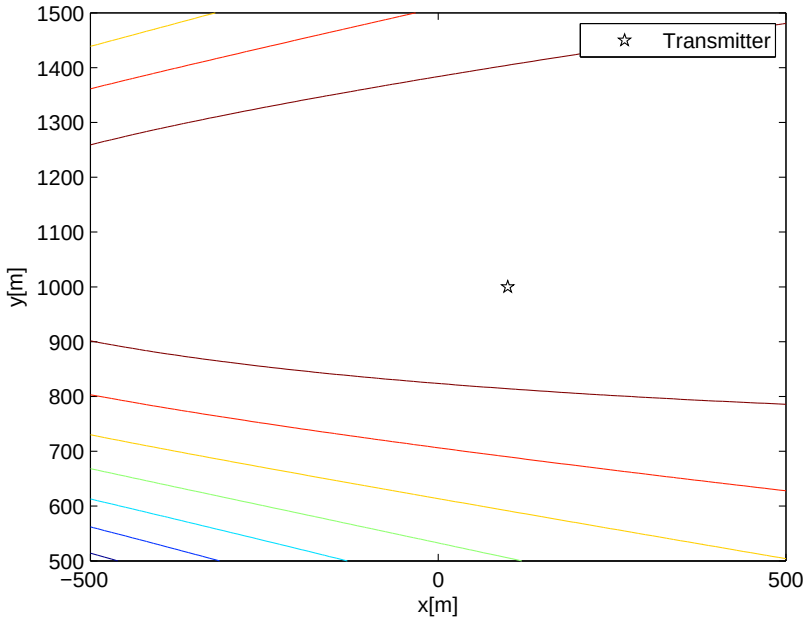

FIGURE 6.20: Wide view contour plot of the conventional two-step cost function, for a linear receivers array and a pulse signal

6.5.3 Random Signals

We continue by examining the contour plots of the various cost functions for random signals. Since the properties of the cost function strongly depend on the properties of the signal, it is interesting to examine the cost function of different signals. In this subsection, we use the same random signal described by figure (6.6) and figure (6.7), with the transmitter parameters described above.

Circular Array of Receivers

Figure (6.21) presents the contour plot of the unknown signals one-step cost function for a circular array of receivers, figure (6.22) presents the contour plot of the known signals one-step cost function and figure (6.23) presents the contour plot of the conventional two-step cost function.

We notice that the one-step unknown signals cost function for the random signal has a smaller peak than for the pulse signal, and less ambiguity, as is demonstrated further by figure (6.24).

For the one-step known signals cost function we see that there is a slightly larger peak than the unknown-signals cost function. Some significant ambiguity is also apparent, as can be further seen in figure (6.25).

We notice that for this scenario geometry, where the transmitter is located near the center of the circular array of receivers, the peak of the one-step cost functions is circular.

We notice that the width of the peak around the transmitter is rather small. In order to find the peak for performing the position estimation, a high resolution grid is required.

The cost function is clearly not convex outside of the area of the peak, so gradient based search methods can be used only for performing fine tuning once the peak was found, and cannot be used in order to find the peak.

As can be seen in figure (6.23), the peak of the conventional two-step cost function around the real position of the transmitter is rather wide, there are no apparent ambiguities, and the cost-function is convex for a wide area.

As can be seen further in a wider view of the conventional cost function in figure (6.26), the cost-function maintains its convexity for a much wider area than the one-step methods. Thus, using gradient based methods, and avoiding grid search is possible with the conventional cost function.

Linear Array of Receivers

Figure (6.27) presents the contour plot of the unknown signals one-step cost function for a circular array of receivers, figure (6.28) presents the contour plot of the known signals one-step cost function and figure (6.29) presents the contour plot of the conventional two-step cost function.

We notice that the one-step unknown signals cost function for the random signal has slightly less ambiguity than for the pulse signal, as is demonstrated further by figure (6.30). As in the case of the pulse signal, we see that the peak of the one-step unknown signals method has an elliptical shape.

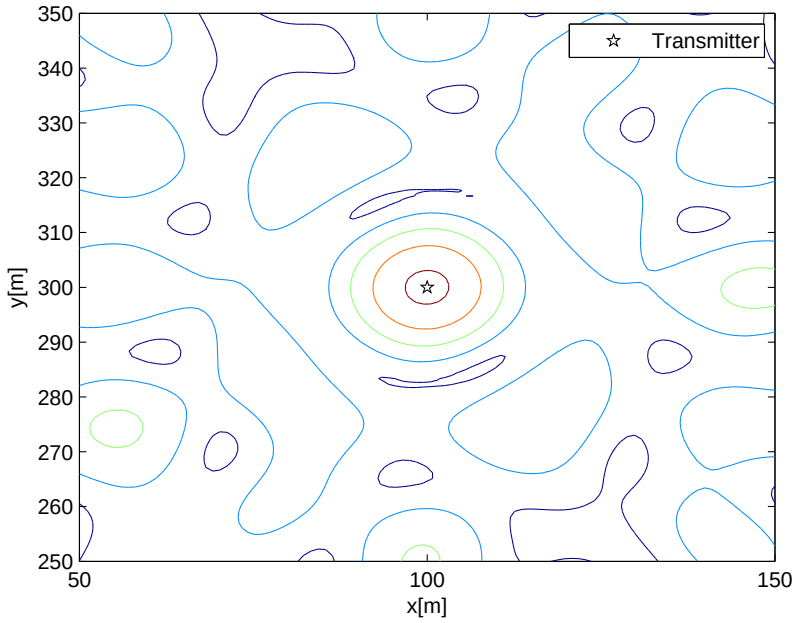

FIGURE 6.21: Contour plot of the unknown signals cost function, for a circular receivers array and a random signal

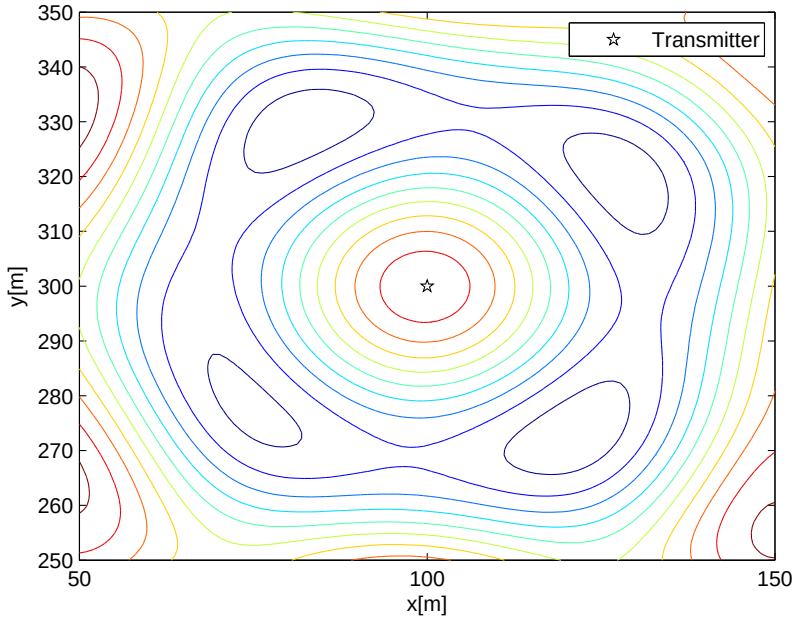

FIGURE 6.22: Contour plot of the known signals cost function, for a circular receivers array and a random signal

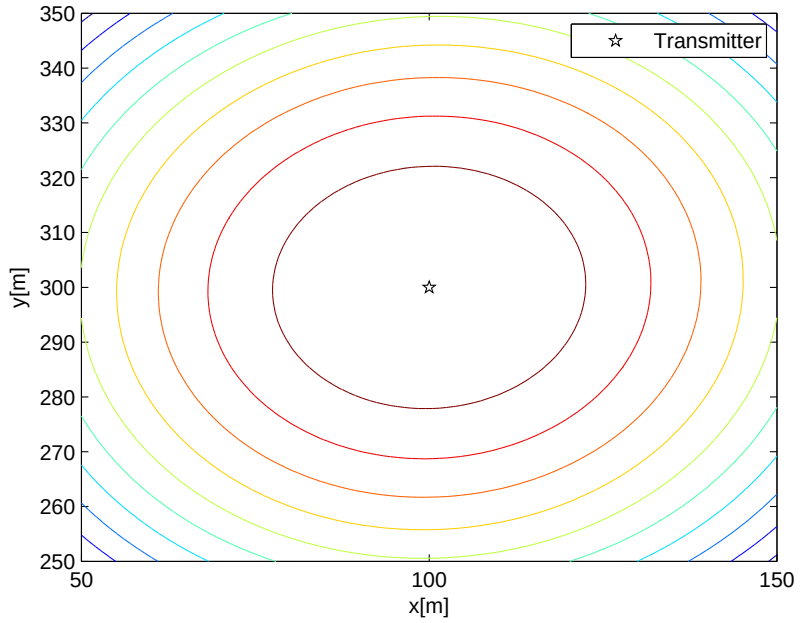

FIGURE 6.23: Contour plot of the conventional two-step signals cost function, for a circular receivers array and a random signal

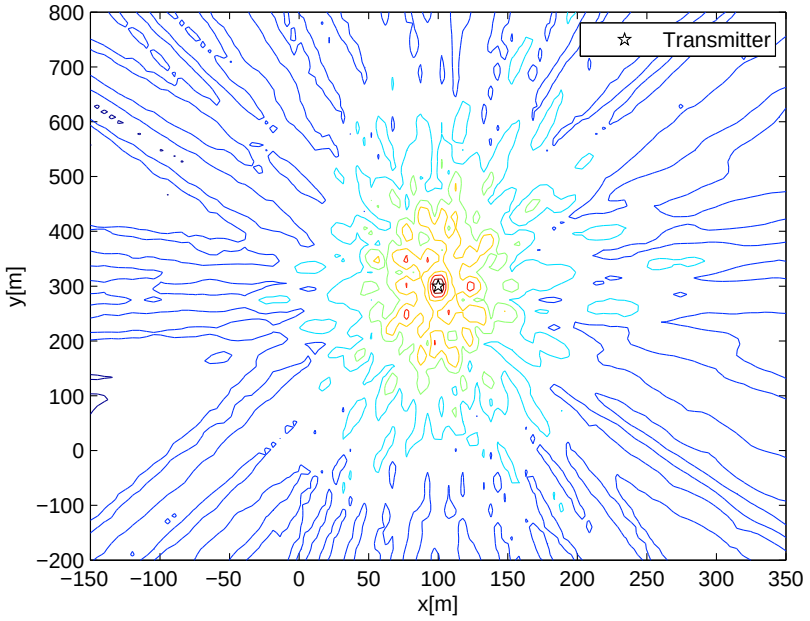

FIGURE 6.24: Wide view contour plot of the unknown signals cost function, for a circular receivers array and a random signal

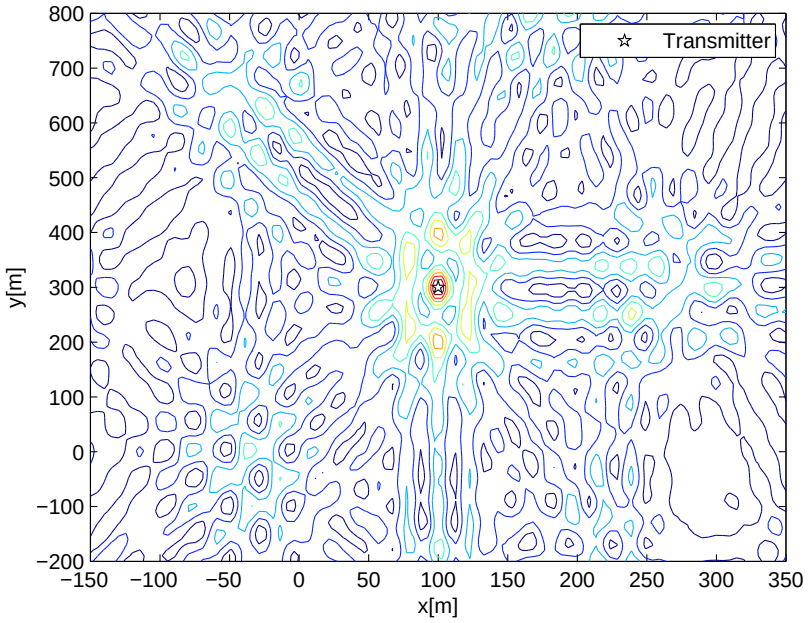

FIGURE 6.25: Wide view contour plot of the known signals cost function, for a circular receivers array and a random signal

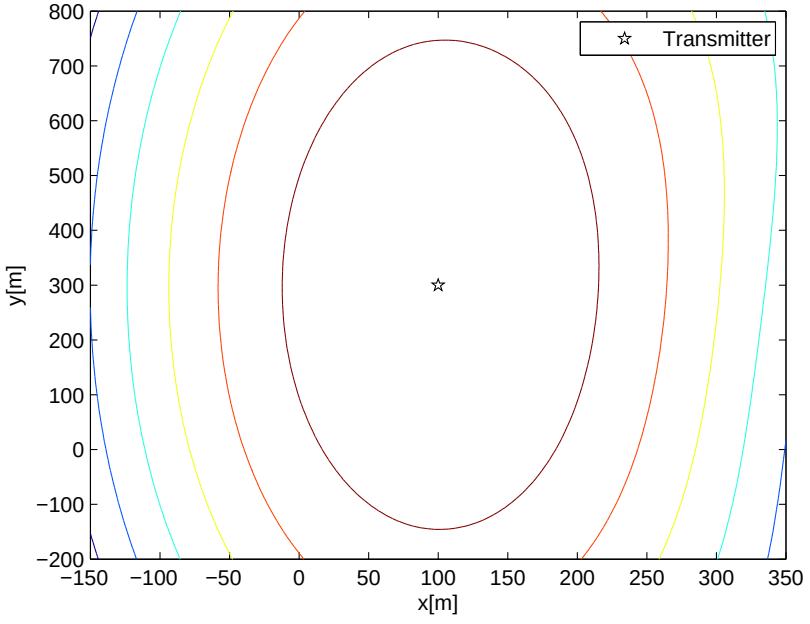

FIGURE 6.26: Wide view contour plot of the conventional two-step cost function, for a circular receivers array and a random signal

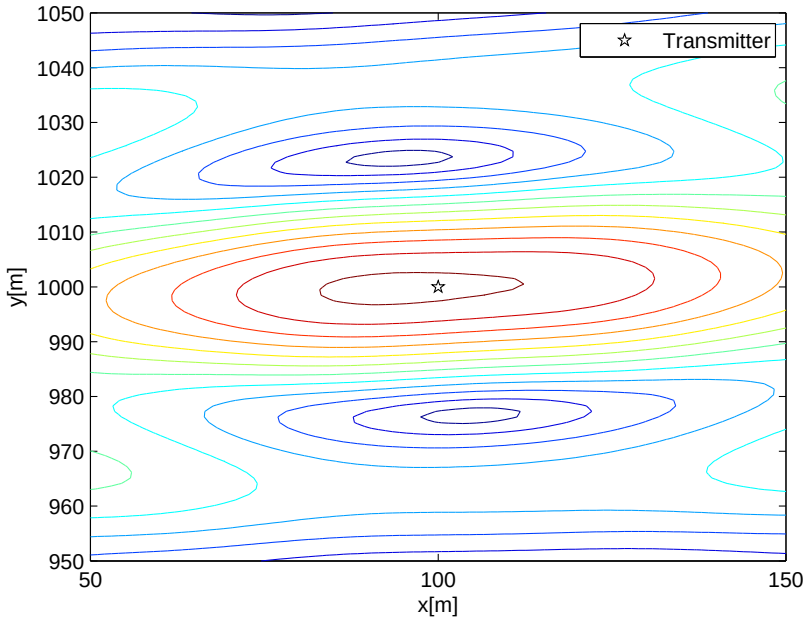

FIGURE 6.27: Contour plot of the unknown signals cost function, for a linear receivers array and a random signal

The one-step known signals cost function for the random signal shows great similarity to the known signals cost function for the pulse signal. Significant ambiguity around the main peak is demonstrated by figure (6.30).

We notice that the width of the peak of the one-step methods around the transmitter is rather small. In order to find the peak for performing the position estimation, a high resolution grid is required.

The cost function is clearly not convex outside of the area of the peak, so gradient based search methods can be used only for performing fine tuning once the peak was found, and cannot be used in order to find the peak.

As can be seen in figure (6.29), the peak of the conventional two-step cost function around the real position of the transmitter is rather wide, there are no apparent ambiguities, and the cost-function is convex for a wide area.

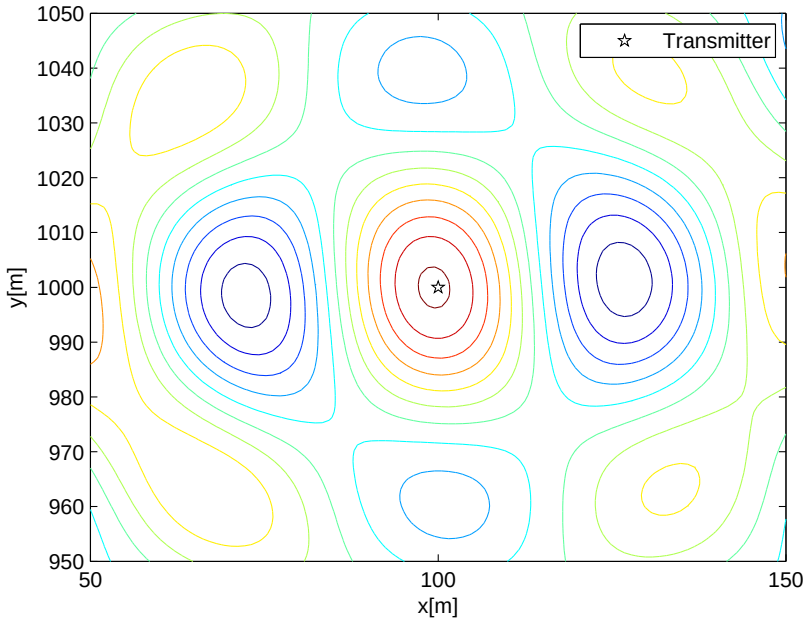

FIGURE 6.28: Contour plot of the known signals cost function, for a linear receivers array and a random signal

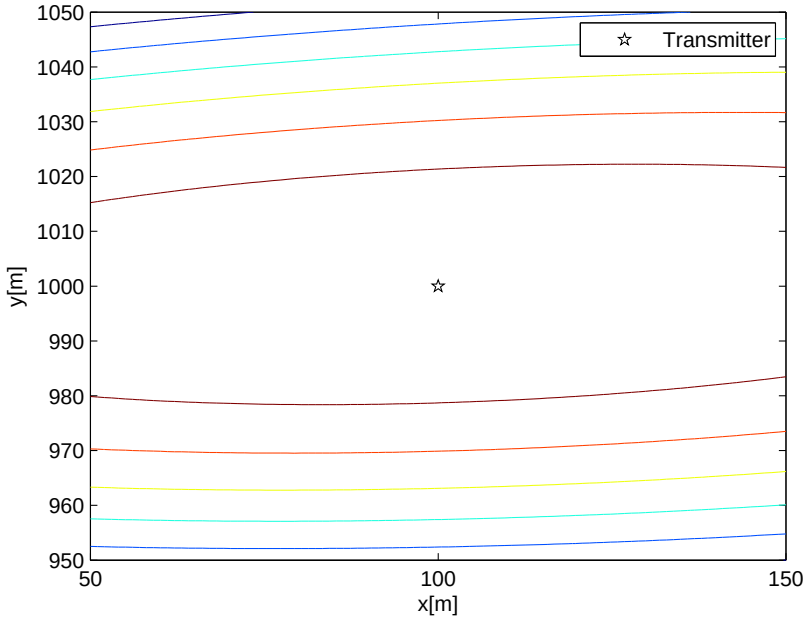

FIGURE 6.29: Contour plot of the conventional two-step signals cost function, for a linear receivers array and a random signal

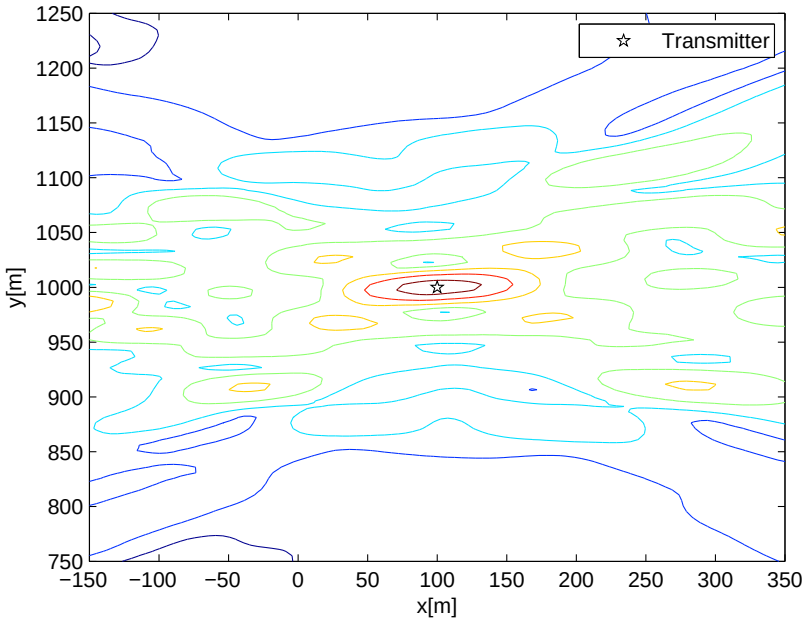

FIGURE 6.30: Wide view contour plot of the unknown signals cost function, for a linear receivers array and a random signal

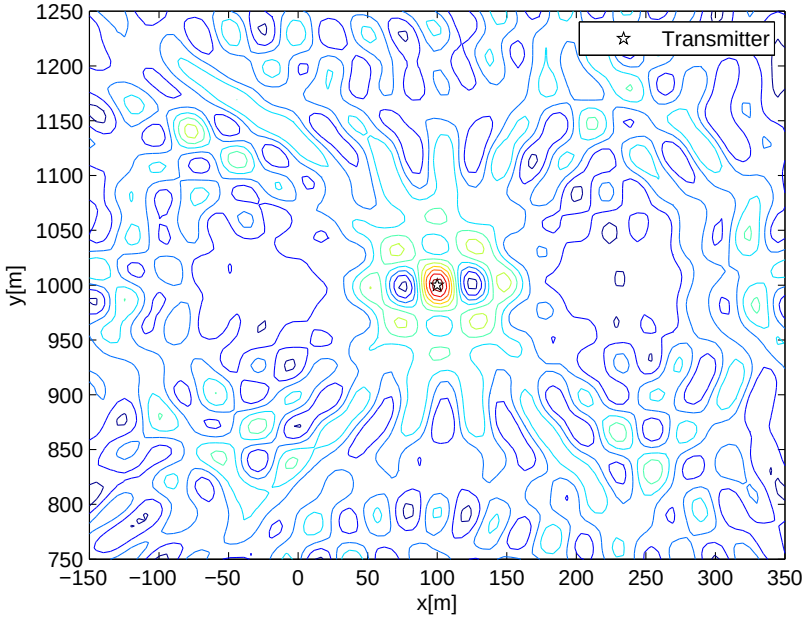

FIGURE 6.31: Wide view contour plot of the known signals cost function, for a linear receivers array and a random signal

6.6 Performance Vs. Transmitter Position

In this section we explore the relation between the performance of the algorithm, and the scenario geometry. We explore the expected performance of the algorithm for different positions of the transmitter in relation to the receivers array. We present the results of this simulation for a circular array of receivers and for a linear array of receivers. Nevertheless, this method could be applied to any arbitrary array of receivers, and could be used in order to design optimal receivers geometry for a given scenario.

Designing an optimal receivers array strongly depends on the characteristics of the problem, on its constraints and on the definition of the goals of the system [20]. Possible constraints could be the number of available receivers and the area on which they can lye. Possible definitions of the goals of the system could be maximizing the performance for a single possible transmitter position, or maximizing the average performance over an area on which the transmitter lies. Since the problem of designing an optimal receivers array depends on describing a specific scenario, we will only describe a method that enables customizing the design for a specific scenario.

In order to estimate the performance of the algorithm in this section, we only used the results of the CRB, and did not use true simulation results of our suggested algorithm. The main reason for doing that is that in order to create a good quality contour plot of the expected performance, the performance has to be evaluated in many different positions. Performing Monte-Carlo simulations shows much better computational complexity than calculating the CRB at a given position, and as we know from theory and as we presented in the previous simulations, the performance of our estimator is asymptotically efficient, so that calculating the CRB gives us a good estimate of the performance of our algorithm.

For each receiver array geometry we created a two contour plots, one for the position estimation performance, and one for the velocity estimation performance. The height of every point on the plot represents the calculated CRB for a transmitter with the above parameters, transmitting from that point. In order to make the plots more informative, we present the calculated CRB on a logarithmic scale, where the height of every point

is the $\log_{10}$ of the CRB at that point. The contour lines are equally on a logarithmic scale.

The parameters used for the simulation in this section are similar to the parameters used in the above sections. For this simulation, we used 512 samples of a random signal, transmitted with a carrier frequency of 1[GHz], and sampled with a $2^{15} \simeq 32$[KHz] sampling frequency with a 25[dB] SNR in all of the receivers. The velocity of the transmitter in all of the simulations in this section is $[200, 200]$[m/s].

Circular Receivers Array

For analysing the circular receivers array scenario, we used the receivers array described in figure (6.1), where there are 6 receivers arranged on a circle with a radius of 1[km].

From figures (6.32) and (6.33) we can learn that for this scenario, the spatial behaviour of the estimation performance of the position and of the estimation performance of the velocity is quite similar.

From both figures, we can learn that the best estimation performance of a circular array is inside the circle. We can see that the estimation performance is almost uniform inside the circle, where there is slightly better performance near the center of the circle.

Outside the circle, we can see that the performance decreases the farther the transmitter is from the center of the circle.

Here, an interesting phenomenon can be noticed. While the position estimation performance is more or less isotropic, the velocity estimation performance declines dramatically when the moving away from the center of the circle in the direction of the speed of the transmitter. We can explain the decline in performance on that line, in the fact that on the line that goes through the center of the circle in the direction of the velocity of the transmitter, the differential Doppler effect is minimal, and the difference between the received frequency in the receivers is minimal. Thus, the estimation of the velocity, whose information is found only in the frequency difference is affected.

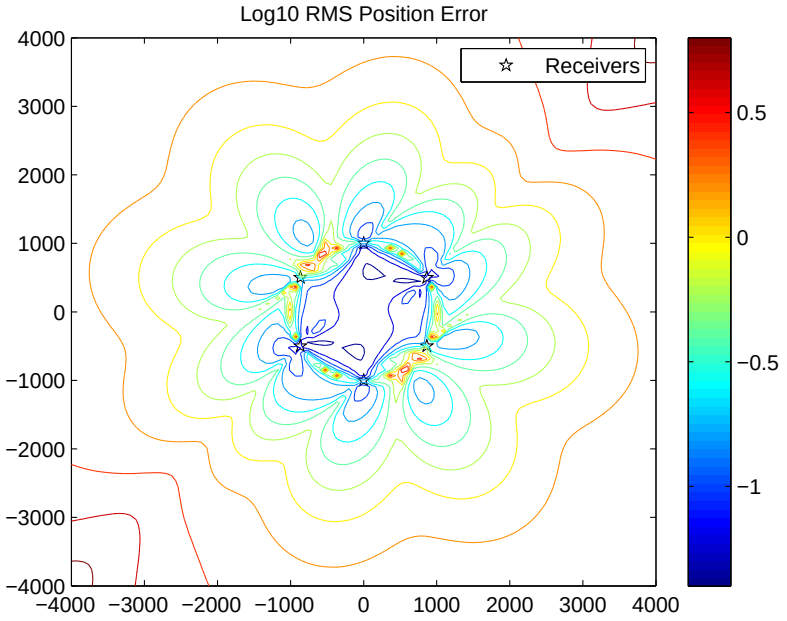

FIGURE 6.32: Position Estimation Preformance Vs. Position for a circular array and a random signal. We can see that the best performance is achieved inside the circle, where the performance of the algorithm is almost uniform. Outside the circle, the performance decreases as we move away from the center of the circle.

This phenomenon can be observed also in the position estimation performance, but it is less dominant, since the information about the position of the transmitter is found both in the time difference, and in the frequency difference of the received signals.

Linear Receivers Array

For analysing the linear receivers array scenario, we used the receivers array described in figure (6.10), where there are 6 receivers that are equally spaced on a 2[km] long line on the x-axis.

From figures (6.34) and (6.35) we can learn that for this scenario, the spatial behaviour of the estimation performance of the position and of the estimation performance of the velocity is quite similar.

From both figures, we can learn that the best estimation performance of a linear array is achieved as close as possible to the center of the array. We can see that the farther the transmitter is from the center of the array, the worse the performance.

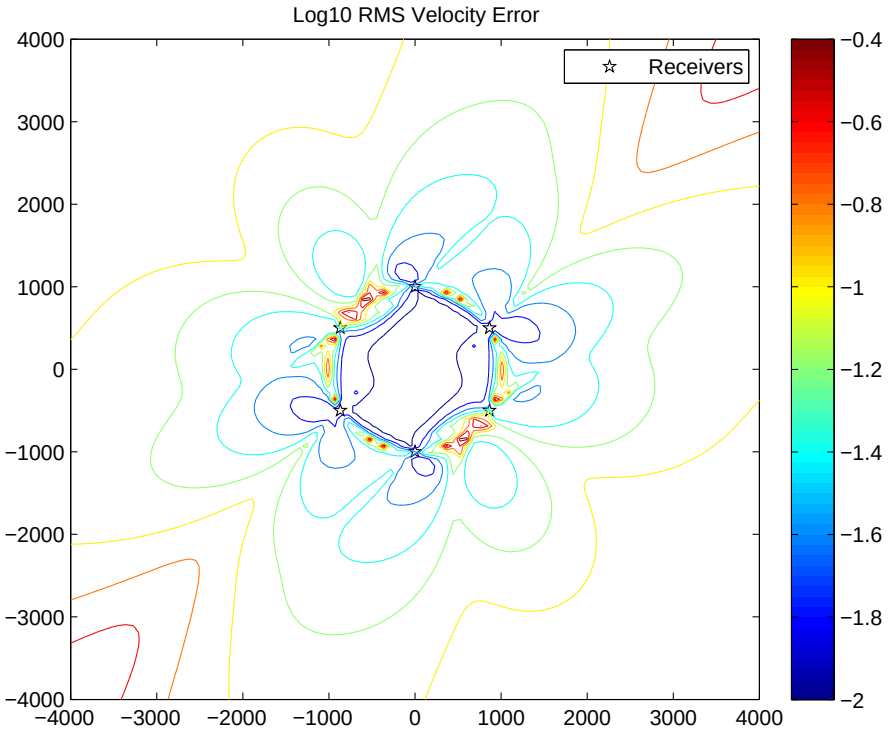

FIGURE 6.33: Velocity Estimation Preformance Vs. Position for a circular array and a random signal. We can see that the best performance is achieved inside the circle, where the performance of the algorithm is almost uniform. Outside the circle, the performance decreases as we move away from the center of the circle. It is interesting to notice, that the performance is worst on the line that goes through the center of the circle in the direction of the velocity of the transmitter.

We notice an interesting phenomenon that occurs on the line on which the receivers lye. On that line, the performance decreases dramatically as we move further away from the receivers array. We can notice this phenomenon both in the position estimation performance and in the velocity estimation performance. This decrease of performance occurs because on that line, the Doppler shift received by all of the receivers is identical, thus, the differential Doppler zeros in all of the receivers, regardless of the velocity of the transmitter or its position on that line. The effect is much more dominant in the velocity estimation, because the velocity estimation depends only on the Doppler shifts, as opposed to the position estimation that also depends on the time delays.

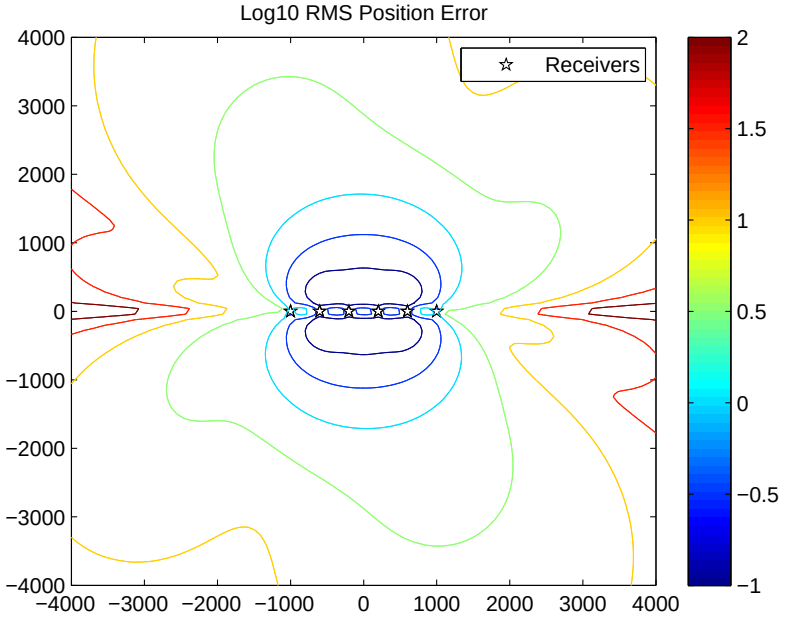

FIGURE 6.34: Position Estimation Preformance Vs. Position for a linear array and a random signal

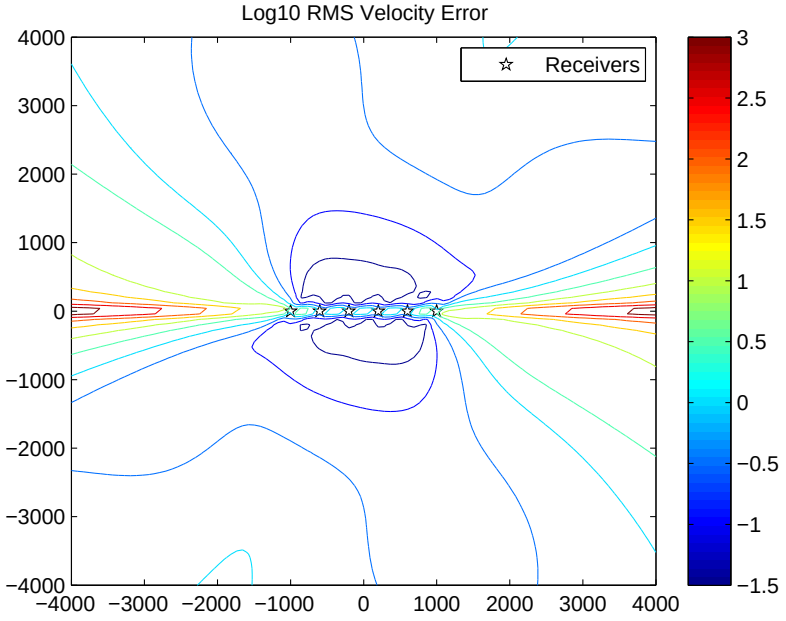

FIGURE 6.35: Velocity Estimation Preformance Vs. Position for a linear array and a random signal

Random Receivers Array

In order to examine a more "realistic" scenario, and in order to see how we can use the intuition acquired in the circular and linear array examples, we examine the performance of a randomly placed receivers array.

In the examined scenario, 6 receivers were placed randomly around the origin. All other scenario parameters, including the velocity of the transmitter are identical to the two previous scenarios.

As can be seen in figure (6.36) and in figure (6.37) similar behaviour to the previous scenarios is observed. We can see that the position estimation performance is more isotropic,while the velocity estimation performance is more direction dependent. Similarly to the previous scenarios, we can relate that phenomenon to the fact that the information about the velocity is found only in the Doppler shift of the signals, while the information about the position is found both in the Doppler shifts and in the time delays of the signals.

We can also notice that, similarly to the previous scenarios, the best performance is achieved in the area contained by the receivers. The performance gradually drops as the transmitter is positioned further away from the array of receivers.

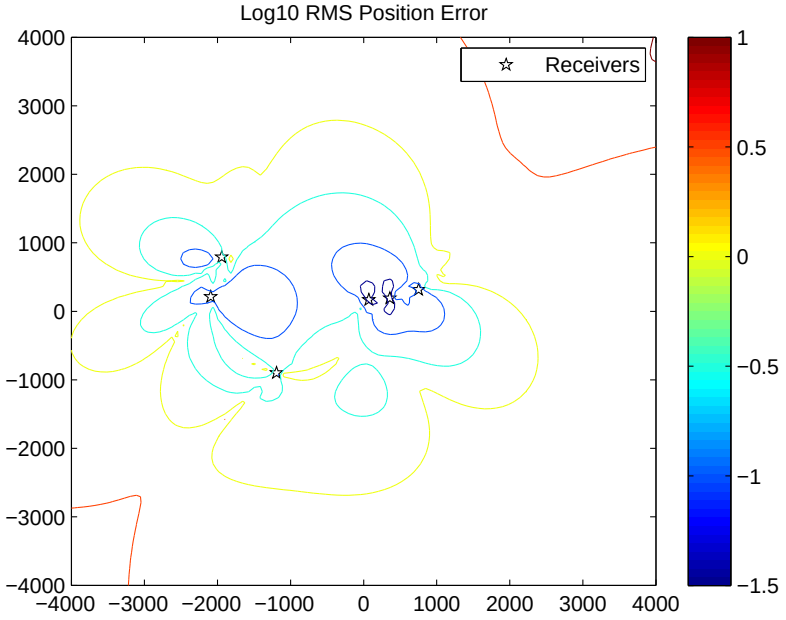

FIGURE 6.36: Position Estimation Preformance Vs. Position for a random array and a random signal

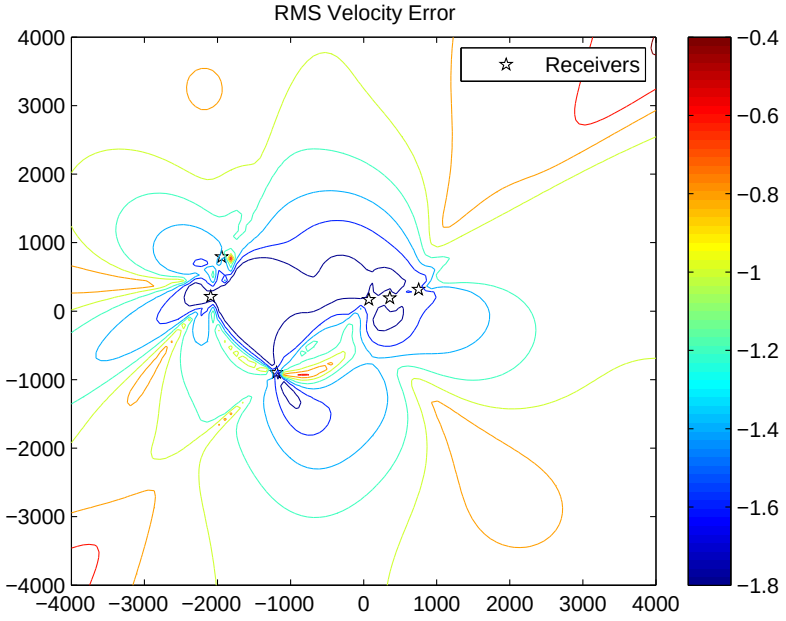

FIGURE 6.37: Velocity Estimation Preformance Vs. Position for a random array and a random signal

Chapter 7

Summary and Future Work

In this work, we suggested a direct algorithm for passive geolocation of a moving radio transmitter using an array of stationary receivers. This method is an extension of the conventional DPD method, to the case in which the transmitter is moving. While the conventional DPD method handles the stationary transmitter scenario, the suggested algorithm handles the scenario in which the transmitter is moving.

For the derivation of the algorithm, we defined a model for the scenario, and expressed the ML cost function for both the known and unknown signal scenario. We then explored the characteristics of the ML cost function , and developed its derivatives. Later, we suggested several algorithms for finding the maximum of the cost function, each relevant to a different scenario.

Later, we derived the Cramar-Rao lower bound of the scenario in order to compare the performance of the suggested algorithm to the theoretical bound.

Finally, we compared the performance of the suggested algorithm with the performance of conventional methods and with the lower bound using Monte-Carlo simulations. The suggested algorithm showed better performance than conventional methods, especially in lower SNR.

There are, of course, many unexplored matters, that were left out of the scope of this work. Future work could be held in the following directions:

- This work considered the estimation of the position and velocity of the transmitter in only a single lag. In realistic scenarios, the moving transmitter is tracked during several lags. An interesting direction would be to develop an algorithm that samples the transmitter in several lags, and takes into consideration the motion model of the transmitter in order to achieve better performance.

- This work handled only a single moving transmitter. It would be interesting to explore the scenario in which there are several moving transmitters.

- In this work, we assumed that certain parameters, such as the position of the receivers is known in an infinite accuracy. It would be interesting to explore the sensitivity of the estimation to errors to the position of the receivers.

- We developed only the known signals Cramer-Rao lower bound. Treating the signals as unknown stochastic signals and developing the unknown signals lower bound is an interesting direction.

- In this work, we developed a method to analyse the performance of the algorithm based on the scenario parameters and the transmitted signal. It would be interesting to develop a method to find the optimal transmitted signal that would give the best estimation performance for a given scenario. This could be very helpful for developing beacon signals.

Bibliography

[1] J.J. Bussgang J.M. Zagami, S. A. Parl and K.D. Melillo. Providing universal location services using a wireless e911 location network. *IEEE Commun. Mag.*, 1998.

[2] M. Hata and T. Nagatsu. Mobile location using signal strength measurements in a cellular system. *IEEE Transactions on Vehicular Technology*, 1980.

[3] D. Musicki and W. Koch. Geolocation using tdoa and fdoa measurements. In *Information Fusion, 2008 11th International Conference on*.

[4] D. Musicki, R. Kaune, and W. Koch. Mobile emitter geolocation and tracking using tdoa and fdoa measurements. *Signal Processing, IEEE Transactions on*, 58(3):1863 –1874, 2010. ISSN 1053-587X. doi: 10.1109/TSP.2009.2037075.

[5] D.J. Torrieri. Statistical theory of passive location systems. *IEEE Transactions on Aerospace and Electronic Systems*, 1984.

[6] Y.T. Chan and F.L. Jardine. Target localization and tracking from doppler shift measurements. *IEEE Journal of Oceanic Engineering*, 1990.

[7] Y.T. Chan and J.J. Towers. Passive localization from doppler shifted frequency measurements. *IEEE Transactions on Signal Processing*, 1992.

[8] R. Bardelli D.P. Haworth, N.G. Smith and T. Clement. Interference localisation for the eutelsat satellite system. In *Global Telecommunications Conference, 1995. GLOBECOM '95., IEEE.*

[9] K.C. Ho and Y.T. Chan. Geolocation of a known altitude object from tdoa and fdoa measurements. *IEEE Transactions on Aerospace and Electronic Systems*, 1997.

[10] K.C. Ho and Wenwei Xu. An accurate algebraic solution for moving source location using tdoa and fdoa measurements. *Signal Processing, IEEE Transactions on*, 52 (9):2453 – 2463, 2004. ISSN 1053-587X. doi: 10.1109/TSP.2004.831921.

[11] A.J. Amar and A.J. Weiss. Direct position determination of multiple radio signals. *Proc. IEEE Int. Conf. Acoustics, Speech, and Signal processing*, 2004.

[12] A.J. Weiss. Direct position determination of narrowband radio frequency transmitters. *IEEE Signal Processing Letters*, 2004.

[13] Alon Amar and A.J. Weiss. Localization of narrowband radio emitters based on doppler frequency shifts. *IEEE Trans. on Signal Processing*, 2008.

[14] A.J. Weiss and A. Amar. Direct geolocation of stationary wideband radio signal based on time delays and doppler shifts. pages 101 –104, aug. 2009. doi: 10.1109/SSP.2009.5278630.

[15] S. Stein. Differntial delay/doppler ml estimation with unknown signals. *IEEE Trans. on Signal Processing*, 1993.

[16] C. Knapp and G. Carter. Time delay estimation in the presence of relative motion. In *Acoustics, Speech, and Signal Processing, IEEE International Conference on ICASSP '77.*, volume 2, pages 280 – 283, May 1977. doi: 10.1109/ICASSP.1977.1170252.

[17] Y.T Chan and K.C Ho. A simple and efficient estimator for hyperbolic location. *IEEE Trans. on Signal Processing*, 1994.

[18] P. C. Chestnut. Emitter location accuracy using tdoa and differential doppler. *IEEE Trans. on Aerospace and Electronic Systems*, 1982.

[19] *Nonlinear Programming*, chapter 1 - Unconstrained Optimization. Athena Scientific, 1999.

[20] R. Ren, M.L. Fowler, and N.E. Wu. Finding optimal trajectory points for tdoa/fdoa geo-location sensors. In *Information Sciences and Systems, 2009. CISS 2009. 43rd Annual Conference on*, pages 817 –822, 2009. doi: 10.1109/CISS.2009.5054830.